

High-throughput sequencing and transcriptomics

Dave Ting Pong Tang

November 27, 2014

Abstract

The development of DNA sequencing has allowed us to fully determine the genetic make-up of all organisms. Technological innovations in DNA sequencing from the last two decades has massively scaled up the process of DNA sequencing in a time- and cost-effective manner and these advancements made it possible to fully sequence the genomes of various organisms, including humans. With the completion of various genome projects, the focus has now shifted towards identifying functional elements in genomes. In particular, the field of transcriptomics aims to identify, annotate, and analyse the transcribed products of the genome. Traditionally, transcriptome profiling has relied on microarray technologies but with the advent of high-throughput sequencing, the ability to profile transcripts accurately and in an unbiased manner has transformed the study of transcriptomes. However the applications of high-throughput sequencing to transcriptomics is relatively immature as developments have occurred in the last 5-6 years. This thesis focuses on the interpretation of high-throughput transcriptome sequencing data through the use of bioinformatic methods.

In the first study of this thesis, biases and technical artefacts in a transcriptome technology known as nano cap analysis gene expression (nanoCAGE) were investigated. We found that biases were introduced through the use of molecular barcodes and developed several strategies for coping with such biases. In the second study, we captured and analysed the transcriptional output of cells with induced DNA damage using small RNA sequencing. We observed a previously uncharacterised class of small RNAs that formed near the DNA break site that were necessary in establishing the DNA damage response. In the third study, we studied the expression of a class of small RNAs called Piwi-interacting RNA (piRNAs) in mice with a Mecp2 knock-out (KO). Our analysis indicated that piRNAs are over-expressed in the cerebellum of mice with a Mecp2 KO, which may be due to proposed role of Mecp2 in silencing transposons. In the fourth and last study, we focused on transcripts that initiated from repetitive elements (REs) and characterised their expression patterns across a wide panel of cell lines, tissues, and primary cells. We demonstrated that REs may drive the expression of long non-coding RNAs and enhancer RNAs, and their expression patterns are tissue specific.

High-throughput sequencing has transformed the field of transcriptomics by revealing a much more complex picture of transcription than previously anticipated. The layers of complexity include the expression of multiple classes of RNA species, each performing various regulatory roles, random transcriptional events or transcriptional noise, and complexity perpetrated from technical artefacts. In order to separate noise from signal requires an understanding of the different technologies, careful scrutiny of the data, and the application of appropriate bioinformatic methods.

Nederlandse Samenvatting

Recente ontwikkelingen op het gebied van DNA sequentie analyse hebben geleid tot zogenaamde “high-throughput sequencing”. Dit heeft DNA sequentie analyse mogelijk gemaakt die zowel tijds- als kostenbesparend werkt.

Met het gereedkomen van de sequentie van het humane genoom en de sequentie van de genomen van andere species, is de nadruk bij genoom sequentie analyse komen te liggen op de identificatie van kleine functionele elementen in het DNA. Het veld van transcriptoom analyse heeft zich voornamelijk gericht op de correcte annotatie en data analyse van de getranscribeerde producten. De introductie van high-throughput sequencing in transcriptoom analyse heeft een unbiased en accurate screening van het transcriptoom mogelijk gemaakt, en heeft daarmee inzicht geboden in de grote complexiteit van bijvoorbeeld het humane genoom. Echter alle methoden zijn nog relatief nieuw en niet gematureerd, eigenlijk allemaal ontwikkeld in de laatste 5-6 jaar. Daarom vinden er continu verbeteringen aan deze methoden plaats. In mijn dissertatie besteed ik daarom veel aandacht aan het gebruik van bio-informatica methoden om het transcriptoom beter te kunnen analyseren.

In hoofdstuk 2 richt ik mij daarom op de mogelijke bias en technische artefacten die bij de transcriptoom analyse voor kunnen komen, in het bijzonder die bij de “nano-CAGE” analyse kunnen optreden. In het bijzonder vond ik artefacten die werden geïntroduceerd door het gebruik van moleculaire barcodes en ik heb verschillende methoden ontwikkeld om hier om op een juiste wijze mee om te gaan.

In hoofdstuk 3 heb ik mij gericht op het analyseren van het transcriptoom van cellen met geïnduceerde DNA schade gebruik makend van sequentie analyse van “small RNAs”. Hierbij ontdekten we een nieuwe vorm van RNA molekulen, die worden gevormd dicht op de plaatsen van DNA schade. Deze RNAs vormen de respons op de DNA schade.

In hoofdstuk 4 heb ik me gericht op het bestuderen van transcripten die ontstaan uit repetitieve elementen (RE) in het DNA. Ik heb daarbij het expressie profiel van deze transcripten voor een groot aantal cellijnen, weefsels, en primaire cellen in kaart gebracht. Ik heb daaruit geconcludeerd dat RE’s belangrijk zijn voor de expressie van de “long non-coding RNAs” en “enhancer RNAs”, waarbij hun expressie tissue specifiek is.

In conclusie, high-throughput sequentie analyse heeft het veld van transcriptoom analyse wezenlijk veranderd door veel meer complexiteit van transcriptie aan te tonen dan daarvoor voor mogelijk werd gehouden. De lagen van complexiteit die we daarbij hebben ontdekt omvatten meerdere klassen van RNA’s, ieder met een eigen regulatoire rol, random transcriptionele gebeurtenissen ook wel “random noise” genoemd, en inzicht in de complexiteit van de technische artefacten. Het scheiden van technische variatie van het echte signaal vergt begrip van de verschillende technologieën, diepgaande data analyse, en de ontwikkeling van adequate bio-informatische methoden.

List of publications

1. Dave T. P. Tang, Charles Plessy, Md Salimullah, Ana Maria Suzuki, Raffaella Calligaris, Stefano Gustincich, and Piero Carninci. Suppression of artifacts and barcode bias in high-throughput transcriptome analyses utilizing template switching. *Nucleic Acids Research*, 41(3):e44, 2013. doi: 10.1093/nar/gks1128
2. Sofia Francia, Flavia Michelini, Alka Saxena, Dave Tang, Michiel de Hoon, Viviana Anelli, Marina Mione, Piero Carninci, and Fabrizio d'Adda di Fagagna. Site-specific DICER and DROSHA RNA products control the DNA-damage response. *Nature*, 488(7410):231–235, 2012
3. Alka Saxena, Dave Tang, and Piero Carninci. piRNAs warrant investigation in rett syndrome: An omics perspective. *Disease markers*, 33(5): 261–275, 2012
4. Dave Tang and Piero Carninci. The regulated expression of repetitive elements across human cell types and tissues. *In preparation*, 2014

Other publications

5. Yuki Hasegawa, Dave Tang, Naoko Takahashi, Yoshihide Hayashizaki, Alastair R. R. Forrest, the FANTOM consortium, and Harukazu Suzuki. Ccl2 enhances pluripotency of human induced pluripotent stem cells by activating hypoxia related genes. *Sci. Rep.*, 4, Jun 2014
6. Dave Tang, Ana Maria Suzuki, Raffaella Calligaris, Stefano Gustincich, and Piero Carninci. Deep transcriptome sequencing of whole blood samples from Parkinson's disease patients. *In preparation*, 2014

Contents

1	Introduction	10
1.1	A brief history of DNA	10
1.2	The Central Dogma of Molecular Biology	11
1.3	Transcription	12
1.3.1	Transcriptional regulation	13
1.3.2	DNA accessibility	15
1.4	DNA sequencing	16
1.4.1	Next-generation sequencing	18
1.4.2	Third generation sequencing and beyond	20
1.5	Expression analysis	20
1.5.1	Transcriptome profiling	21
1.5.2	Transcriptional complexity	24
1.5.3	Defining a gene	24
1.5.4	Non-coding RNAs	25
1.6	Repetitive mammalian genomes	26
1.6.1	Junk DNA	27
1.6.2	Impact of transposable elements on genomes	27
1.7	Bioinformatics and genomics	29
1.7.1	High-throughput sequencing data	29
1.7.2	Analysing expression datasets	30
2	Template switching artefacts	33
3	Role of small RNAs in DNA damage repair	46
4	Rett syndrome and piRNAs	55
5	Regulated expression of repetitive elements	64
6	General discussion	86
6.0.3	Artefacts and biases in high-throughput sequencing . . .	86
6.0.4	Pervasive transcription and functional RNA products . .	87
6.0.5	The repetitive human genome	88

List of Figures

1.1	DNA base pairing	11
1.2	The central dogma	12
1.3	Core promoter elements	13
1.4	DNA transcription	14
1.5	DNA packaging	16
1.6	Radioactively labelled sequencing gel	18
1.7	Sanger sequencing	19
1.8	Developments in next generation sequencing	21
1.9	Cap Analysis Gene Expression protocol	23
1.10	Coverage of repetitive elements in vertebrate genomes	28

List of Tables

1.1	Table of histone modifications	17
1.2	Table of non-coding RNAs	26

List of Abbreviations

3D	Three-dimensional.
A	Adenine.
ANOVA	Analysis of variance.
ASC	Adult stem cell.
BP	Base pair.
BRE	B recognition element.
C	Cytosine.
CAGE	Cap analysis gene expression.
CCL2	chemokine (C-C motif) ligand 2.
cDNA	Complementary DNA.
CGI	CpG islands.
ChIP	Chromatin immunoprecipitation.
CPAT	Coding-potential assessment tool.
CRT	Cyclic reversible termination.
dATP	Deoxyadenosine triphosphate.
DBD	DNA-binding domain.
dCTP	Deoxyguanosine triphosphate.
ddNTP	Dideoxynucleotide triphosphate.
DDR	DNA damage response.
dGTP	Deoxycytidine triphosphate.
DNA	Deoxyribonucleic acid.
dTTP	Deoxythymidine triphosphate.
emPCR	Emulsion PCR.
ENCODE	Encyclopedia of DNA elements.
ERV	Endogenous retrovirus.
ESC	Embryonic stem cell.
FANTOM	Functional annotation of the mammalian genome.
FDR	False discovery rate.
G	Guanine.
GO	Gene ontology.

HGP	Human genome project.
iPSC	Induced pluripotent stem cell.
LINE	Long interspersed elements.
lncRNA	Long non-coding RNA.
LTR	Long terminal repeat.
MBD	methyl-CpG binding domain.
MECP2	methyl CpG binding protein 2.
miRNA	Micro RNA.
mRNA	Messenger RNA.
NaCl	Sodium chloride.
nanoCAGE	Nano Cap analysis gene expression.
ncRNA	Non-coding RNA.
PAGE	Polyacrylamide gel electrophoresis.
PCR	Polymerase chain reaction.
PET	Paired-end ditag.
piRISC	piRNA-induced silencing complex.
piRNA	Piwi-interacting RNA.
Pol I	RNA polymerase I.
Pol II	RNA polymerase II.
Pol III	RNA polymerase III.
pre-miRNA	Precursor miRNA.
pri-miRNA	Primary miRNA.
QC	Quality control.
qRT-PCR	Quantitative real-time polymerase chain reaction.
RABS	Repeat-associated binding sites.
RAP	Repeat Analysis Pipeline.
RE	Repetitive elements.
RIDL	Repeat Insertion Domains of LncRNAs.
RNA	Ribonucleic acid.
RNA pol	RNA polymerase.
RT	Reverse transcriptase.
RTT	Rett syndrome.
SAGE	Serial analysis gene expression.
SAM	Sequence alignment/map.
SBL	Sequencing by ligation.
SBS	Sequencing by synthesis.
SINE	Short interspersed elements.
SNA	Single-nucleotide addition.
SOLiD	Sequencing by Oligonucleotide Ligation and Detection.

T	Thymine.
TBP	TATA binding protein.
TE	Transposable element.
TF	Transcription factor.
TFBS	Transcription factor binding site.
TFIIB	Transcription factor IIB.
TMM	Trimmed mean of M values.
tRNA	Transfer RNA.
TS	Template switching.
TSS	Transcription start site.
TU	Transcriptional unit.
TUF	Transcripts of unknown function.
U	Uracil.

Chapter 1

Introduction

1.1 A brief history of DNA

In the winter of 1868/9, Swiss physician and biologist, Johannes Friedrich Miesscher isolated an unknown substance from the nuclei of cells (Dahm, 2008). This substance was unlike anything he had observed before; it was resistant to protease, lacked sulphur, and contained a large amount of phosphorous. He recognised that he had isolated a novel substance and as it was from the nucleus, he named it nuclein. In 1881, Albrecht Kossel determined that nuclein was composed of five bases: adenine (A), cytosine (C), guanine (G), thymine (T), and uracil (U). Later in 1889, Richard Altmann discovered that nuclein was acidic (due to the presence of phosphorous) and renamed nuclein to nucleic acid. The basic component of deoxyribonucleic acid (DNA) was deduced by Phoebus Levene in 1909, who discovered that DNA consisted of an acid, an organic base, and a sugar. Levene also showed that these components were linked together as phosphate-sugar-base to form units, which he termed nucleotides. This sugar-phosphate backbone forms the structural framework of nucleic acids and makes DNA highly stable. In 1928, Frederick Griffith demonstrated that heritable traits could be transferred between dead and live bacteria and that provided the first clue that a “transforming factor” existed (Griffith, 1928). It wasn’t until 1944, when Oswald Avery, Colin MacLeod, and Maclyn McCarty demonstrated that deoxyribonucleo-depolymerase (an enzyme that degrades DNA) destroyed the “transforming factor”, that it was hypothesised DNA was the genetic material (Avery et al., 1944). This was later confirmed in 1952 by Alfred Hershey and Martha Chase, by demonstrating that when bacteriophages infected bacteria, only their DNA would enter into the cytoplasm of the bacteria, while their protein remained outside (Hershey and Chase, 1952).

While Levene proposed that DNA was made up of equal amounts of A, C, G, and T, it was later discovered by Erwin Chargaff that DNA had a one-to-one ratio of pyrimidine (C, T, and U) and purine (A and G) bases (Chargaff et al., 1952, Elson and Chargaff, 1952); this became known as Chargaff’s rules. This observation by Chargaff and insights gained from Rosalind Franklin were necessary for the deduction of the three-dimensional (3D) structure of DNA.

by Francis Crick and James Watson in 1953 (Watson and Crick, 1953). The 3D structure of DNA demonstrated how adenines paired with thymines and cytosines paired with guanine (Figure 1.1); this became known as Watson-Crick base pairing and explained how genetic information could be copied due to the complementary nature of DNA.

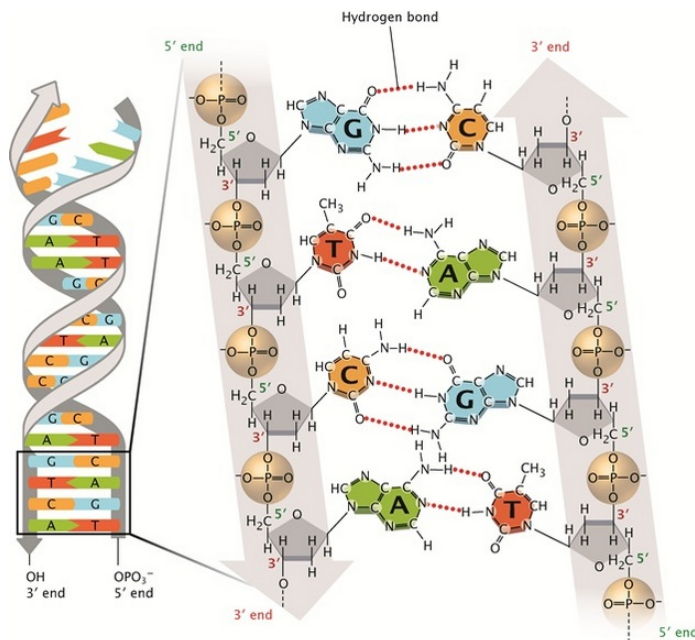


Figure 1.1: The structure of DNA is based on the repeated pattern of deoxyriboses and phosphate groups, forming the sugar-phosphate backbone, and the base pairing of the four bases, adenine (A), cytosine (C), guanine (G), and thymine (T). Two hydrogen bonds connect A to T and three hydrogen bonds connect C to G. Image used with permission from Nature Education 2013.

1.2 The Central Dogma of Molecular Biology

In 1958, Francis Crick wrote a seminal paper on protein synthesis, where he described the importance of proteins in living organisms and first proposed the central dogma of molecular biology (Crick, 1958). Crick described how DNA or ribonucleic acid (RNA) could be used as templates for proteins and further described the possible directions of information flow between DNA, RNA, and protein. However, he noted that once information had been transferred from either DNA or RNA to protein, it was not possible for information to flow back to nucleic acids (Figure 1.2). In 1970, an enzyme known as reverse transcriptase (RT) was discovered (Temin and Mizutani, 1970, Baltimore, 1970), which allowed RNA to be used as a template for producing DNA. In light of this and due to the misunderstanding of the central dogma, Crick restated the central dogma (Crick, 1970): “The central dogma of molecular biology deals with the detailed residue-by-residue transfer of sequential information. It states that such information cannot be transferred from protein to either protein or nucleic acid.”

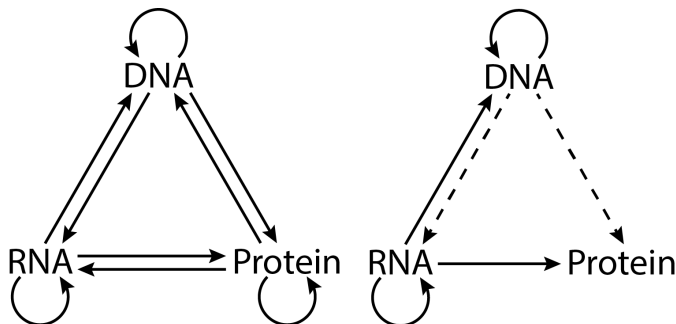


Figure 1.2: All possible information transfer pathways between DNA, RNA, and protein are shown on the left. Probable (solid arrows) and possible (dotted arrows) information transfer pathways, as originally proposed in 1958 by Francis Crick (Crick, 1958), are shown on the right. The Central Dogma of Molecular biology states that once information has been transferred to a protein, it is not possible for this information to be transferred back to the nucleic acids.

Prior to proposing the central dogma, Crick had predicted the existence of “adaptors” that would transfer information from RNA to protein in 1955 (Newton, 2013). Crick proposed that there were twenty adaptors and special enzymes, one for each amino acid; the enzymes would join a particular amino acid to its own special adaptor. This theory was later confirmed by the discovery of transfer RNA (tRNA) in 1958 (Hoagland et al., 1958). The discovery of messenger RNA (mRNA) in 1961 (Brenner et al., 1961) demonstrated the flow of information from DNA to RNA and from RNA to protein. In 1962, the DNA code used for encode the amino acids of proteins was deduced (Matthaei et al., 1962). Matthaei and colleagues demonstrated that an artificially created RNA, composed entirely of uracils, would produce a protein composed entirely of phenylalanine. The full code, known as the genetic code, was cracked three years later in 1965 (Nirenberg et al., 1965) and defined how information was encoded in DNA to produce amino acids. Nirenberg and colleagues deduced that three nucleotides defined a codon, which are translated into one of the 20 standard amino acids.

1.3 Transcription

Transcription is the process by which a particular segment of DNA is processed into RNA by the enzyme RNA polymerase (RNA pol). There are three different types of RNA polymerases in eukaryotic cells: Pol I transcribes DNA that encode most of the ribosomal RNAs (rRNAs); Pol II transcribes DNA that encode mRNAs and other non-coding RNAs; and Pol III transcribes the genes for small regulatory RNA molecules, such as tRNAs. The first step in transcription is initiation, whereby RNA pol binds upstream of the DNA to be transcribed, at a region known as the promoter (Figure 1.4). A promoter can be classified by their distance from the transcription start site (TSS), which are the first nucleotides transcribed by RNA pol. The core promoter for a region to be transcribed, i.e. the transcript, by Pol II is usually found immediately upstream of the TSS and contains specific DNA sequences or elements that are necessary for transcription. The core promoter elements include the TATA box

(usually located 25 to 35 bases upstream of the TSS), the transcription factor IIB recognition element [also known as the B recognition element, (BRE)], the initiator element (Inr), the downstream promoter element (DPE), and CpG islands (CGIs) (Figure 1.3). The proximal promoter lies \sim 250 bp of the TSS and contains primary regulatory elements. Distal promoters do not have a fixed distance from the TSS but are usually further upstream and contain additional regulatory elements.

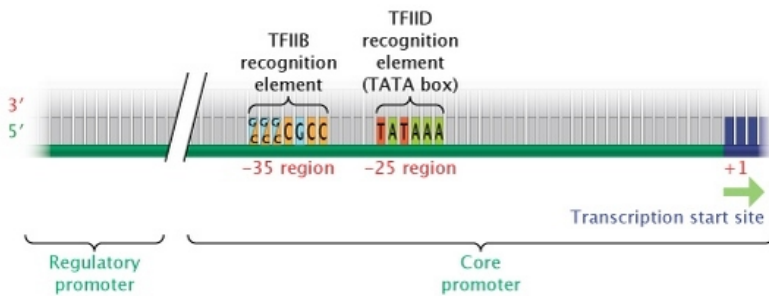


Figure 1.3: Core promoter elements recognised by RNA Pol II include the transcription factor IIB recognition element and the TATA box, which are located around 35 and 25 bp upstream of the transcription start site (TSS), respectively. Various regulatory elements that regulate transcription may lie further upstream. Image used with permission from Nature Education 2014.

Once transcription has initiated, RNA pol and its associated proteins unwind the DNA double helix; once unwound, RNA pol reads the template DNA strand and adds nucleotides to the 3' end of a nascent RNA transcript. Transcription is terminated when the RNA polymerase reaches the termination site and the mRNA transcript and RNA pol are released (Figure 1.4). Transcription results in two main classes of RNA transcripts: (1) Protein-coding transcripts, where the RNA known as mRNA can be further translated into a protein molecule and (2) Non-coding transcripts, where the RNA molecule is the functional product.

1.3.1 Transcriptional regulation

The regulation of transcription ensures that transcripts are expressed in the correct spatial and temporal manner; this is necessary for maintaining cellular identity and for responding appropriately to environmental cues. Transcriptional regulation is achieved through interactions directly related to the DNA sequence and modifications not directly related to the DNA sequence. A class of regulatory proteins that plays a role in controlling the rate of transcription are transcription factors (TFs). These proteins can activate or enhance transcription by binding to specific DNA sequences and recruiting RNA polymerase (Lee and Young, 2000). TFs characteristically contain DNA-binding domains (DBDs), which allow them to bind specifically to DNA regions, known as transcription factor binding site (TFBS). One particular group of regulatory DNA that TFs bind to are known as enhancer sequences, which as the name suggests, enhances in the rate of transcription. Enhancer sequences can be located thousands of nucleotides away from the promoter they interact with, as they are brought into proximity to the promoter by the physical looping of DNA. In

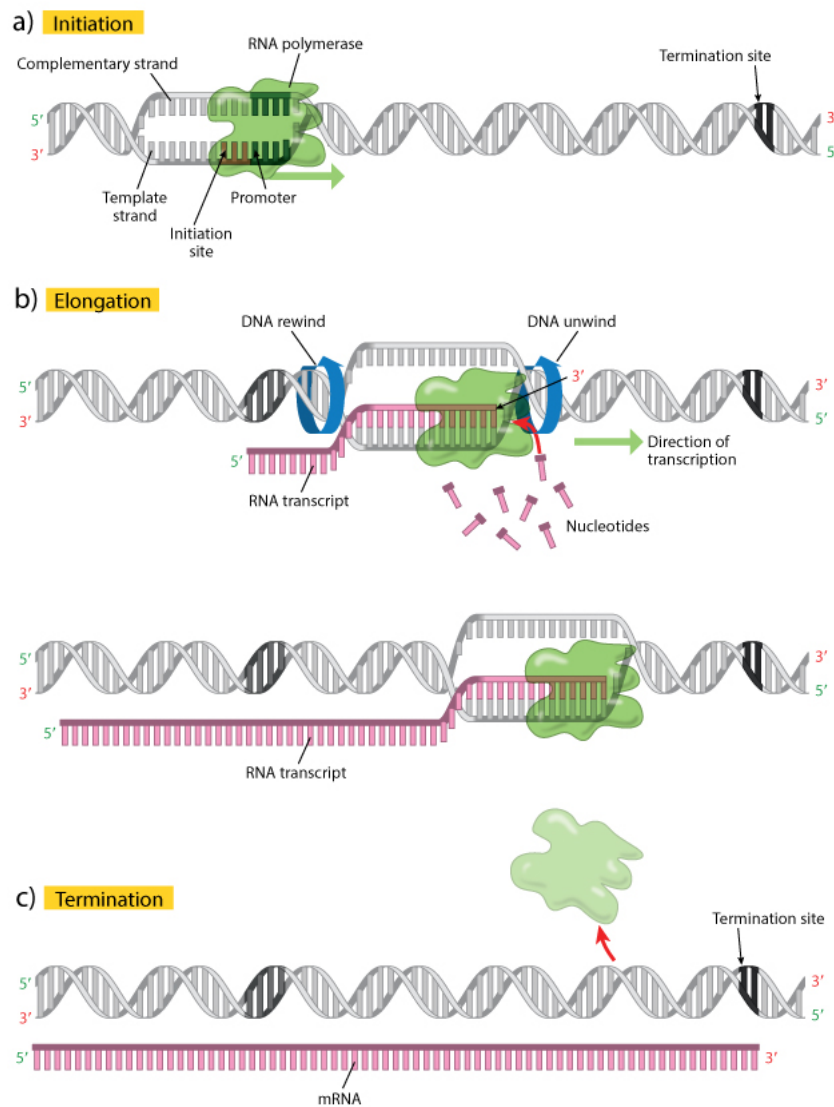


Figure 1.4: The process of transcription can be broadly grouped into three stages: a) initiation, b) elongation, and c) termination. Initiation involves the binding of RNA polymerase (shown as a large green blob) to the promoter and the DNA double helix starts to separate. RNA polymerase starts reading the sequence on the template strand in the 5' to 3' direction (green arrow). The elongation step involves the movement of RNA polymerase along the DNA strand producing a growing RNA transcript chain, which continually closes and opens the DNA strand. The nucleotides are shown as pink T-shaped molecules and the red arrow indicates that they are added at the 3' end of the nascent transcript. The termination step occurs once the RNA polymerase reaches the termination site, and the RNA transcript and RNA polymerase are separated from the DNA. Image used with permission from Nature Education 2013.

addition, enhancers may be positioned in both forward and reverse orientations, and located either upstream or downstream from its associated promoter and still affect transcription.

DNA is a physical entity; mechanical and biochemical factors inside cells that act on DNA also regulate transcription. This type of regulation is known as epigenetic regulation, which refers to effects that are caused by changes in the DNA sequence. An example of a biochemical modification is DNA methylation, which is the covalent addition of a methyl group to the 5 position of cytosines. DNA methylation is an important regulator of gene transcription and high levels of methylation typically lead to gene silencing. In addition, mechanical factors such as the structural compaction of DNA can regulate transcription by limiting the accessibility of DNA to TFs and RNA pol. This compaction is achieved mainly via histones, which are a family of small and positively charged proteins that fold negatively charged DNA in the form of electrostatic interactions; this folding helps condense DNA and the resulting DNA-histone complex is called chromatin. Chromatin possesses a fundamental repeating structure (Van Holde et al., 1974), known as the nucleosome, which is the structural and functional unit of chromatin. Nucleosomes are structured with two of each of the following histones: H2A, H2B, H3, and H4, and forms a histone octamer that binds and wraps about 146 base pairs of DNA. The H1 histone protein binds to DNA that links nucleosomes, called linker DNA, wrapping another 20 bps of DNA and stabilising the linker DNA. Chromatin is found in two varieties: heterochromatin, which features DNA tightly wrapped into a 30 nm fibre, and euchromatin where DNA is lightly packed as nucleosomes (Figure 1.5).

1.3.2 DNA accessibility

Chromatin structure and nucleosome positioning are altered in order for the transcriptional and replication machinery to be able to access parts of the genome for transcription. Chromatin structure can be relaxed by biochemically modifying histones, to strengthen or weaken its association with DNA. Generally speaking, there are two major mechanisms by which chromatin is made more accessible via histone modifications:

1. Histones can be enzymatically modified by the addition of acetyl, methyl, or phosphate groups.
2. Histones can be displaced by chromatin remodelling complexes, thereby exposing underlying DNA sequences to polymerases and other enzymes.

Importantly, these two processes are reversible, so modified or remodelled chromatin can be returned to its compact state after transcription and/or replication are complete. The nomenclature for histone modifications is defined by the name of the histone, followed by the single-letter amino acid abbreviation and its position, and then an abbreviation of the enzymatic modification; for example, H3K27ac indicates the acetylation of lysine 27 on H3. Specific histone modifications are associated with different biological states; for example, acetylation removes the positive charge on histones, thereby decreasing the interaction between histones and DNA, loosening chromatin, and allowing transcriptional activation to take place. On the other hand, the tri-methylation of lysine 27 on histone H3, i.e. H3K27me3, is associated with the inhibition of transcription (Young et al., 2011). Given that distinct histone modifications can either be implicated in the activation or repression of transcription, a “histone code” has been proposed (Jenuwein and Allis, 2001) and the profiling of the

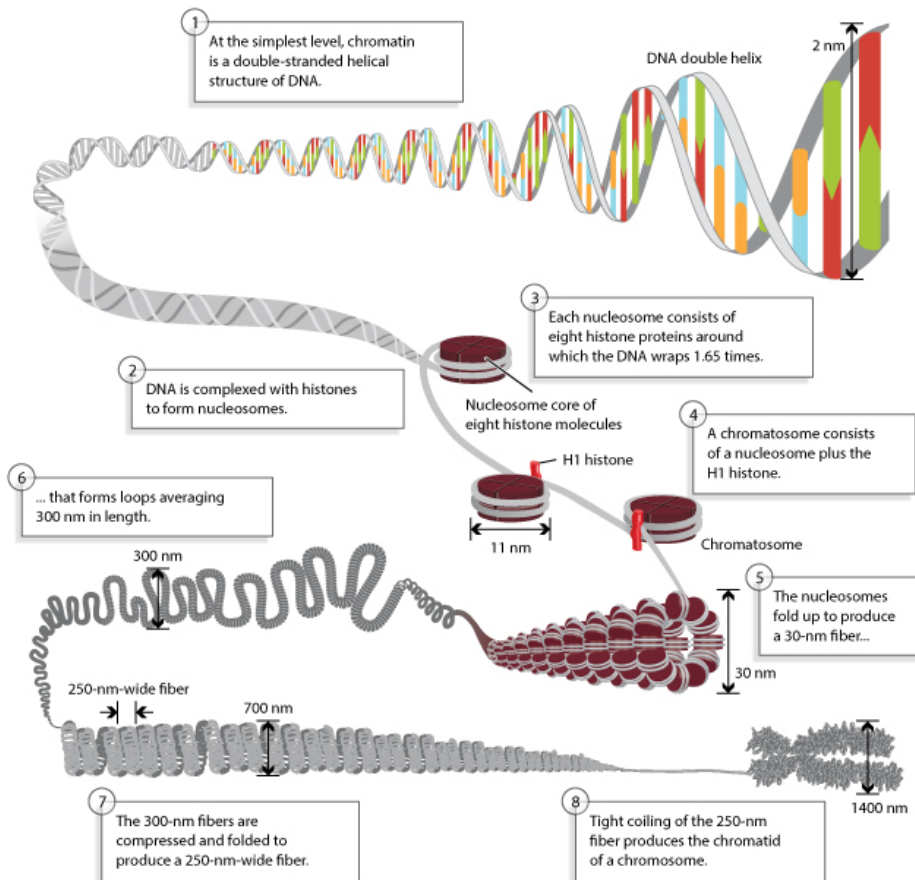


Figure 1.5: DNA is compacted at various levels: 1) as a double-stranded helical structure, 2 and 3) as nucleosomes, which consists of eight histone molecules with DNA wrapped around 1.65 times, 4) as a chromatosome, which consists of the nucleosome and a H1 histone, 5) as a 30 nm fiber of folded nucleosomes, 6) as looped nucleosomes that are on average 300 nm in length, 7) as compressed 300 nm fibers, producing a 250 nm fiber, and finally 8) as chromatids of a chromosome. Image used with permission from Nature Education 2013.

histone states provides insights into the transcriptional state of a DNA region. Table 1.1 summarises a list of histone modifications and variants profiled by the ENCODE project (Bernstein et al., 2012).

1.4 DNA sequencing

DNA sequencing is the process of determining the exact order of nucleotides within a DNA molecule. The first generation of DNA sequencing methods (Sanger and Maxam-Gilbert sequencing) were developed in the 1970s and were very labour intensive, requiring four separate polyacrylamide gel electrophoresis (PAGE) runs, for the determining the sequence of each base. The key feature of Sanger sequencing (Sanger et al., 1977) was the use of chain-terminating dideoxynucleotide triphosphates (ddNTPs). The structure of a normal nucleotide (dNTP), consists of a 3' hydroxyl (OH) group in the pentose sugar;

Histone modification or variant	Signal characteristics	Putative functions
H2A.Z	Peak	Histone protein variant (H2A.Z) associated with regulatory elements with dynamic chromatin
H3K4me1	Peak/region	Mark of regulatory elements associated with enhancers and other distal elements, but also enriched downstream of transcription starts
H3K4me2	Peak	Mark of regulatory elements associated with promoters and enhancers
H3K4me3	Peak	Mark of regulatory elements primarily associated with promoters/transcription starts
H3K9ac	Peak	Mark of active regulatory elements with preference for promoters
H3K9me1	Region	Preference for the 5' end of genes
H3K9me3	Peak/region	Repressive mark associated with constitutive heterochromatin and repetitive elements
H3K27ac	Peak	Mark of active regulatory elements; may distinguish active enhancers and promoters from their inactive counterparts
H3K27me3	Region	Repressive mark established by polycomb complex activity associated with repressive domains and silent developmental genes
H3K36me3	Region	Elongation mark associated with transcribed portions of genes, with preference for 3' regions after intron 1
H3K79me2	Region	Transcription-associated mark, with preference for 5' end of genes
H4K20me1	Region	Preference for 5' end of genes

Table 1.1: Summary of histone modifications and variants profiled by the ENCODE project (Bernstein et al., 2012).

chain-terminating ddNTPs lack the OH group that is necessary for the formation of the phosphodiester bond between one nucleotide and the next during DNA strand elongation. The idea was to set up a reaction with a mixture of dNTPs [deoxyadenosine triphosphate (dATP), deoxyguanosine triphosphate (dGTP), deoxycytidine triphosphate (dCTP), deoxythymidine triphosphate (dTTP)] and a particular ddNTP in a ratio of 300:1. Most of the times, the DNA will be elongated but if a ddNTP is incorporated into the growing DNA strand, strand elongation is terminated. This results in DNA fragments of varying lengths, where the last base of these fragments corresponding to the ddNTP used. By performing the same reaction for the other three ddNTPs and loading the fragments of each reaction onto separate PAGE lanes, the DNA bases can be deduced by reading the four lanes (Figure 1.6).

The Maxam-Gilbert sequencing method (Maxam and Gilbert, 1977) relies on the use of chemicals that can cleave specific bases in contrast to chain-terminating ddNTPs. Dimethyl sulfate was used to cleave purine bases (A and G) and hydrazine was used to cleave pyrimidine bases (C and T). To distinguish the purines, an adenine-enhanced cleavage step is carried out, which cleaves adenines preferentially. To distinguish the pyrimidines, NaCl is used with hy-

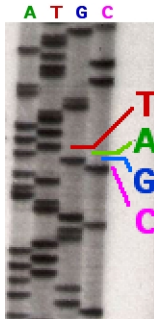


Figure 1.6: PAGE, which has a 1 bp resolution, is used to separate the radioactively labelled DNA fragments from each reaction using specific chain-terminating ddNTPs. By reading the DNA fragments, the sequence of the DNA can be deduced. Image used under the terms and agreement of the Wikipedia GFDL.

drazine to suppress the reaction of thymines. As with Sanger sequencing, the DNA fragments are separated using PAGE, and the DNA bases are deduced by reading the gel.

Sanger sequencing became the *de facto* method for DNA sequencing due to its comparative ease and the use of fewer toxic materials than Maxam-Gilbert sequencing. A further improvement to Sanger sequencing replaced the need to radioactively label the DNA fragments by using chemically synthesised fluorescent oligonucleotide primers (Smith et al., 1986). Four different fluorophores were used for each ddNTP reaction allowing all four reactions to be co-electrophoresed and the DNA sequence was deduced by reading the fluorescence colours (Figure 1.7). The development of a fluorescence detection apparatus linked to a computer that processed the data created the world's first partially automated DNA sequencer (Smith et al., 1986); this development was key towards the success of the Human Genome Project (HGP). For over 25 years since its inception, Sanger sequencing was the method of choice for DNA sequencing.

1.4.1 Next-generation sequencing

The next wave of DNA sequencing techniques, the so-called next-generation (next-gen) or second generation sequencing, started with various strategies that relied on a combination of template preparation, sequencing, and imaging that allowed thousands to billions of sequencing reactions to be performed simultaneously (Metzker, 2010). Next-gen sequencing relies on the clonal amplification of templates and uses *in vitro* cloning rather than bacterial cloning; the two most common methods of clonal amplification are emulsion polymerase chain reaction (emPCR) (Dressman et al., 2003) and solid-phase amplification (Fedorco et al., 2006). With emPCR individual DNA molecules are isolated with primer-coated beads in water-in-oil microreactors and clonal amplification leads to thousands of copies of the DNA molecule in an emulsion. 454 pyrosequencing and Sequencing by Oligonucleotide Ligation and Detection (SOLiD) sequencing employ emPCR and the amplification products are deposited into individual wells for sequencing. Solid-phase amplification relies on a lawn of high-density primers that are covalently attached on a slide surface (also known as a flow cell) and bind to DNA molecules that have been ligated with sequencing adaptors.

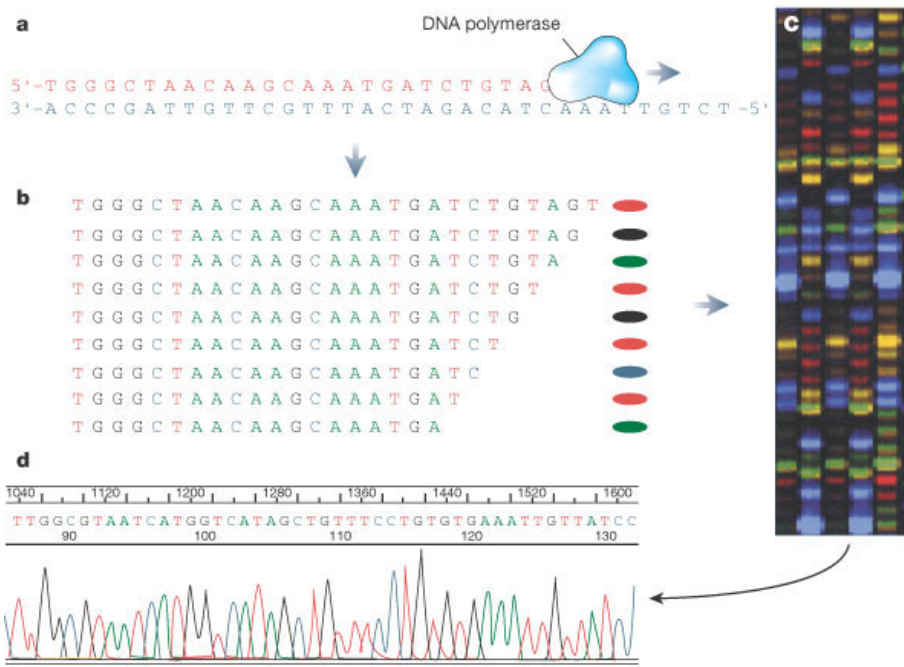


Figure 1.7: a) DNA polymerase synthesises a complementary strand of DNA, however when a b) fluorescently labelled chain-terminating ddNTP base is incorporated, synthesis terminates producing DNA fragments of various sizes. c) As each terminator are fluorescently labelled with different dyes, each fragment will fluoresce a particular colour and the d) sequence trace is read by a computer that determines the sequence based on the coloured peaks.

The two methods allow each DNA template to be spatially separated and allow massively parallel sequencing to take place.

Sequencing can take place via the use of DNA polymerase, which is commonly known as sequencing-by-synthesis (SBS), or via the use of DNA ligase, which is known as sequencing-by-ligation (SBL). SBS can be further classified into cyclic reversible termination (CRT), single-nucleotide addition (SNA), and real-time sequencing (Metzker, 2010). CRT uses reversible terminators and initial developments used the dideoxynucleotides chain terminators used in Sanger sequencing. The concept of CRT is that a DNA polymerase incorporates one fluorescently modified nucleotide, which has a reversible terminator that terminates DNA synthesis. Unincorporated nucleotides are washed away and fluorescence imaging takes place to determine the identity of the incorporated nucleotide. The last step removes or cleaves the reversible terminator and the fluorescent dye, and the cycle is repeated. The CRT method is used in Solexa/Illumina and Helicos single-molecule fluorescent sequencing. SBL relies on DNA ligase and uses either one-base-encoded or two-base-encoded probes that are fluorescently labelled. The probes hybridise to its complementary sequence on the primed template and DNA ligase is added to join the probe to the primer. Non-ligated probes are washed away followed by fluorescence imaging and cleavage of the fluorescent dye and the cycle is repeated. The SBL method is used in SOLiD sequencing.

1.4.2 Third generation sequencing and beyond

The third generation of sequencing refers to single-molecule sequencing technologies, which has the capacity for generating longer read lengths at potentially cheaper costs (Schadt et al., 2010). One of the major advantages of single-molecule sequencing is that polymerase chain reaction (PCR) is not required, and therefore amplification biases and PCR mutations are eliminated. Furthermore, by employing third generation sequencing, quantitative applications of sequencing, such as RNA sequencing, can give a much more representative picture of the true abundance of RNA molecules. The HeliScope sequencer was the first commercially available single-molecule sequencer, which was based on the work of Stephen Quake and colleagues (Braslavsky et al., 2003). HeliScope sequencing utilises billions of primed single-molecule templates that are covalently attached to a solid support and uses CRT but with slight differences from Solexa/Illumina sequencing. HeliScope sequencing uses Helicos Virtual Terminators, which differ from the reversible terminators used in Solexa/Illumina sequencing and dye labelled nucleotides are added individually in the predetermined order of C, T, A, and G, followed by fluorescence imaging.

With the advent of high-throughput sequencing we now have the capacity to sequence an entire human genome in a matter of days. In addition, we have just recently arrived in the \$1,000 genome era, whereby we can sequence the entire genome of an individual at a 30x depth (the minimum depth required for clinical applications) for around 1,000 US dollars (USD). In contrast, the HGP, which gave us the first glimpse of the human genome (Lander et al., 2001) costed approximately 2.7 billion fiscal year 1991 US dollars (NHGRI, 2010). Further developments in sequencing by various companies are aiming towards longer read lengths at a higher output (Figure 1.8). Currently, different sequencers either have very long reads but at a low-throughput or have a high-throughput of shorter reads; as such, each sequencer fills a particular niche. *De novo* assembly of genomes requires longer reads for less ambiguity and the quantification of RNA requires higher throughput in order to accurately sample the vast RNA population.

1.5 Expression analysis

Transcription of a region of DNA results in the expression of an RNA transcript. A transcript may be constitutively expressed, i.e constantly expressed, or expressed according to the current cellular requirements. By comparing transcript levels between different conditions, insight can be gained on the possible function of a particular transcript. Of note is that the amount of a specific transcript in a cell at a given time is not only influenced by the rate of transcription but also by the stability of the transcript; a rapidly degraded transcript may appear to be lowly transcribed. Northern blotting (Alwine et al., 1977) was one of the first methods for quantifying the expression level of specific RNA transcripts. This technique involves the electrophoretic separation of purified RNA, followed by immobilising the RNA onto a blotting membrane; detection of the transcript is achieved by hybridising a specific probe that is complementary to part of the transcript. The relative amount of a specific transcript can be estimated by comparing the strength of signals from different samples; this estimate as-

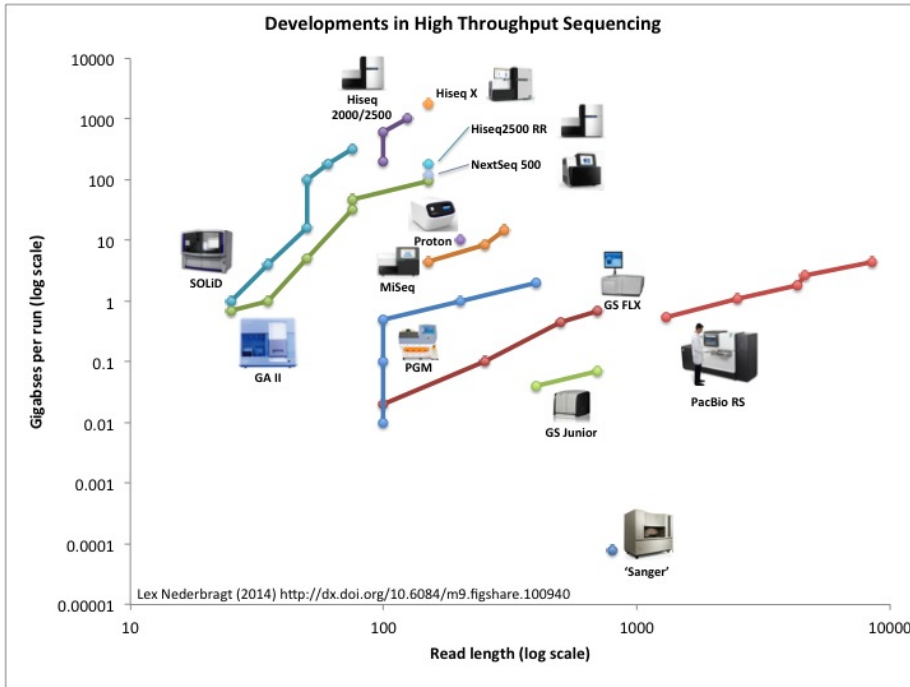


Figure 1.8: Read length (\log_{10}) versus gigabases per run (\log_{10}) for various high-throughput sequencer (Nederbragt, 2012). Currently, the HiSeq X, the sequencer that bought us into the \$1,000 genome era, provides the highest throughput. Image used under the terms and agreement of the CC-BY license.

sumes that an equivalent amount of total RNA was used per sample and this is verified by using a probe that detects a constitutively expressed transcript. Northern blotting is also useful for determining the size of a specific transcript and is commonly used for detecting alternatively spliced transcripts; however, Northern blotting is not very sensitive for estimating transcript abundance.

The most sensitive method of detecting specific transcript levels is quantitative real-time polymerase chain reaction (qRT-PCR), which is able to detect sparse levels of transcripts, down to the level present in single cell. The method employs the use of a fluorescent dye and PCR, where the primer pairs are designed to be specific for a given transcript. By measuring the number of cycles that is required for the formation of a detectable amount of product, which is known as the cycle threshold (C_t) value, the transcript levels can be estimated by comparing the results to qRT-PCR experiments performed using standard samples (Livak and Schmittgen, 2001); lower C_t values indicate higher amounts of initial template. It should be ensured that the PCR step is equally efficient for different transcripts by proper primer design, as a more efficient PCR will result in a lower C_t value compared to a less efficient PCR.

1.5.1 Transcriptome profiling

Transcriptome profiling refers to the expression profiling of the complete collection of transcripts in a cell at a specific time point. Transcripts associated with

a particular biological process or disease state can be identified by profiling all transcripts and in addition, the interplay between transcripts can be inferred by studying transcripts with similar expression patterns. One of the first technologies that allowed the simultaneous profiling of thousands of transcripts at once were microarrays (Schena et al., 1995). DNA probes that are complementary to specific DNA sequences, such as complementary DNAs (cDNA) or genomic regions, are attached to a solid surface and fluorescently labelled target sequences are hybridised onto the surface. Target sequences that complement the probe sequences hybridise to the probe and the signal intensity provides a measure of the expression strength of a particular transcript. In one of the first application of microarrays, researchers were able to observe the change in expression levels of 700 mRNAs during a switch from aerobic to anaerobic respiration in yeast cells (DeRisi et al., 1997). However, microarrays have several limitations, which includes requiring *a priori* knowledge of the genome or transcript sequences, high background levels from cross-hybridisation (Okoniewski and Miller, 2006), and a limited dynamic range in quantifying expression.

In contrast to the hybridisation approach of microarrays, sequencing-based approaches have been developed for transcriptome profiling. Prior to the advent of next-gen sequencing, sequencing approaches were based on the sequencing of short tags; these tagging approaches were cost-effective, as only short fragments of cDNAs were sequenced. Typically type IIS restriction enzymes were used to create tags, which were then concatenated, cloned, and sequenced. A technology called Serial Analysis of Gene Expression (SAGE) (Velculescu et al., 1995) was the first tag-based approach, which created 9 to 10 bp long tags that generally corresponded to the 3' end of the transcripts. A similar technology known as Massive Parallel Signature Sequencing (MPSS), was later developed, which is similar to SAGE but employs different biochemical steps and a different sequencing approach (Brenner et al., 2000). MPSS was an improvement to SAGE in that it produced longer tags (16-20 bp) and libraries that were 20 times larger than typical SAGE libraries (Brenner et al., 2000). Another tagging method known as the paired-end ditag (PET) approach, prepared ditags that corresponded to the 5' and 3' end of the same full-length cDNA (Ng et al., 2005). The PET approach allows the mapping of cDNA boundaries, helps resolve ambiguous tag mappings by using the paired-end information, and has the potential to detect unconventional fusion transcripts and rearrangement events. The SAGE approach also gave rise to Cap Analysis Gene Expression (CAGE) (Shiraki et al., 2003), which combines the tagging strategies of SAGE with a molecular technique known as Cap-Trapper (Carninci et al., 1996, 1997). The CAGE protocol captures all capped transcripts and sequences a short tag (20 or 27 nt depending on which restriction enzyme is used) that corresponds to the 5' end of an RNA transcript (Figure 1.9).

With the arrival of next-gen sequencing, the SAGE and CAGE methods were adapted to high-throughput sequencers (Matsumura et al., 2003, Takahashi et al., 2012). The short-read and high-throughput nature of next-gen sequencing suited tag-based approaches aptly, as the tag lengths were in the size range of reads produced by the sequencer. Whole transcriptome shotgun sequencing or simply RNA sequencing (RNA-Seq) methods were later developed to sequence entire populations of RNA. RNA-Seq refers to the fragmentation of RNA followed by deep-sequencing on next-gen sequencing platforms (Wang et al., 2009); the fragmentation step is required due to the short-read nature of

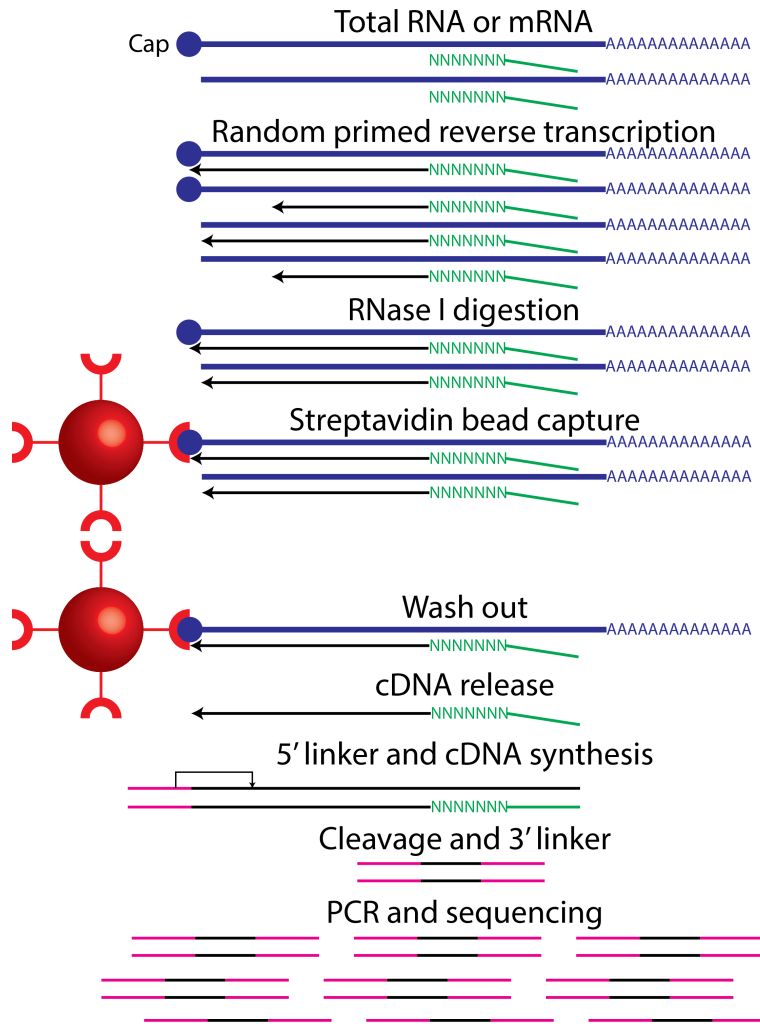


Figure 1.9: The Cap Analysis Gene Expression (CAGE) protocol starts with synthesising cDNA from either total RNA or mRNA by using random or oligo dT primers (only random primers are shown here). Reverse transcription takes place in RNAs with or without a cap and to full or partial completion; the RNase I digestion removes partially reverse transcribed RNA as they are not protected by a full double strand. The 5' end of cDNAs are selected by streptavidin beads and unbound cDNA are washed out. After release from the bead, a linker is attached to the 5' end of the single-stranded cDNA; this linker contains recognition sites that allow the endonuclease cleavage. Lastly a linker is attached to the 3' end of the tag sequence, which is amplified and directly sequenced.

next-gen sequencers. Typically, RNA-Seq methods enrich for transcripts with a poly-A tail; this enrichment step is carried out to avoid rRNA sequences, which make up a large fraction of the total RNA population. One major difference between RNA-Seq and the tag-based approaches is that the entire length of the RNA is sequenced in RNA-Seq; the advantage in this is that alternative splicing patterns can be inferred. However tag-based approaches, such as CAGE, can be used in a complementary nature to RNA-Seq (Kawaji et al., 2014), since

transcript boundaries are defined clearly in CAGE.

1.5.2 Transcriptional complexity

Several landmark studies have revealed that the transcriptional landscape is much more complex than previously anticipated. The functional annotation of the mammalian genome (FANTOM) project, which began as an initiative to sequence and functionally annotate mouse full-length complementary DNA (cDNA) (Kawai et al., 2001), revealed that the transcriptome was dominated by transcripts that had no apparent coding potential (Okazaki et al., 2002). The FANTOM consortium also revealed massive antisense transcription (Katayama et al., 2005), which is transcription arising from the strand opposite the sense strand, and extensive alternative promoter usage (Carninci et al., 2005). Tiling arrays, which are microarrays designed to interrogate a genome at evenly spaced intervals, revealed that a large fraction of genomic bases were transcribed (Bertone et al., 2004, Kapranov et al., 2002, Cheng et al., 2005). This observation that a large percentage of mammalian genomes are transcribed became known as pervasive transcription (Kapranov et al., 2007), however these claims made on the basis of tiling arrays were questioned (van Bakel et al., 2010). However, the Encyclopaedia of DNA elements (ENCODE) project, which endeavours to identify all functional elements in the human genome, observed that mammalian genomes were pervasively transcribed (Bernstein et al., 2012, Birney et al., 2007). These claims were based on the use of various genome-wide biochemical assays and multiple lines of evidence. However, it is not known whether these products of transcription are functional or not, as they do not overlap known genes.

1.5.3 Defining a gene

The idea of a gene dates back to Gregor Mendel and his plant breeding experiments that demonstrated that discrete traits could be inherited from parents to offspring. The term “gene” was coined in 1909 by Wilhelm Johannsen to describe the Mendelian units of heredity. Genes were later described as the precursors to proteins, in the “one gene, one polypeptide” hypothesis, when it was observed that mutations in *Neurospora* genes would cause defects in different steps of metabolic pathways (Beadle and Tatum, 1941). After the determination of the genetic code (see section 1.2), a gene was recognised as a stretch of DNA that coded for a protein in an open reading frame (ORF). The discovery of introns (Chow et al., 1977, Berk and Sharp, 1977), altered the ORF concept, in that genes were now composed of both protein-coding regions (exons) and the non-coding regions (introns). The trend had been that each time a major discovery had been made, the definition of a gene was revised. Thus in light of pervasive transcription members of the ENCODE consortium suggested that the definition of a gene needs to be updated yet again (Gerstein et al., 2007). The definition they proposed was: “A gene is a union of genomic sequences encoding a coherent set of potentially overlapping functional products” (Gerstein et al., 2007). This definition is similar to the idea of a transcriptional unit (TU), proposed by the FANTOM consortium, which is a segment of the genome that shares common core of genetic information and is able to generate transcripts (Okazaki et al., 2002).

1.5.4 Non-coding RNAs

The protein-centric view of genes segregated RNA as either being coding RNA, the mRNAs, or RNA with no coding potential, known as non-coding RNAs (ncRNAs). Historically, it was believed that there were only a few ncRNA families, such as the tRNAs, rRNAs, and the spliceosomal RNAs, all of which existed to aid protein translation. NcRNAs exist as single-strand nucleic acid molecules, which tend to fold on themselves due to the hydrophobic nature of bases, to form localised double-stranded regions that form structures called hairpins or stem-loop structures. NcRNAs can be broadly classified as short or small RNAs, which are defined as being <200 nucleotides long, or as long non-coding RNAs (lncRNAs), which are >200 nucleotides in length; these size cut-offs correspond to the commonly used size selections in biochemical fractionations and does not have any biological implications.

One of the most well studied classes are the micro-RNAs (miRNAs), which were first observed in *Caenorhabditis elegans* (Lee et al., 1993). MiRNAs are typically 20-24 nucleotides in length and function as regulators of expression by base-pairing with complementary sequences within mRNAs (commonly to the 3' untranslated region (UTR)). Another class of well known ncRNAs are the Piwi-interacting RNA (piRNA), which were first observed in drosophila (Aravin et al., 2001). PiRNA are typically between 24 and 32 nucleotides long and are thought to be involved in gene silencing, especially in silencing transposable elements (TEs), by forming the piRNA-induced silencing complex (piRISC). The characterisation of full-length cDNAs revealed another class of RNAs known as lncRNAs (Okazaki et al., 2002). Unlike miRNAs and piRNAs, they are not as well characterised and are usually described with respect to protein-coding genes as sense, antisense, bidirectional, intronic, and intergenic (Ponting et al., 2009). LncRNAs have been dismissed due to lack of sequence conservation (Wang et al., 2004) and have been suggested to be products of transcriptional noise (Huttenhofer et al., 2005). While there have been several well documented cases of lncRNAs, it has been suggested that more experimental work needs to be performed on lncRNAs to find out how many are indeed functional (Kung et al., 2013).

The list of ncRNAs (Table 1.2) has increased over the last 20 years due to technological advances, such as RNA-Seq. These include, but are not limited to, promoter upstream transcripts (Preker et al., 2008), long intergenic non-coding RNAs (Cabili et al., 2011, Ulitsky et al., 2011, Kedersha and Rome, 1986), transcription start site-associated RNA (Valen et al., 2011), enhancer RNAs (Kim et al., 2010), promoter-associated short RNAs and termini-associated short RNAs (Kapranov et al., 2007), double strand break-induced small RNAs (Wei et al., 2012) or DNA damage RNAs (Francia et al., 2012), competing endogenous RNAs (Tay et al., 2014), and transcription initiation RNAs (Taft et al., 2009). Despite an abundance of ncRNA classes, many of these ncRNAs are supported only by transcriptional data, since validation studies have only been performed in a low-throughput manner. As the genome is pervasively transcribed, transcription by itself is not enough evidence to support function. Newer technologies, such as parallel analysis of RNA structure (Kertesz et al., 2010) and fragmentation sequencing (Underwood et al., 2010), that focus on the structural properties of RNA may provide more clues to the extent of functionality of ncRNAs.

Non-coding RNA	Typical size (bp)	Putative functions
Transcription initiation RNA	17-18	Transcriptional regulation
Micro-RNA	20-24	Silencing of targeted messenger RNA
DNA damage RNA	22-23	Establishing the DNA damage response
Promoter-associated short RNA	22-200	Unknown
Piwi-interacting RNA	24-32	Silencing of transposable element
Enhancer RNA	50-2000	Transcriptional regulation
Transfer RNA	73-94	Translation of messenger RNA
Long intergenic non-coding RNA	>200	Chromatin modification
Ribosomal RNA	1,900 and 5,000	Protein synthesis
Competing endogenous RNA	Undefined	Micro-RNA sponge

Table 1.2: A list of various non-coding RNAs, their size profiles, and putative functions.

1.6 Repetitive mammalian genomes

The discovery that cells contained a large fraction of repetitive DNA was made by measuring the re-association rates of DNA strands after denaturation (Britten and Kohne, 1968). The characterisation of repetitive elements (REs) was possible with the release of the mouse (Waterston et al., 2002) and human (Lander et al., 2001, Venter et al., 2001) genome sequences, which showed that these genomes are indeed largely made up of REs. The two major groups of REs are tandem repeats, which include different classes of satellite repeats, and interspersed repeats, which are mostly made up of transposable elements (TEs) (Jurka, 1998). Within TEs are two main classes: Class I TEs or retrotransposons, which are DNA elements that are transcribed into RNA, reverse transcribed back to DNA, and transposed to a new location in the genome (a copy-and-paste mechanism), and Class II TEs or DNA transposons, which simply excise their DNA sequence from one location to another via transposase enzymes (a cut-and-paste mechanism). As retrotransposons are able to produce a copy of themselves before propagation, they are more numerous than DNA transposons. The retrotranspon known as the Alu element, has an estimated copy number of more than one million, making them the most abundant RE in the human genome (Lander et al., 2001).

There are various methods for identifying REs in genomes, which can be broadly categorised into *de novo*, homology, structure, and comparative genomic based methods (Bergman and Quesneville, 2007). For the initial mouse and human genome sequencing projects, REs were catalogued using a popular software called RepeatMasker, which identifies REs by using homology-based methods to search against a database of consensus repeats (Tarailo-Graovac and Chen, 2009), such as the Repbase Update database (Jurka et al., 2005). One of the main drawbacks of identifying REs in this manner is the reliance on sequence homology and a single consensus sequence, resulting in missing REs with an extensive number of mutations. Recently, RepeatMasker has incorporated the use of profile Hidden Markov Models to annotate REs (Wheeler et al., 2013); profile methods use an alignment of multiple representative sequences rather than a single consensus and are more sensitive than single sequence searches.

However, REs not contained within databases may still be missed and *de novo* methods may be the key to identifying these repeats. It has been proposed that up to two-thirds of the human genome may be made up of repetitive elements based on a *de novo* identification method (de Koning et al., 2011).

1.6.1 Junk DNA

Historically, TEs have been labelled as purely selfish elements that have no function or provide no selective advantage to an organism (Doolittle and Sapienza, 1980, Orgel and Crick, 1980) and were considered as junk DNA. The term “junk DNA”, was popularised by Susumu Ohno (Ohno, 1972), who used it to describe pseudogenes, which are gene copies that have no known biological function. In its modern day usage, “junk DNA” is used to describe DNA sequence that does not play a functional role in an organism. The question of how much of the human genome is functional was also addressed by Susumu Ohno, who used a fixed mutation rate (each locus has a 10^{-5} probability of sustaining a deleterious mutation) to estimate the number of functional loci (Ohno, 1972). Given this mutation rate, he predicted that the human genome could not have more than 30,000 loci under selection, as this would guarantee a progressive decline in genetic fitness, leading to mutational meltdown (Palazzo and Gregory, 2014). In stark contrast to the estimation made by Susumu Ohno, the ENCODE project reported that 80% of the human genome has a biochemical function (Bernstein et al., 2012), to which junk DNA was immediately dismissed (Pennisi, 2012). This lead to several critiques (Graur et al., 2013, Doolittle, 2013, Eddy, 2012), which all raised the issue of whether biochemical activity is enough to assert function.

One peculiar observation among eukaryotic genome sizes, known as the C-value enigma, is the lack of correlation between genome sizes and organismal complexity (Gregory, 2001). The genome size variation among eukaryotes can be partially explained by the presence or absence of TEs (Kidwell, 2002), which raises the question of whether or not these sequences are necessary or simply junk. To answer this question, the *Fugu rubripes* genome was sequenced to provide a useful reference for annotating functional elements in the human genome (Aparicio et al., 2002). The fugu has one of the smallest vertebrate genomes; at 390 Mb less than 10% of the genome is made up of REs, compared to 50% in the human genome (Figure 1.10). An even more extreme example, is the genome of the carnivorous bladderwort plant, *Utricularia gibba*, which is 82 Mb in size and is almost devoid of REs (Ibarra-Laclette et al., 2013). At least in these two organisms, their genomes suggest that “junk DNA” is not essential.

1.6.2 Impact of transposable elements on genomes

Genome evolution has been largely affected by TEs, which have the ability to move around within genomes. The activity of TEs have led to insertion mutations and genomic instability, but have also contributed to genetic innovation (Cordaux and Batzer, 2009). Despite the dismissal that TEs are purely selfish and are non-essential elements, the possibility that some TEs may become useful was speculated:

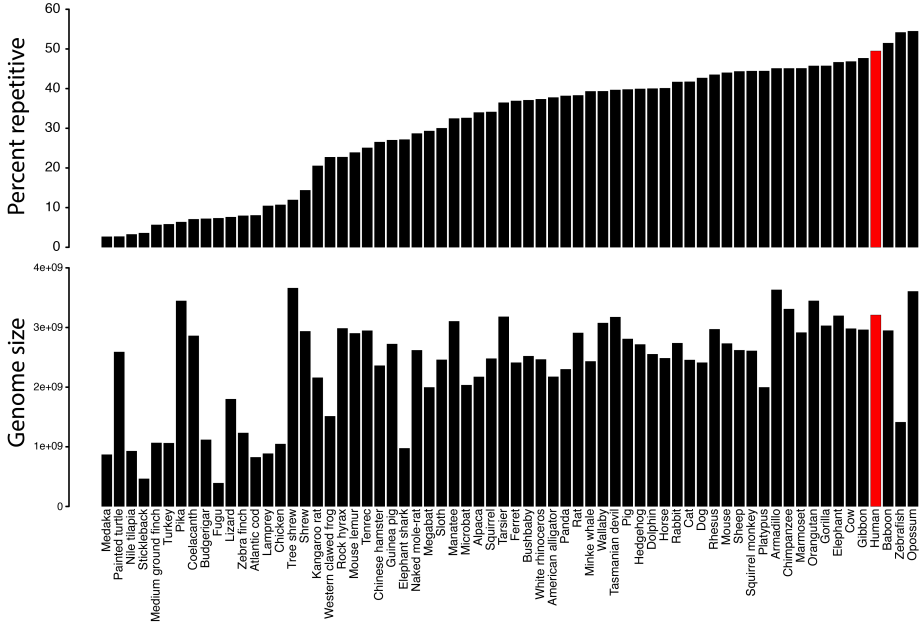


Figure 1.10: The total coverage, in percentage, of repetitive elements in 66 vertebrate genomes as annotated by RepeatMasker and their respective genome sizes in base pairs; the human genome is shown in red (Tang, 2014). Image used under the terms and agreement of the CC-BY license.

“It would be surprising if the host genome did not occasionally find some use for particular selfish DNA sequences, especially if there were many different sequences widely distributed over the chromosomes. One obvious use ... would be for control purposes at one level or another. This seems more than plausible.”

— Orgel and Crick 1980

While the estimated number of active TEs in the human genome is less than 0.05% (Mills et al., 2007), it is clear that TEs have impacted the evolution of genomes. There is increasing evidence that TEs have served as a source for evolutionary innovation by contributing to the evolution of regulatory networks (Feschotte, 2008), influenced alternative splicing (Lev-Maor et al., 2008), drove the evolution of lncRNAs (Kapusta et al., 2013), and provided alternative promoters for genes (Cohen et al., 2009). These examples illustrate the process of exaptation, where a character (the TE) becomes co-opted for a new function that it was not originally functional for (Gould and Vrba, 1982). As speculated by Orgel and Crick, there may be many other examples of TE exaptation, however, large-scale analysis of TE expression have been limited. This was due to cross-hybridisation problems with repetitive sequences in microarrays and the short read nature of current high-throughput sequencers.

In one of the first genome-wide profiling studies of TE expression, it was revealed that a large number of transcriptional events initiate within TEs in a tissue specific manner (Faulkner et al., 2009). Many of these TSSs were validated experimentally to show that TEs served as alternative promoters. In order to deal with the multi-mapping nature of reads corresponding to TEs, a

probabilistic method called multi-map rescue was implemented (Faulkner et al., 2008), which allowed reads to be assigned probabilistically based on the nearby region. Another genome-wide study examining the methylation patterns of TEs revealed tissue-specific methylation patterns (Xie et al., 2013). In this study, the authors developed the Repeat Analysis Pipeline (RAP), to deal with ambiguously mapped reads, in a manner that aggregates reads to families of repeats (Day et al., 2010). Both of these studies illustrate the importance of developing specific methodologies for analysing TEs and that TEs have been important in regulating the expression of genes.

1.7 Bioinformatics and genomics

Modern day high-throughput sequencers generate a large amount of data and dedicated informatics tools for storing, managing, and the analysis of such data sets are absolutely necessary. Bioinformatics can be thought of as a subset of informatics that deals with biological data, though historically it was defined as “the study of informatic processes in biotic systems” (Hogeweg, 2011). The HGP was one of the first large scale international research efforts, which demonstrated how bioinformatics was crucial towards the successful completion of the project (Stein, 1996). Furthermore, the HGP also set the stage for data sharing by establishing important principles, known collectively as the “Bermuda Principles”, that promoted the rapid and public sharing of human genome information. These set of commitments left a lasting legacy in large genomic science projects such as The International HapMap Project, ENCODE and modENCODE, and The Cancer Genome Atlas, where data are made freely available prior to publication (Contreras, 2011). By opening such resources, researchers are able to integrate and leverage these datasets for generating testable hypotheses.

While many of the foundations in bioinformatics were related to molecular evolution and population genetics, the availability of complete genome sequences has opened up an entire research discipline called genomics. The field of genomics is also closely tied with bioinformatics, as genomics studies typically deals with large amounts of data, corresponding to features of genomes. There are several sub-branches within genomics; the field of functional genomics focuses on the dynamic aspects of genomes, such as transcription, interactions between proteins and genomic regions, and DNA methylation patterns. Functional genomics, as the name suggests, attempts to discover and establish function to elements in the genome and usually employing the use of high-throughput methods for genome-wide screening.

1.7.1 High-throughput sequencing data

The FASTQ format was formally defined in 2010 (Cock et al., 2010) and has become the *de facto* format for storing raw high-throughput sequencing data. FASTQ is similar to the FASTA format but with the addition of quality scores, known as the Phred quality score, for each sequenced nucleotide and is usually the starting point of bioinformatic pipelines. Typically, quality control (QC) steps are carried out next to remove potential artefacts and low quality reads; one such tool known as TagDust (Lassmann et al., 2009), removes reads

that match sequences used during the library preparation, such as primer and adaptor sequences. Other QC steps include removing reads containing undetermined bases, as they indicate poor overall read quality; for sequencers that output reads of different lengths, reads outside the main length distribution are removed; quantifying highly over-represented 10-mers can also be implemented as a QC step (Lassmann et al., 2011), to identify potential artefactual sequences.

In order to put sequencing reads into context, reads are mapped onto their corresponding reference genome; various tools are available for aligning high-throughput sequencing reads. Traditional tools such as BLAST (Altschul et al., 1990) and BLAT (Kent, 2002) are unable to cope with the large quantity and short length of reads from high-throughput sequencers. One popular short-read alignment tool, BWA (Li and Durbin, 2009), implements the Burrows–Wheeler transform to deal with millions to billions of short reads. The Burrows–Wheeler transform allows a large mammalian genome, for example human, to be indexed and stored efficiently into memory (Trapnell and Salzberg, 2009). The Sequence Alignment/Map (SAM) format (Li et al., 2009a) is the standard file format for storing sequence alignments and contains all the information for reconstructing an alignment. In addition the SAM format contains information on where a read maps on the genome, the quality of the mapping, and depending on the alignment program, other mapping statistics. The open source program SAMTools (Li et al., 2009b), provides various utilities for the processing and analysis of alignments stored in the SAM format. In order to save disk space, SAM files are typically stored as BAM files, which are simply their binary equivalent. Recent developments have introduced a newer format known as CRAM, based on a newer compression method (Hsi-Yang Fritz et al., 2011), which further compresses BAM files but are still processable using SAMTools.

The BED format is another standard file format used for storing the location of a set of features (or even sequencing reads) with respect to a reference genome and has been popularised by the UCSC Genome Browser (Kent et al., 2002). Due to the popularity of the BED format, a suite of tools released as BEDTools (Quinlan and Hall, 2010), provides various routines for comparing genomic features stored in BED format. A common task in processing RNA-Seq data involves intersecting mapped reads to known genomic features, such as genes, to associate a read to a gene and thereby quantifying its expression. In addition to this, the proximity of elements on a chromosome may indicate potential functional interactions, thus reads may be annotated with respect to the physical distance, i.e. spatially, to genomic features. For example, promoters are usually upstream and nearby the genes that it initiates transcription for, thus CAGE reads are associated with nearby gene models in this manner.

1.7.2 Analysing expression datasets

Expression data sets are typically represented as matrices; for example, if we let A be an $m \times n$ matrix, where a_{ij} are elements of A , then the i^{th} row would represent the transcriptional response of the i^{th} transcript and the j^{th} column would represent the expression profile of the j^{th} assay:

$$A = \begin{bmatrix} a_{11} & \cdots & a_{1j} & \cdots & a_{1n} \\ \cdot & & \cdot & & \cdot \\ a_{i1} & \cdots & a_{ij} & \cdots & a_{in} \\ \cdot & & \cdot & & \cdot \\ a_{m1} & \cdots & a_{mj} & \cdots & a_{mn} \end{bmatrix}$$

Typically, two or more groups of assays are produced, such as a set of control experiments versus a set of treated experiments, and the aim is to find differentially expressed transcripts between the two conditions. Data normalisation is required prior to comparing assays to ensure that experimental factors (not including the experimental treatment) that cause differences are accounted for. For example, a library that has been sequenced twice as much as another library will have most of its transcript as seemingly expressed twice as much. One way to account for this is to normalise reads by counts or tags per million (TPM); to normalise by TPM the i^{th} gene in the j^{th} assay:

$$TPM_{a_{ij}} = \frac{a_{ij} \times 1000000}{\sum_{i=1}^m a_{mj}}$$

Other methods include normalising the expression by the length of a transcript, known as reads per kilobase of transcript per million mapped reads or fragments per kilobase of transcript per million mapped reads, for RNA-Seq experiments where reads are generated throughout the length of the transcript, quantile normalization, which is a technique for making two distributions identical in statistical properties (Bolstad et al., 2003), and trimmed mean of M values (TMM), which is a normalisation method that takes into account differences in the RNA population from different samples by scaling the expression (Robinson and Oshlack, 2010).

After the appropriate normalisation methods have been carried out, the testing of differential expression is performed by comparing the amount of variation between groups against the amount of variation within groups for a particular transcript, which is similar to carrying out a t -test or analysis of variance (ANOVA). However, the simple assumptions of these tests are not met due to the heteroscedastic and non-normal distribution properties of high-throughput sequencing data. RNA-Seq expression is measured by digital counts of reads, meaning that expression levels are discrete, and the variance is modelled using discrete probability distributions. In a pioneering study examining the reproducibility of RNA-Seq, it was noted that the variation between technical replicates was close to the shot noise limit (Marioni et al., 2008). Thus it was suggested that the Poisson model was sufficient in modelling the variance and used for testing differential expression. However, it was demonstrated that the Poisson model underestimated the effects of biological variability, i.e. the variation between two different biological samples is greater than Poisson variation (Anders and Huber, 2010). This can be accounted for by modelling variance under a negative binomial model, which has been implemented for differential expression analysis in the edgeR package (Robinson et al., 2010) from Bioconductor (Gentleman et al., 2004).

The correlation of transcriptional responses or expression profiles can be calculated to identify transcripts expressed in a similar manner or assays with a

similar profile, respectively. Correlation measures such as Pearson’s product-moment correlation coefficient or Spearman’s rank correlation coefficient are typically used and can be used as a measure of co-expression, i.e. transcripts with a similar transcriptional response are assumed to be co-expressed. Other measures of similarity or rather dissimilarity include metrics such as the Euclidean, maximum, Manhattan, Canberra, Jaccard, and Minkowski distances. Hierarchical clustering is usually performed in an agglomerative manner to reveal the topology of distance matrices and visualised using dendograms to revealing the most similar transcripts or assays. The visualisation of expression datasets include heatmaps, which transforms the expression matrix into colours representing the relative expression strength and are commonly arranged according to the hierarchical clustering structure (Eisen et al., 1998). Graphs can also be used to represent associations of transcripts or assays, which can leverage methodologies developed in graph theory.

Expression datasets are usually large and therefore subjected to the multiple testing problem, whereby significant p-values are observed due to the large number of statistical inferences that are carried out. Several techniques are used to account for this, such as the Bonferroni correction or false discovery rate (FDR) control (Benjamini and Hochberg, 1995) and these techniques generally require a higher p-value significance threshold to compensate for the number of inferences made. A FDR of 10% means that it is expected that 10% of our statistical inferences are false positives and the FDR is the p-value at which to draw a threshold. It is important to account for multiple testing when performing numerous statistical tests, which is common when analysing high-throughput expression datasets.

Chapter 2

Template switching artefacts

In this work, we studied the transcriptional landscape in whole blood using a technology called nano Cap Analysis Gene Expression (nanoCAGE). While it was expected that the variability between samples would be high due to the heterogeneous nature of whole blood, unexpectedly, samples prepared with the same or similar barcodes had very similar expression profiles regardless of biological origin. This affected differential expression analyses whereby the estimation of variability was increased due to biological replicates having very different expression profiles. In order to adjust for the barcode bias, we identified template-switching artefacts that caused the bias, and developed a bioinformatic solution for removing these artefacts and improved the nanoCAGE protocol to mitigate the barcode bias. This work laid the groundwork for analysing transcriptome profiling using high-throughput sequencing, by understanding how technical artefacts and biases are able to form and affect downstream analyses.

Suppression of artifacts and barcode bias in high-throughput transcriptome analyses utilizing template switching

Dave T. P. Tang¹, Charles Plessy¹, Md Salimullah¹, Ana Maria Suzuki¹, Raffaella Calligaris², Stefano Gustincich² and Piero Carninci^{1,*}

¹Omics Science Center, RIKEN Yokohama Institute, 1-7-22 Suehiro-cho, Tsurumi-ku, Yokohama, Kanagawa 230-0045, Japan and ²Sector of Neurobiology, International School for Advanced Studies (SISSA), via Bonomea 265, 34134 Trieste, Italy

Received March 13, 2012; Revised September 27, 2012; Accepted October 23, 2012

ABSTRACT

Template switching (TS) has been an inherent mechanism of reverse transcriptase, which has been exploited in several transcriptome analysis methods, such as CAGE, RNA-Seq and short RNA sequencing. TS is an attractive option, given the simplicity of the protocol, which does not require an adaptor mediated step and thus minimizes sample loss. As such, it has been used in several studies that deal with limited amounts of RNA, such as in single cell studies. Additionally, TS has also been used to introduce DNA barcodes or indexes into different samples, cells or molecules. This labeling allows one to pool several samples into one sequencing flow cell, increasing the data throughput of sequencing and takes advantage of the increasing throughput of current sequences. Here, we report TS artifacts that form owing to a process called strand invasion. Due to the way in which barcodes/indexes are introduced by TS, strand invasion becomes more problematic by introducing unsystematic biases. We describe a strategy that eliminates these artifacts *in silico* and propose an experimental solution that suppresses biases from TS.

INTRODUCTION

Reverse transcriptase (RT) has been widely used for the construction of cDNA libraries since its discovery (1,2) and has been subsequently used for gene expression studies. One intrinsic property of RT is that once it has reached the 5' end of a RNA molecule, the 7-methylguanosine at the cap site is reverse transcribed to cytosine residues (3). This activity at the cap site has

also been previously demonstrated on RNAs with an artificial adenosine cap, which was reverse-transcribed to thymidine (4). In addition to this mechanism, RT also exhibits terminal transferase activity that allows the addition of non-templated nucleotides (predominantly cytidines) once it reaches the 5' end of a RNA molecule, especially in the presence of manganese (5). Combined, these two mechanisms form a cytosine overhang at the 3' end of the cDNA after reverse transcription and serves as a useful marker for the 5' site of the RNA. These properties have been taken advantage of in the construction of full-length cDNA libraries (6). More specifically, the library construction method uses oligonucleotides incorporating a stretch of consecutive ribo-guanosine nucleotides, r(G)₃, at the 3' end of the first strand cDNA that allows for the hybridization of the oligonucleotide with the cytosine overhang. Once hybridized, the RT then switches templates and starts polymerizing the oligonucleotide, thereby incorporating the oligonucleotide sequence with the cDNA sequence. This process is known as the template-switching (TS) mechanism.

Following original cDNA cloning protocols (6,7), several high-throughput transcriptome analyses protocols have incorporated the TS mechanism (8–12). The TS oligonucleotide used for the hybridization to the cytosine overhang is further used for incorporating priming sites for downstream steps in the respective protocols. Furthermore, in the experiments conducted by Plessy *et al.* (9) and Islam *et al.* (10), the TS oligonucleotide was used to incorporate DNA barcode sequences (also known as DNA indexes) into its cDNA libraries, allowing for pooled or multiplexed reactions. By including a set of known sequences (i.e. barcodes) directly upstream of the r(G)₃ in the TS oligonucleotide, these sequences become identifiers for different samples. The pooling of several samples into a single sequencing reaction is a common strategy towards minimizing costs and labor (13) and increases the data throughput.

*To whom correspondence should be addressed. Tel: +81 45 503 9222; Fax: +81 45 503 9216; Email: carninci@riken.jp

Given the constant increase of number of reads per sequencer run, techniques for multiplexing libraries are flourishing. For example, the current protocol of the HiSeq 2000 sequencer can produce up to 3 billion single reads that pass filtering on a single flow cell run (http://www.illumina.com/systems/hiseq_systems/hiseq_2000_1000/performance_specifications.ilmn). Methods that measure transcript expression levels by their 5'-end such as STRT (14), CAGE (15) or nanoCAGE (16) have a reduced complexity compared with RNA-Seq, and therefore take a particular advantage of multiplexing. In addition to TS, there are ligation- and polymerase chain reaction (PCR)-based methods that have been used for introducing barcodes into samples for multiplexed experiments. In single-read libraries using restriction enzymes to cleave sequence tags, the barcode is often added by ligation at the 5' or 3' end of the construct, like for CAGE (15), the cleaved version of nanoCAGE (9), SAGE protocols such as HT-SuperSAGE (17) or small RNA libraries (18). However, studies have demonstrated that ligation-based methods are heavily biased due to RNA ligases having sequence-specific biases (19,20). One strategy used for dealing with ligation-based biases has been to standardize the sequence at the end of the RNA adaptor that will be ligated (18). Another proposed strategy was to use a pool of RNA adaptors (20); however, Alon *et al.* (19) have further suggested that barcodes should be introduced via PCR-based methods, such as Illumina's industry standard known as TruSeq. TruSeq uses 6-nt barcodes, which are detected as a separate step after sequencing the forward read or its mate pair. Read indexes are primed with a separate oligonucleotide, which gives a lot of flexibility in their placement in the 5' and 3' linkers. The designers of TruSeq protocols took this opportunity to place the index far from the reaction sites, usually in the tail of the primers. However, the indexes are introduced at a late step in the reaction, as there are no universal primers that would amplify the libraries and keep the indexes at the same time. As a consequence, it does not allow the pooling of the samples at early preparation steps, and for this reason, strategies where barcodes can be introduced as early as possible, such as via TS or ligation-based methods, are still preferred in situations that strongly benefit in terms of cost or logistics from early pooling. The question of which multiplexing approach to take is highly dependent on the nature of the research. For example, in a study by Kivioja *et al.* (21), they describe a method for introducing unique molecular identifiers via TS for quantifying transcript numbers. These identifiers are random bases in the TS oligonucleotides and function like random barcodes that index RNAs molecules instead of indexing samples. Double-stranded ligation and PCR are ruled out as alternatives for introducing indexes. In the case of ligation, it would be too difficult to produce the double-stranded adaptors because random sequences will not be reverse complementary. Indexing via PCR would be too late, as the purpose of these identifiers is to detect PCR duplicates. Lastly, Kivioja *et al.* (21) have envisioned that unique molecular identifiers can be combined with sample barcodes.

One of the main advantages of using TS is the lack of purification and adaptor ligation steps, which eliminates ligation-introduced biases and also minimizes the loss of material. This has made TS highly suitable in studies working with a limited amount of RNA (9,10,12,22,23). Although TS is an inherent property of RTs, and is therefore only implemented in transcriptome studies, we may see an increase in the use of TS due to the growing interest in single cell transcriptomics (24). There are, however, intrinsic problems associated with the TS mechanism, such as the concatenation of TS oligonucleotides due to cycles of terminal transferase activity and TS oligonucleotide hybridization (25). Another issue that we address here is the interruption of first strand synthesis via strand invasion. Although TS is most efficient when RT has reached the end of the RNA template, the TS oligonucleotide may hybridize to the first strand cDNA due to sequence complementarity before the RT has finished polymerizing. This creates first strand cDNAs that are artificially shorter than the RNA due to the incomplete reverse transcription process. Furthermore, although this is usually a systematic bias, this becomes more problematic in protocols using varied TS oligonucleotides for barcoding purposes, as the strand invasion process is dependent on the oligonucleotide sequence. We study in detail the artifacts and biases created by strand invasion in a protocol using the TS mechanism and demonstrate how it is possible to remove such artifacts *in silico*. Lastly, we propose possible experimental strategies that may help reduce such artifacts and biases in protocols that use TS, and demonstrate it with the nanoCAGE protocol.

MATERIALS AND METHODS

NanoCAGE libraries were prepared from total RNA isolated from human whole blood samples (200 ng per sample) and rat whole body RNA (500 ng per sample) according to a previously published protocol (16), and sequenced using the Illumina GAIIX instrument on five (four for blood samples and one for rat samples) sequencing lanes. These quantities of starting material are well above the recommended quantity of 50 ng, and we therefore expected that the difference would not cause one set of samples to underperform compared with the other set. Blood samples were collected in PAXgene blood RNA tubes (PreAnalytix) following manufacturer's instructions from seven donors (four male and three females) of the same ethnicity with an average age of 67 years and a standard deviation of 6.6 years and were labeled as 14–20P. Blood samples were collected following a fasting period and at the same hour of the day to help reduce variability. The rat whole body RNA were a generous donation from Dr. Alistair Forrest and are commercially available from BioChain (<http://www.biocat.com/products/R4434567-1-BC>).

We processed all five lanes of sequencing from the nanoCAGE libraries as follows. Using the FASTX-Toolkit (http://hannonlab.cshl.edu/fastx_toolkit/), we extracted raw tags and distributed them into their respective samples based on their barcode sequence. Raw reads that

did not match a barcode sequence were discarded mainly owing to poor or ambiguous base calling. Barcode sequences (and the common spacer sequence in the rat libraries) and the leading guanosines were trimmed off from the sequenced read. Next, we filtered out artifactual reads using TagDust (26), a program that filters out reads resembling the primer, linker and adaptor sequences used during library construction, using a false discovery rate of 0.01. Lastly, reads mapping to the ribosomal sequences U13369.1, NR_003285.2, NR_003286.2 and NR_003287.2 with ≤ 2 mismatches were considered to be ribosomal sequences and removed (Supplementary Table S1). After all pre-processing stages, reads were mapped to the hg19 or rn4 genome depending on the sample using BWA (27) with a mismatch threshold of 2. Using SAMTools (28), we selected reads with a mapping quality (MAPQ) of 10 (90% accuracy) or better.

Identifying barcode-biased tags in the whole blood libraries

For the 21 human whole blood libraries, we used 14 barcodes, consisting of 12 unique barcode sequences (ACATAC, AGTACG, ATCACG, CACGAT, CGATA C, GAGACG, GCTATA, GCTCAG, GTAGTG, GTAT AC, TATGTG and TCGACG) where the mean Hamming distance between all pairwise barcodes is 4.32. For each sample, three libraries were made using two barcodes, i.e. one technical replicate was made with one barcode sequence, and the other two technical replicates made with the other barcode sequence (Table 1).

Next, using a present/absent criterion, we identified reads among technical replicates that were only present when using one barcode and absent when the other barcode is used. We used a threshold of ≥ 21 raw reads for our present criteria (Supplementary Table S4). Marioni *et al.* (29) reported that if technical replicates are sequenced, the read counts for a particular feature should vary according to the Poisson distribution. Thus, it is unlikely that our selected reads are a consequence of natural variation but rather are attained by the use of a different barcode sequence. Sequence logos (30) were created by extracting the nine nucleotides upstream of these mapped reads, and the sequence enrichment was calculated using unique upstream sequences.

Filtering strand invasion artifacts

From our selection of barcode-biased reads, we observed that the upstream region of these reads showed sequence complementary to the tail of the TS oligonucleotide (Figure 2), which is a consequence of strand invasion. This served as a marker for strand invasion artifacts, which was subsequently used as our strategy for their removal. Thus, once reads were mapped to a reference, the nine nucleotides immediately upstream were extracted, and using a global alignment approach (31), they were aligned to the last nine nucleotides of the TS oligonucleotide used for construction of that particular library. The edit distance was used as a metric for the alignment, and a single mismatch or gap constituted an edit distance of one. A perfect alignment would thus have zero edits.

Table 1. A summary of the biological and technical replicates used in this study, along with the barcodes and the number of reads that were mapped at a MAPQ of ≥ 10

Samples	Technical replicate	Barcodes	Number of reads mapping at q10
Human	14P	1 GCTATA	597909
		2 CACGAT	711936
		3 CACGAT	960204
	15P	1 GTAGTG	445901
		2 CGATAC	592336
		3 CGATAC	674823
	16P	1 TATGTG	1040935
		2 GAGACG	1163416
		3 GAGACG	756476
	17P	1 ACATAC	722023
		2 GCTCAG	538660
		3 GCTCAG	695706
	18P	1 ATCACG	685146
		2 GTATAC	889014
		3 GTATAC	884897
	19P	1 CACGAT	371069
		2 TCGACG	663186
		3 TCGACG	420775
	20P	1 CGATAC	741908
		2 AGTACG	1195816
		3 AGTACG	1431334
Rat	1 ACAGAT	927429	
	2 ATCGTG	849609	
	3 CACGAT	793598	
	4 CACTGA	810155	
	5 CTGACG	863029	
	6 GAGTGA	895320	
	7 GTATAC	1005221	
	8 TCGAGC	823343	

We observed the enrichment of at least two guanosine nucleotides directly upstream of where a strand invasion artifact mapped. Thus, we imposed this criterion to our filtering strategy; reads were only considered to be artifacts if two of the three nucleotides directly upstream were guanosines. Lastly, as an indication of the edit distance threshold to use for data filtering, we filtered libraries using edit distances of zero to five and measured the Spearman's rank correlation coefficient between technical replicated libraries at each threshold. The filtering strategy was implemented using Perl, and an executable version of the script is available as supplementary data.

Specificity and sensitivity

The specificity of a method relates to the ability of identifying negative results, assessed by the number of false positives. We created a negative set, i.e. putatively non-biased reads, by selecting for the least variable reads among technical triplicates. We first normalized reads by tags per million, and selected the top 20% of least variable reads among replicates. In contrast, the sensitivity refers to the ability of identifying positive results, assessed by the number of true positives. We created a positive set, i.e. strand invasion artifacts, in the same manner that

we identified barcode-biased tags described above. With our negative and positive sets, we then applied our barcode filtering scheme described above with an edit distance of four. The specificity was calculated as the ‘number of true negatives/(number of true negatives + number of false positives)’, and the sensitivity was calculated as the ‘number of true positives/(number of true positives + number of false negatives)’.

Differential expression analysis

For the comparison of different libraries, we used a previously developed read/tag clustering method (32), as opposed to comparing individual reads. The clustering method aggregates reads that are mapped within a window of 20 nucleotides into single entity clusters; the expression of the cluster is the summation of all tags within the cluster. We conducted our differential expression analyses on tag clusters present among technical replicates using the edgeR_2.4.1 package (33) on R version 2.14.1. Within a technical triplicate set, technical replicates made with one barcode were tested against technical replicates made with the other barcode. For the comparison of the rat libraries, we arbitrarily tested the libraries made with the ACAGAT, ATCGTG, CACGAT and CACTGA barcodes against the libraries made with the CTGACG, GAGTGA, GTATAC and TCGAGC barcodes. We used an independent filtering criterion (34), selecting for tag clusters with ≥ 10 raw reads. The standard edgeR pipeline was carried out using a common dispersion approach (and tag-wise dispersion for the rat libraries) and the Benjamini and Hochberg’s (35) approach for controlling the false discovery rate. Tag clusters with an adjusted *P*-value of ≤ 0.01 were defined as differentially expressed.

RNA-Seq data sets

We processed two independently produced RNA-Seq data sets, made using two different protocols (10,36). Briefly, Islam *et al.* analysed the single cell transcriptomes of mouse embryonic fibroblasts and embryonic stem cells. The Islam *et al.* RNA-Seq libraries, which was made using TS and in a manner very similar to nanoCAGE, was downloaded directly from the author’s website and was processed in the same manner as our nanoCAGE libraries owing to the similarity between the protocols. Briefly, Guttman *et al.* produced RNA-Seq libraries from mouse embryonic stem cells, neuronal precursor cells and lung fibroblasts by mRNA fragmentation and random-primed reverse transcription. The Guttman *et al.* data set was downloaded from the DNA Data Bank of Japan under the accession number SRP002325, and the sequenced reads were mapped using TopHat (37) on the default settings. After all pre-processing steps, we compared the derived transcript structures between the fibroblasts libraries made by Islam *et al.* and by Guttman *et al.* In addition, we also compared different fibroblast libraries made with different barcodes in the Islam *et al.* data set.

RESULTS

Barcode specific reads in nanoCAGE libraries

Total RNA, isolated from whole blood samples derived from seven donors, was used to prepare 21 separate nanoCAGE libraries where each sample was made in triplicate (Table 1). Furthermore, libraries were prepared together to help limit batch effects. To study the effect of using different TS oligonucleotides and thus the barcode sequence, we prepared the same sample identically except for the TS oligonucleotides used; two barcodes were used per technical triplicate. As there are an odd number of replicates, two of the three replicates were prepared with one barcode and the remaining replicate prepared with the other barcode. NanoCAGE libraries were prepared following a previously published protocol (16). The 21 nanoCAGE libraries were then sequenced in multiplex using Illumina’s GAIIX instrument on four sequencing lanes.

Sequenced reads in the nanoCAGE protocol represent the site at which TS occurred (Figure 1), which represents the 5' end of a RNA molecule and thus the putative transcriptional starting site (TSS) (9). Hence, to identify artifacts, we could compare nanoCAGE reads that do not map to known promoters of transcripts, although these could represent previously uncharacterized transcripts. A more definitive approach not requiring transcript annotations is to search for intra sample differences, i.e. reads present only in one set of barcoded technical replicates. To correctly identify the corresponding transcript for a sequenced read, we selectively analysed 16 281 067 reads that could be mapped to the genome with 90% confidence (MAPQ of ≥ 10) (27). Finally, from this set, we identified 132 980 barcode specific reads, i.e. reads present only in one set of technical replicates using a particular barcode and not the other, where the variance is unlikely due to Poisson noise (see ‘Materials and Methods’ section).

From our barcode specific nanoCAGE reads, we analysed the region directly surrounding the reads. Interestingly, the upstream sequence of these barcode biased reads revealed an enrichment of nucleotides that resembled the 3' end of the TS oligonucleotide used for that library (Figure 2). The sequence logos illustrate an enrichment of guanosines at positions -1 to -3, which corresponds to the r(G)₃ tail of the TS oligonucleotide, whereby positions -4 to -9 show a varied enrichment of nucleotides that resemble the barcode used to produce the library, especially positions -4 to -6 (Figure 2). These results suggest the hybridization of the TS oligonucleotide to a complementary region on the first strand cDNA, i.e. strand invasion, and thus produces TS artifacts in a barcode dependent manner (Figure 1B). Although the r(G)₃ tail of the TS oligonucleotide preferentially binds to the cytosine overhang created by the RT (9), the increase in sequence complementarity in the 3' tail of the TS oligonucleotide may increase the hybridization of the TS oligonucleotide to the first strand cDNA (Figure 1B).

Filtering out strand invasion artifacts

Artifactual reads need to be removed before they are used for further downstream analyses (26). The TS mechanism

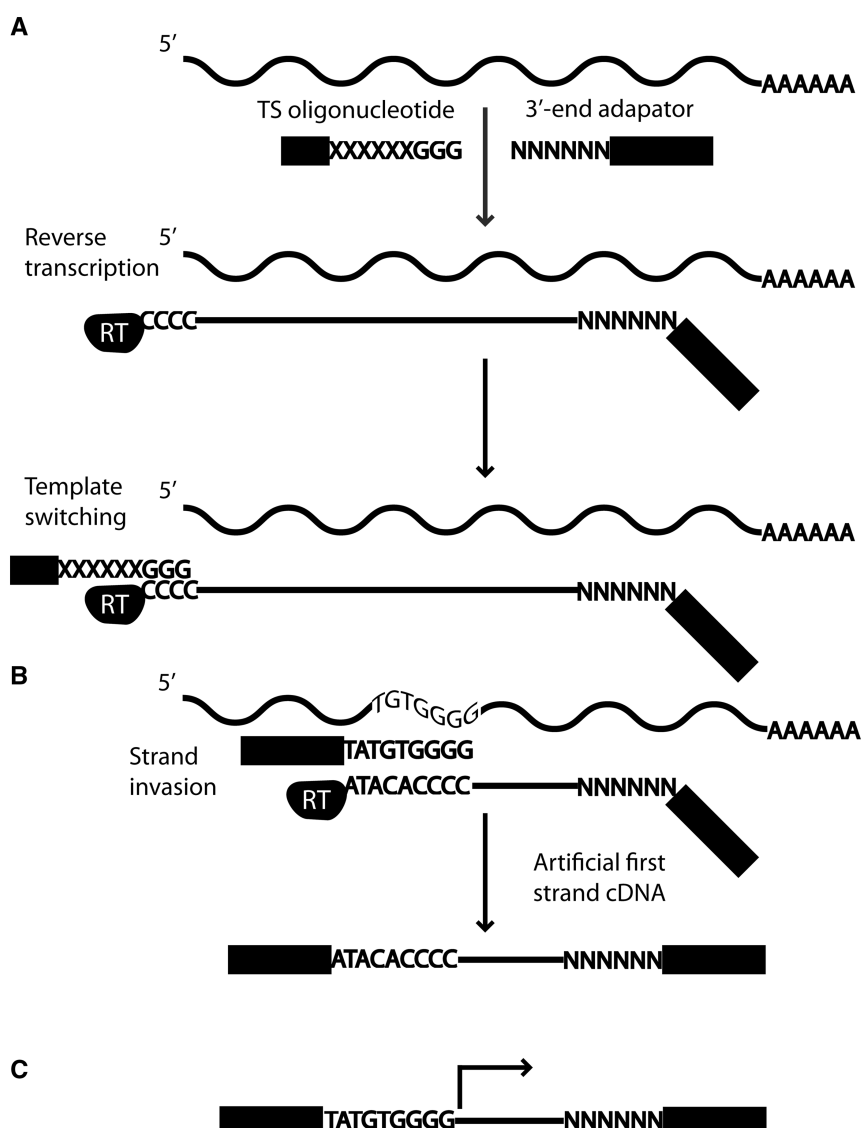


Figure 1. (A) The TS mechanism is used for first strand cDNA synthesis. First, an oligonucleotide hybridizes to the RNA molecule, and RT starts polymerizing. Once the RT reaches the 5' end of the RNA, a cytosine overhang is formed. The TS oligonucleotide containing three riboguanosines hybridizes to the cytosine overhang and the RT switches template and polymerizes the TS oligonucleotide. (B) However, during RT synthesis, if the polymerized region has sequence complementarity with the 3' tail of the TS oligonucleotide, it may invade and hybridize with the first strand cDNA. RT then switches template and polymerizes the TS oligonucleotide. However, this strand invasion process has resulted in a cDNA that is shorter than the RNA. (C) With the nanoCAGE protocol, sequencing begins just upstream of the site of TS, which includes the barcode and the riboguanosine linker sequence. The barcode and linker sequences are trimmed off during processing steps, and the final read sequence is indicated by the black arrow.

is expected to occur at the cytosine overhang created by the RT (Figure 1A); thus, the sequence immediately upstream of a nanoCAGE tag should exhibit sequence complementarity only on a random basis, although this is largely dependent on the makeup of the genome. Under these assumptions, we devised a strategy for removing strand invasion artifacts by aligning the sequence immediately upstream of reads to the 3' tail of the TS oligonucleotide. We chose to align the nine nucleotides directly upstream of a read (Figure 1C) to the last nine nucleotides of the TS oligonucleotide owing to the enrichment profiles previously observed (Figure 2).

Next, we analysed a range of sequence complementarity scores to determine the optimal threshold for classifying

reads as artifacts. First, we carried out a global alignment (31) between the sequence upstream of a read and the TS oligonucleotide tail for all libraries. We directly used the edit distance of an alignment as a measurement of the sequence complementarity, where gaps and mismatches were individually constituted as one edit; a perfect alignment would thus have zero edits. In addition, we only classified reads as artifacts if two or more of the three nucleotides directly upstream were composed mainly of guanosines (see ‘Materials and Methods’ section). Lastly, we filtered out reads on a range of edit distances, from zero to five, and found that by removing such noise, we had technical replicates that correlated better with each other (Supplementary Table S2).

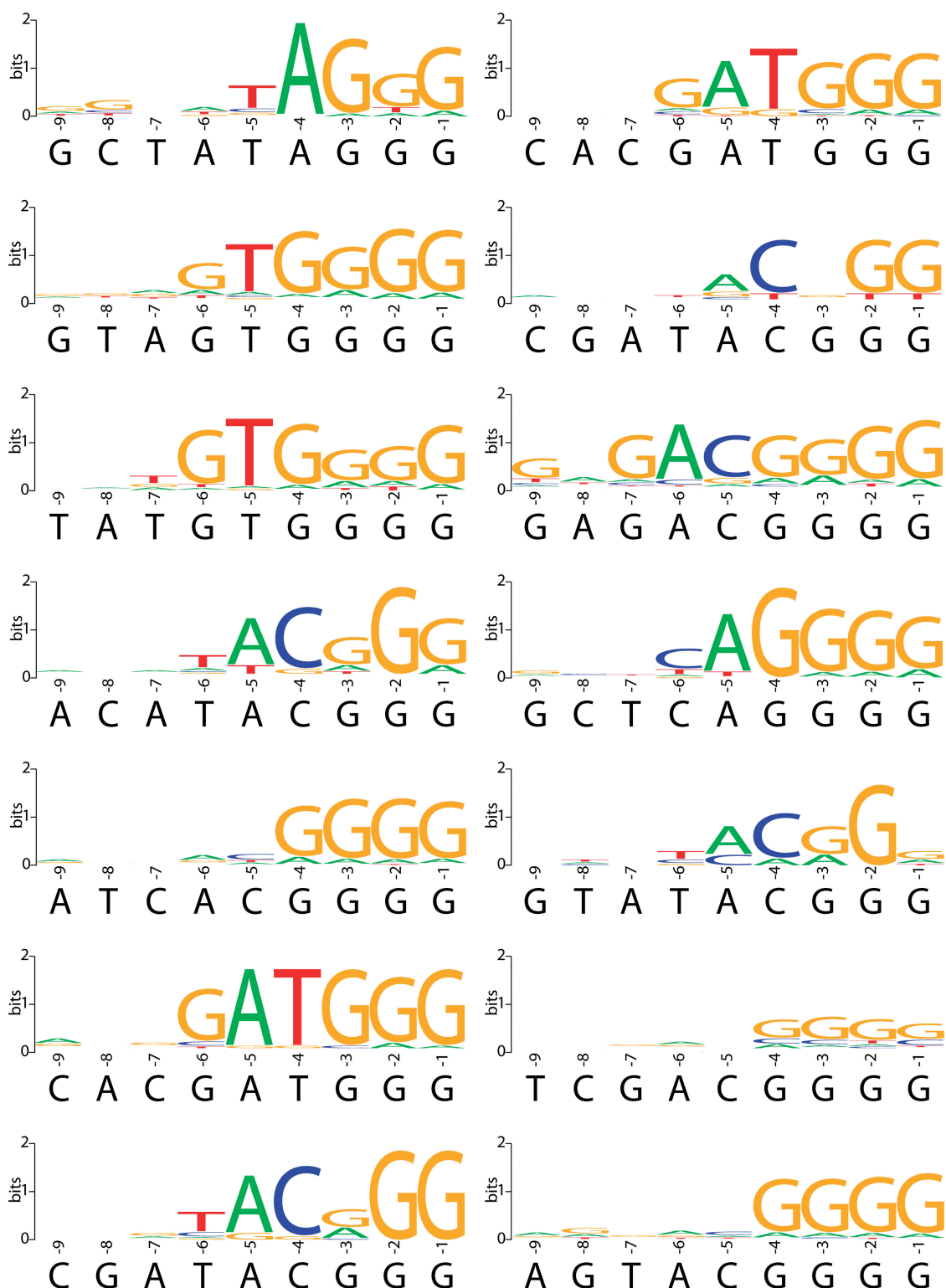


Figure 2. By preparing technical triplicates with different barcodes, we could identify reads present in a barcode specific manner, i.e. barcode-biased reads. The sequence logos were created using the sequence directly upstream of individually mapped barcode biased reads. The barcode sequence used to prepare each library and the three riboguanosines of the TS oligonucleotide are shown directly below the corresponding sequence logos. The enrichment profiles closely resemble the tailing sequence of the TS oligonucleotide used to construct that particular library.

Effects of artifact filtering on library correlation

A common metric used to determine library similarity is by correlation. We assessed the correlation of technical replicates after our filtering strategy at various thresholds. Given the nature of CAGE reads and promoters, we first clustered reads into what are known as ‘tag clusters’ (32), enabling us to measure the correlation of libraries. Tag clusters are representative of putative promoter regions whereby the number of reads mapping to these regions represents the level of expression (see ‘Materials and Methods’ section). We calculated the Spearman’s rank correlation coefficient between all technical replicates, given the skewed expression rate of blood transcripts, i.e. the distribution of transcript expression is not linear; so we used a non-parametric measure of correlation. The distribution of transcripts in blood is largely skewed by the presence of globin transcripts, which resulted in the under sequencing of other transcripts. This under sampling resulted in an increase of noise, especially for transcripts that are lowly expressed, and subsequently lower correlations between replicates. The removal of globin transcripts would not significantly affect the Spearman’s rank correlation coefficient owing to the way the correlation is calculated. For technical replicates made with different barcodes, we observed a general increase in correlation between the libraries as we relaxed the similarity threshold, i.e. increasing the edit distance (Supplementary Table S2). The increase in correlation was the direct consequence of removing library specific reads, i.e. TS artifacts. The opposite effect, a decrease in correlation after read filtering, was observed when comparing technical replicates with the same barcode (Supplementary Table S2). The correlation of technical replicates was inflated owing to TS artifacts, and the removal of these reads decreased the correlation. For the comparison of libraries with different barcodes, the majority of correlations increased until an edit distance of four. This was due to the decrease in stringency, which resulted in real signal being removed by random chance that a loose alignment could be formed between the upstream sequence and the tail sequence of the TS oligonucleotide. Although the correlations between technical replicates are considered moderate, we demonstrated that we are able to identify TS artifacts, and the removal of these artifacts resulted in higher correlations between technical replicates.

Effects of artifact filtering on differential expression detection

One of the core analyses conducted on transcriptome data is a statistical test that detects differential expression of transcripts. An observed difference is statistically significant only when the observed difference is greater than expected from random variation. Transcripts may be spuriously detected as differentially expressed owing to the introduction of experimental variations such as from using different barcodes. We tested this notion by conducting differential expression analyses using edgeR (33) on technical replicated libraries before artifact filtering, after filtering and after randomly removing reads (Figure 3). Given that our analyses were carried out on

technical replicates, we would expect to find very few tag clusters that are detected as differentially expressed. However, a fraction of tag clusters were detected as differentially expressed between technical replicates before filtering (Supplementary Table S3). In all cases, the removal of strand invasion artifacts decreased the number of differentially expressed candidates (Supplementary Table S3). Using an edit distance of four for barcode filtering, on average, we observed a roughly 10-fold decrease in the number of differentially expressed candidates. In contrast, removing random reads resulted in a slight decrease of 1.2-fold in differentially expressed candidates.

Sensitivity and specificity of artifact filtering

We have experimentally prepared our libraries in such a way that we can identify TS artifacts. Using a set of nanoCAGE reads that were identified as TS artifacts (see ‘Materials and Methods’ section), i.e. true positives, we applied our filtering strategy to measure the sensitivity of the method. Reads not detected as artifacts in this set were considered as false negative. Using an edit distance metric of four, the average sensitivity was ~94.3% across the entire data set; we could detect 125 357 of the 132 980 true positives (Supplementary Table S4).

The specificity of a method gives an estimate of the number of false positives. This measure is important for quantifying the potential amount of signal that is removed due to the random chance that the upstream region of a read resembles the 3' tail of the TS oligonucleotide. To determine a true negative set, i.e. not barcode biased, we selected reads with the lowest amount of variance between the technical replicates (see ‘Materials and Methods’ section), and if any of these reads were filtered out, they were considered false positives. Of the subset of reads we considered to be a true negative set ($n = 135\,613$), on average $6.7\% \pm 2.1$ of these reads were considered false positives (Supplementary Table S5). However, one should consider that even our true negative set may contain strand invasion artifacts, i.e. a false positive in the sense of being a true negative, and we only examined a small proportion of the total number of reads in a library; in reality, the false positive rate is likely to be much lower.

Degree of bias from different barcode sequences

Strand invasion occurs during first strand cDNA synthesis, and successful hybridization depends on the degree of sequence complementarity between the cDNA and the 3' tail of the TS oligonucleotide. Therefore, the number of TS artifacts becomes a function of the number of RNA molecules that contains sequence complementarity to the TS oligonucleotide. Barcode sequences that occur more prominently among RNA molecules would result in a higher number of TS artifacts. To test this hypothesis, we scanned the genome in a sliding window manner. Given that the last six nucleotides of the TS oligonucleotide are the most important for strand invasion (Figure 2), we tallied the number of all possible 6-mers that end in GGG (total of 64 6-mer combinations) across the human genome (hg19) on both strands. For the sake of simplicity

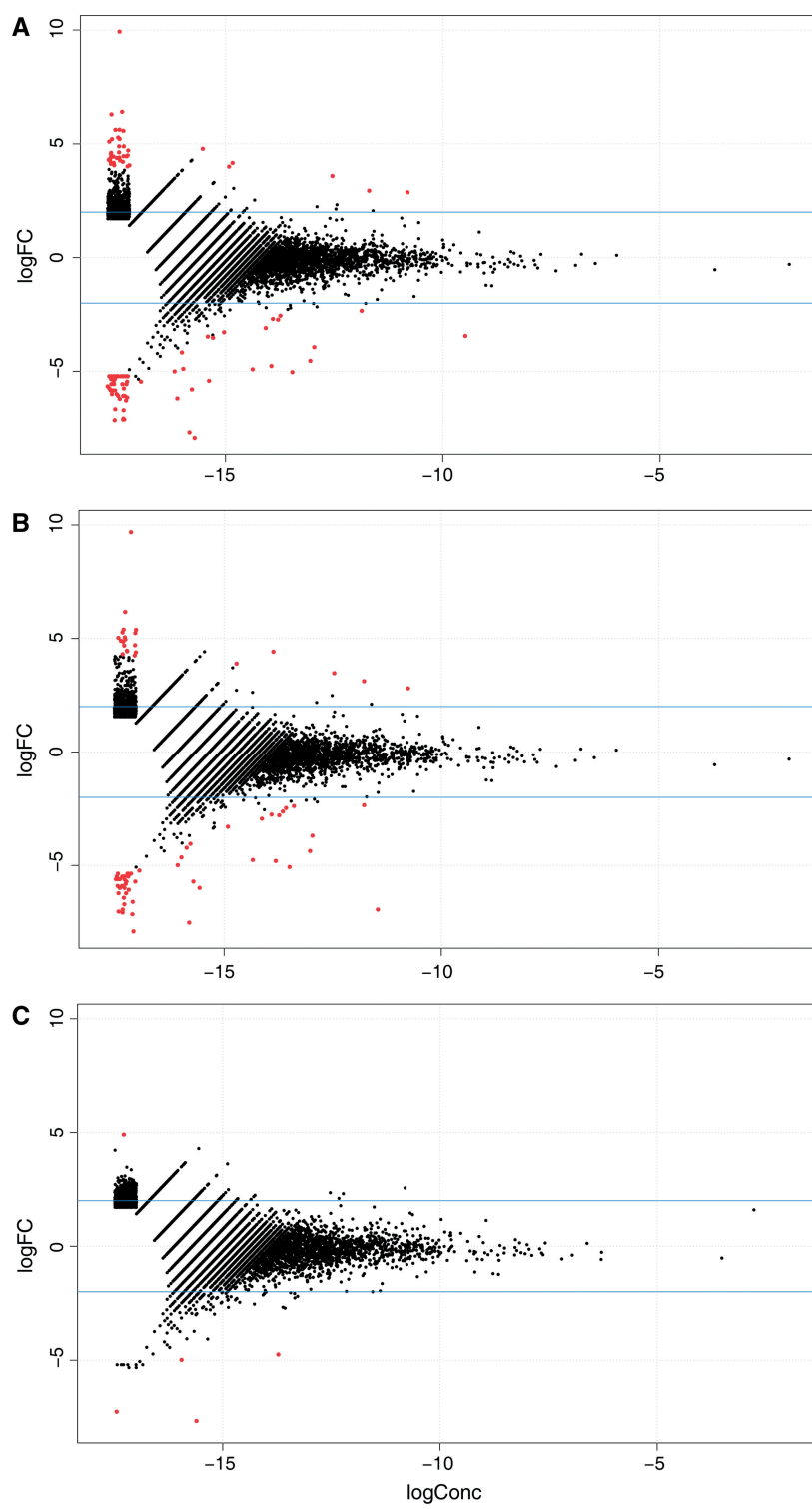


Figure 3. Differential expression analyses were carried out between technical replicates made from different barcode sequences using edgeR. The scatter plots show the log-fold change (y-axis) against the log concentration (x-axis) for tag clusters present among the 14P technical replicates. In red are tag clusters that were detected as differentially expressed at an adjusted P -value ≤ 0.01 . Three separate analyses were carried out: test for differential expression (A) before strand invasion artifacts were filtered out, (B) when random reads were removed and (C) after strand invasion artifacts were filtered out. By removing artifacts, fewer tag clusters were detected as differentially expressed compared with no filtering and removing random reads.

and owing to a lack of a complete transcriptome, we chose to tally this number across the genome as opposed to a defined transcriptome. We previously defined a set of TS artifacts by examining technical replicates made with different barcodes and used this number as an estimate of the number of TS artifacts. We then calculated the Spearman's rank correlation coefficient between the number of TS artifacts and the tallied number for the 6-mer that corresponded to the sequence at the end of the TS oligonucleotide. As expected, a positive correlation (Spearman's rho ~ 0.67) was observed (Supplementary Table S6), which supported the hypothesis that choosing a barcode sequence, which is present more often in the genome, leads to a larger number of strand invasion artifacts.

An experimental strategy for suppressing artifacts and barcode bias

Our results have suggested that first strand cDNAs with regions of sequence complementarity to the last six nucleotides of the TS oligonucleotide are potential sites for strand invasion. Given this information, intuitively it is expected that if the last six nucleotides of the TS oligonucleotide occur more frequently amongst RNA molecules, there would be a higher number of TS artifacts. We established this hypothesis that barcode sequences that are present more frequently in the genome have more strand invasion artifacts (Supplementary Table S6). So to suppress the number of artifacts, one should select barcodes less frequent in the genome. We have also observed that barcodes that end with a guanosine, thus creating a sequence tail of four guanosines in the TS oligonucleotide, have much higher number of TS artifacts (Supplementary Table S6). Furthermore, at transcriptional starting sites, libraries made with a barcode ending with a guanosine have much higher counts of certain transcripts compared with barcodes that do not end with a guanosine (Figure 4); this type of bias cannot be mitigated by our artifact filterer. To suppress this barcoding bias, it is necessary that the sequence directly upstream of the riboguanosines is standardized, a strategy similar to standardizing the adaptor sequence in ligation-based barcoding (18). Additionally, our strategy for the choice of a standard spacer is one that occurs less frequently in the genome. Thus, we can potentially suppress the extent of strand invasion and systematically remove the barcode bias effect.

To test this strategy, we redesigned the TS oligonucleotide to include a 6-nucleotide spacer (GCTATA) directly upstream of the riboguanosines. We produced eight nanoCAGE libraries using eight barcodes from rat whole body RNA, i.e. technical replicates, and sequenced them on one lane on the Illumina GAIIX platform. We processed these libraries in the same manner as our blood nanoCAGE libraries and obtained around 8 million reads in total after processing (Supplementary Table S7). Next, using the tag-clustering method previously described, we aggregated our reads and measured the pairwise correlations of each library; the average Spearman's rank correlation coefficients was ~ 0.75 (Supplementary Table S7),

a vast improvement to the blood nanoCAGE libraries. To investigate how much of the variance in the data is explained by sequencing noise, for each tags per million - normalized tag cluster, we calculated the mean and the exact 95% confidence intervals (CIs) for the mean assuming a Poisson distribution. For each tag cluster and the respective library expression, we tallied the number of times an expression value was inside the CIs; approximately 92% of the total expression values fall inside the 95% CIs. The nanoCAGE protocol is designed to work with few nanograms of total RNAs and require a relatively large number of semi-suppressive PCR cycle, which in addition to the Poisson noise, may account for points that fall outside of the 95% CIs. Semi-suppressive PCR allows the use of random primers, which can capture non-coding RNAs, but, however, shows suboptimal yields at each PCR cycles. Additionally, a second PCR reaction is needed to add sequencing adapters after the semi-suppressive PCR. In summary, although nanoCAGE can also identify non-polyA RNAs from low starting material (9), it requires two PCR cycles, which may be a source of noise.

When we applied the filtering strategy on the libraries made with the common spacer, we found that on average 4.5% \pm standard deviation of 0.12 (Supplementary table S7) of the total reads were detected as putative TS artifacts compared with an average of 11.1% \pm standard deviation of 6.65 (Supplementary Table S1) for the libraries made without the common spacer. By using a common spacer, all libraries had roughly the same number of putative artifacts, i.e. very low standard deviation, which is also lower than the number of putative artifacts detected in most libraries made without the common spacer. Although the older data set detected an average of $\sim 11\%$, the number of artifacts is highly dependent on the barcode (Supplementary Table S1), which is the reason for a much higher strand deviation. For example, by using the GCTCAG barcode without a spacer, up to $\sim 25\%$ of the reads were detected as artifacts. By using a common spacer, the biases will affect the same transcripts in the same way in different samples. This is particularly important when conducting differential expression analyses and because of this, it is not necessary to filter out putative artifacts. To test this, we performed a differential expression analysis on the common spacer libraries, and indeed none of the tag clusters were detected as significantly differentially expressed.

DISCUSSION

The TS mechanism has been exploited in full-length cDNA library construction owing to its technical simplicity (6), in transcriptome analyses due to its ability to mark the 5' end of a RNA molecule (9) and its flexibility in incorporating DNA barcodes for multiplexing (10) and for incorporating DNA fingerprints for quantifying the absolute number of molecules (21). Owing to the elimination of adaptor mediated steps, RNA material can be conserved, making TS an attractive choice when

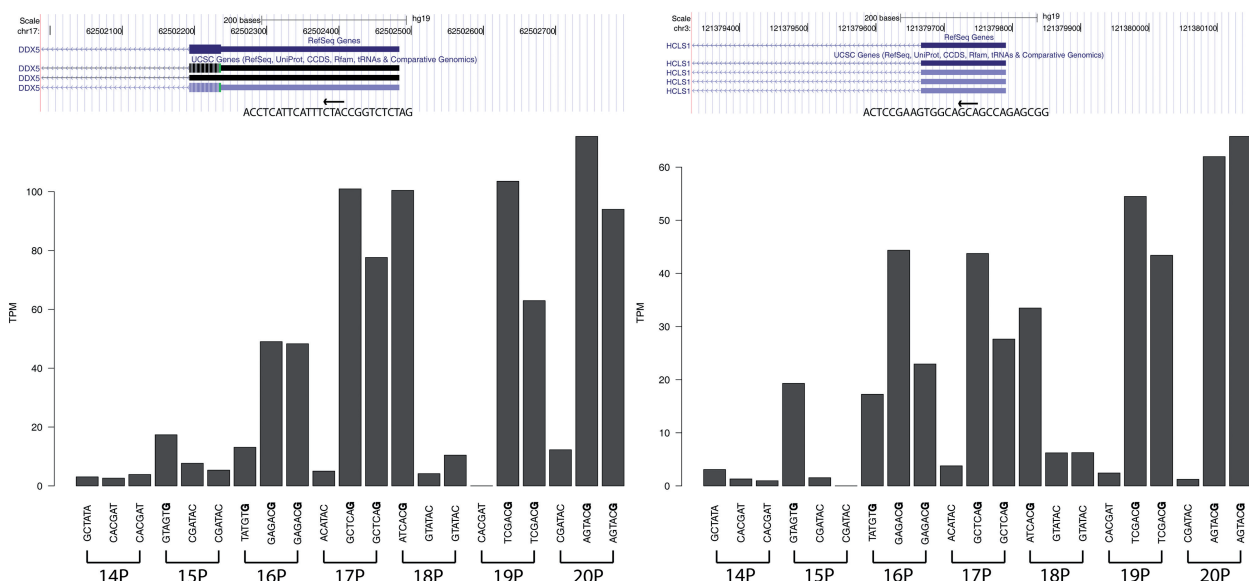


Figure 4. Barcode bias in nanoCAGE technical replicated libraries. The choice of barcode sequence can affect the read count pertaining to the transcriptional starting site. Here, we show two examples for the genes DDX5 and HCLS1, where the read count fluctuates according to the barcode sequence and not by the sequencing depth or by the library. Libraries made with barcodes ending with a guanosine (shown in bold in the bar plot) have a much higher tags per million (TPM) count than barcodes that end with other nucleotides.

working with limited amounts of sample, such as with single cell type analyses (10,12). Furthermore, the decreasing costs of DNA sequencing are driven by an increase of throughput in a constant number of sequencing lanes, which makes multiplex sequencing determinant for cost and time efficiency. Although TS has been used to incorporate barcodes during reverse transcription for multiplexing, one particular drawback of this approach is that the barcode sequences may skew the following reactions, in particular PCR, in favor of one sample. For this reason, strategies where the barcode is added at a last step are sometimes preferred, for instance in the protocols of Illumina's TruSeq product line. Nevertheless, this has the drawback that samples cannot be pooled as early as with TS, which increase the work load and cost of the experiment. In addition, because these two methods of barcoding are directed at different parts of the library constructs, they can be used together to implement combinatorial multiplexing. By combining two barcodes together, the index diversity is greatly increased, and this allows the unique labeling of all transcripts in a sample (38). This approach takes advantage of the very high throughput of current sequencers, which can also be applied to labeling several thousands of low complexity single cell libraries.

Here, we have characterized and investigated a source of bias that is inherent to TS: the production of spurious, sequence-specific reads owing to strand invasion and different hybridization rates as a consequence of choosing different barcodes. We have shown that the extent of strand invasion depends highly on the sequence of the TS oligonucleotide, especially the last six nucleotides. All oligonucleotides in the reverse transcription reactions can interrupt the first-strand cDNA synthesis by strand

invasion, and we have previously observed oligo-dT primers being template switched at the 5' of T-rich regions of the mRNAs (data not shown). This strand invasion becomes more problematic when different sets of TS oligonucleotides are used to barcode specific samples, as this subjects the samples to different degrees of bias. In these multiplexed libraries, the strand invasion artifacts will produce sample-specific signals, which will wrongly suggest correlations or in contrary mask the similarity between related samples. For example, samples using two barcodes that end in the same six nucleotides may artificially cluster together irrespective of the sample condition. Even in non-multiplexed libraries, strand invasion produce shortened cDNAs that can systematically bias expression levels and create artifacts that do not reflect the transcriptome. We compared two different RNA-Seq protocols, one using TS (and with the same multiplexing strategy as nanoCAGE) (10) and another by conventional RNA fragmentation on mouse fibroblasts and observed different coverage patterns (Supplementary Figure S1). The transcript profile observed in the TS RNA-Seq protocol is likely a consequence of strand invasion. Moreover, we have also observed different transcript profiles in biologically replicated samples that were made from different barcodes (Supplementary Figure S2). As we have demonstrated in our work, it is crucial to control strand invasion products especially with respect to introducing barcodes by TS.

It is possible to identify strand invasion products *in silico* and consequently have them removed. We have shown that by analysing the sequence upstream of where a sequenced read maps, artifactual reads could be identified with high specificity and sensitivity. Importantly, by removing such noise, replicated libraries made

using different barcodes correlated better to each other. By performing a differential expression analysis on the filtered data sets, on average, a 10-fold decrease in the number of tag clusters called as differentially expressed was observed. The removal of strand invasion artifacts, which contribute to an increased variance among samples, is crucial in differential expression analyses using digital gene expression data such as CAGE and RNA-Seq. However, it is ideal to design an experimental protocol that limits as much as possible biases that are a consequence of the barcoding strategy (19). We proposed a strategy, which we tested in the nanoCAGE method, by updating the sequence of the TS oligonucleotide by inserting a 6-nucleotide long standard spacer between the barcode and the ribo-guanosines. In addition, we chose a spacer sequence that had less potential for strand invasion. The main purpose of the common spacer is to ensure that any TS bias systematically affects all libraries in the same manner. We confirmed this by conducting a differential expression analysis on the libraries made with the common spacer, and indeed no tag clusters were detected as significantly differentially expressed (Supplementary Table S7). A potential downside to the common spacer approach is the addition of six more nucleotides to a sequenced read. However, when sequenced on a HiSeq instrument with the standard read length of 50 nucleotide, the resulting libraries can be aligned accurately with standard tools such as BWA (27), as 35 informative bases are remaining after removing the barcode, the spacer and the linker. Alternative strategies could be conceived, and the spacer could be extended or replaced by a random sequence (21,39).

We have described in this article an inherent problem that exists with the TS mechanism, which we could suppress by combining experimental and computational strategies; however, TS artifacts cannot be entirely abolished. What distinguishes the artifacts from *bona fide* full-length cDNAs is the presence of the remaining 5' part of the mRNA as a possibly long tail in the mRNA/cDNA/oligonucleotide triplex. By using an experimental protocol called CAP Trapper (40), which is used in CAGE protocols, it is possible to identify this triplex due to the presence of a 7-methylguanosine cap, therefore accurately identifying transcriptional starting sites as opposed to strand invasion products. This concept of combining TS and CAP Trapper has been shown to produce multiplexed libraries that capture promoters with high fidelity (41). However, as this methodology requires additional preparation steps and is not favored in most TS protocols, where the starting material is limited such as in single cell analyses. Despite the remaining artifacts, our proposed strategy allows one to directly compare different samples, such as between normal and diseased samples. Given that TS is garnering interest again, as seen by the number of recent publications that have used TS, it is important that investigators become aware of TS artifacts. It is clear that more investigations are needed to fully understand the TS mechanism, especially with respect to the types of biases that could potentially be introduced.

DATA DEPOSITION

Sequence data have been deposited in the DNA Data Bank of Japan under accession code DRA000552.

SUPPLEMENTARY DATA

Supplementary Data are available at NAR Online: Supplementary Tables 1–7 and Supplementary Figures 1 and 2.

ACKNOWLEDGEMENTS

The authors would like to thank Dr. Michiel de Hoon for assistance with the statistical analyses and Dr. Alistair Forrest for the rat samples.

FUNDING

The European Union Seventh Framework Programme under grant agreement [FP7-People-ITN-2008-238055] ('BrainTrain' project) (to P.C.); the Research Grant for RIKEN Omics Science Center from Ministry of Education, Culture, Sports, Science and Technology; the Grant-in-Aids for Scientific Research (A) No. 20241047 for nanoCAGE (to P.C.); the 7th Framework Programme Dopaminet Project from the EU (to P.C.); the Telethon grant [GGP10224] (to S.G.). Funding for open access charge: the European Union Seventh Framework Programme under grant agreement [FP7-People-ITN-2008-238055] ('BrainTrain' project) (to P.C.).

Conflict of interest statement. None declared.

REFERENCES

- Baltimore,D. (1970) RNA-dependent DNA polymerase in virions of RNA tumour viruses. *Nature*, **226**, 1209–1211.
- Temin,H.M. and Mizutani,S. (1970) RNA-dependent DNA polymerase in virions of *Rous sarcoma* virus. *Nature*, **226**, 1211–1213.
- Hirzmann,J., Luo,D., Hahnen,J. and Hobom,G. (1993) Determination of messenger RNA 5'-ends by reverse transcription of the cap structure. *Nucleic Acids Res.*, **21**, 3597–3598.
- Ohtake,H., Ohtoko,K., Ishimaru,Y. and Kato,S. (2004) Determination of the capped site sequence of mRNA based on the detection of cap-dependent nucleotide addition using an anchor ligation method. *DNA Res.*, **11**, 305–309.
- Schmidt,W.M. and Mueller,M.W. (1999) CapSelect: a highly sensitive method for 5' CAP-dependent enrichment of full-length cDNA in PCR-mediated analysis of mRNAs. *Nucleic Acids Res.*, **27**, e31.
- Zhu,Y.Y., Machleder,E.M., Chenchik,A., Li,R. and Siebert,P.D. (2001) Reverse transcriptase template switching: a SMART approach for full-length cDNA library construction. *BioTechniques*, **30**, 892–897.
- Matz,M., Shagin,D., Bogdanova,E., Britanova,O., Lukyanov,S., Diatchenko,L. and Chenchik,A. (1999) Amplification of cDNA ends based on template-switching effect and step-out PCR. *Nucleic Acids Res.*, **27**, 1558–1560.
- Cloonan,N., Forrest,A.R., Kolle,G., Gardiner,B.B., Faulkner,G.J., Brown,M.K., Taylor,D.F., Steptoe,A.L., Wani,S., Bethel,G. *et al.* (2008) Stem cell transcriptome profiling via massive-scale mRNA sequencing. *Nat. Methods*, **5**, 613–619.
- Plessy,C., Bertin,N., Takahashi,H., Simone,R., Salimullah,M., Lassmann,T., Vitezic,M., Severin,J., Olivarius,S., Lazarevic,D. *et al.* (2010) Linking promoters to functional transcripts in small

- samples with nanoCAGE and CAGEscan. *Nat. Methods*, **7**, 528–534.
10. Islam,S., Kjallquist,U., Moliner,A., Zajac,P., Fan,J.B., Lonnerberg,P. and Linnarsson,S. (2011) Characterization of the single-cell transcriptional landscape by highly multiplex RNA-seq. *Genome Res.*, **21**, 1160–1167.
 11. Ko,J.H. and Lee,Y. (2006) RNA-conjugated template-switching RT-PCR method for generating an *Escherichia coli* cDNA library for small RNAs. *J. Microbiol. Methods*, **64**, 297–304.
 12. Ramskold,D., Luo,S., Wang,Y.C., Li,R., Deng,Q., Faridani,O.R., Daniels,G.A., Khrebtukova,I., Loring,J.F., Laurent,L.C. *et al.* (2012) Full-length mRNA-Seq from single-cell levels of RNA and individual circulating tumor cells. *Nat. Biotechnol.*, **30**, 777–782.
 13. Maeda,N., Nishiyori,H., Nakamura,M., Kawazu,C., Murata,M., Sano,H., Hayashida,K., Fukuda,S., Tagami,M., Hasegawa,A. *et al.* (2008) Development of a DNA barcode tagging method for monitoring dynamic changes in gene expression by using an ultra high-throughput sequencer. *Biotechniques*, **45**, 95–97.
 14. Islam,S., Kjallquist,U., Moliner,A., Zajac,P., Fan,J.B., Lonnerberg,P. and Linnarsson,S. (2012) Highly multiplexed and strand-specific single-cell RNA 5' end sequencing. *Nat. Protoc.*, **7**, 813–828.
 15. Takahashi,H., Lassmann,T., Murata,M. and Carninci,P. (2012) 5' end-centered expression profiling using cap-analysis gene expression and next-generation sequencing. *Nat. Protoc.*, **7**, 542–561.
 16. Salimullah,M., Sakai,M., Plessy,C. and Carninci,P. (2011) NanoCAGE: a high-resolution technique to discover and interrogate cell transcriptomes. *Cold Spring Harb. Protoc.*, **2011**, pdb prot5559.
 17. Matsumura,H., Yoshida,K., Luo,S., Kimura,E., Fujibe,T., Albertyn,Z., Barrero,R.A., Kruger,D.H., Kahl,G., Schroth,G.P. *et al.* (2010) High-throughput SuperSAGE for digital gene expression analysis of multiple samples using next generation sequencing. *PLoS One*, **5**, e12010.
 18. Kawano,M., Kawazu,C., Lizio,M., Kawaji,H., Carninci,P., Suzuki,H. and Hayashizaki,Y. (2010) Reduction of non-insert sequence reads by dimer eliminator LNA oligonucleotide for small RNA deep sequencing. *Biotechniques*, **49**, 751–755.
 19. Alon,S., Vigneault,F., Eminaga,S., Christodoulou,D.C., Seidman,J.G., Church,G.M. and Eisenberg,E. (2011) Barcoding bias in high-throughput multiplex sequencing of miRNA. *Genome Res.*, **21**, 1506–1511.
 20. Jayaprakash,A.D., Jabado,O., Brown,B.D. and Sachidanandam,R. (2011) Identification and remediation of biases in the activity of RNA ligases in small-RNA deep sequencing. *Nucleic Acids Res.*, **39**, e141.
 21. Kivioja,T., Vaharautio,A., Karlsson,K., Bonke,M., Enge,M., Linnarsson,S. and Taipale,J. (2011) Counting absolute numbers of molecules using unique molecular identifiers. *Nat. Methods*, **9**, 72–74.
 22. Goetz,J.J. and Trimarchi,J.M. (2012) Transcriptome sequencing of single cells with Smart-Seq. *Nat. Biotechnol.*, **30**, 763–765.
 23. Fan,J.B., Chen,J., April,C.S., Fisher,J.S., Klotzle,B., Bibikova,M., Kaper,F., Ronaghi,M., Linnarsson,S., Ota,T. *et al.* (2012) Highly parallel genome-wide expression analysis of single mammalian cells. *PLoS One*, **7**, e30794.
 24. Wang,D. and Bodovitz,S. (2010) Single cell analysis: the new frontier in ‘omics’. *Trends Biotechnol.*, **28**, 281–290.
 25. Kapteyn,J., He,R., McDowell,E.T. and Gang,D.R. (2010) Incorporation of non-natural nucleotides into template-switching oligonucleotides reduces background and improves cDNA synthesis from very small RNA samples. *BMC Genomics*, **11**, 413.
 26. Lassmann,T., Hayashizaki,Y. and Daub,C.O. (2009) TagDust—a program to eliminate artifacts from next generation sequencing data. *Bioinformatics*, **25**, 2839–2840.
 27. Li,H. and Durbin,R. (2009) Fast and accurate short read alignment with Burrows-Wheeler transform. *Bioinformatics*, **25**, 1754–1760.
 28. Li,H., Handsaker,B., Wysoker,A., Fennell,T., Ruan,J., Homer,N., Marth,G., Abecasis,G. and Durbin,R. (2009) The sequence alignment/map format and SAMtools. *Bioinformatics*, **25**, 2078–2079.
 29. Marioni,J.C., Mason,C.E., Mane,S.M., Stephens,M. and Gilad,Y. (2008) RNA-seq: an assessment of technical reproducibility and comparison with gene expression arrays. *Genome Res.*, **18**, 1509–1517.
 30. Schneider,T.D. and Stephens,R.M. (1990) Sequence logos: a new way to display consensus sequences. *Nucleic Acids Res.*, **18**, 6097–6100.
 31. Needleman,S.B. and Wunsch,C.D. (1970) A general method applicable to the search for similarities in the amino acid sequence of two proteins. *J. Mol. Biol.*, **48**, 443–453.
 32. Carninci,P., Sandelin,A., Lenhard,B., Katayama,S., Shimokawa,K., Ponjavic,J., Semple,C.A., Taylor,M.S., Engstrom,P.G., Frith,M.C. *et al.* (2006) Genome-wide analysis of mammalian promoter architecture and evolution. *Nat. Genet.*, **38**, 626–635.
 33. Robinson,M.D., McCarthy,D.J. and Smyth,G.K. (2009) edgeR: a Bioconductor package for differential expression analysis of digital gene expression data. *Bioinformatics*, **26**, 139–140.
 34. Bourgon,R., Gentleman,R. and Huber,W. (2010) Independent filtering increases detection power for high-throughput experiments. *Proc. Natl Acad. Sci. USA*, **107**, 9546–9551.
 35. Benjamini,Y. and Hochberg,Y. (1995) Controlling the false discovery rate: a practical and powerful approach to multiple testing. *J. Roy. Stat. Soc. Ser. B*, **57**, 289–300.
 36. Guttman,M., Garber,M., Levin,J.Z., Donaghey,J., Robinson,J., Adiconis,X., Fan,L., Koziol,M.J., Gnirke,A., Nusbaum,C. *et al.* (2010) Ab initio reconstruction of cell type-specific transcriptomes in mouse reveals the conserved multi-exonic structure of lincRNAs. *Nat. Biotechnol.*, **28**, 503–510.
 37. Trapnell,C., Pachter,L. and Salzberg,S.L. (2009) TopHat: discovering splice junctions with RNA-Seq. *Bioinformatics*, **25**, 1105–1111.
 38. Shiroguchi,K., Jia,T.Z., Sims,P.A. and Xie,X.S. (2012) Digital RNA sequencing minimizes sequence-dependent bias and amplification noise with optimized single-molecule barcodes. *Proc. Natl Acad. Sci. USA*, **109**, 1347–1352.
 39. Konig,J., Zarnack,K., Rot,G., Curk,T., Kayikci,M., Zupan,B., Turner,D.J., Luscombe,N.M. and Ule,J. (2010) iCLIP reveals the function of hnRNP particles in splicing at individual nucleotide resolution. *Nat. Struct. Mol. Biol.*, **17**, 909–915.
 40. Carninci,P., Kvam,C., Kitamura,A., Ohsumi,T., Okazaki,Y., Itoh,M., Kamiya,M., Shibata,K., Sasaki,N., Izawa,M. *et al.* (1996) High-efficiency full-length cDNA cloning by biotinylated CAP trapper. *Genomics*, **37**, 327–336.
 41. Batut,P.J., Dobin,A., Plessy,C., Carninci,P. and Gingeras,T.R. (2012) High-fidelity promoter profiling reveals widespread alternative promoter usage and transposon-driven developmental gene expression. *Genome Res.*, **23**, 169–180.

Chapter 3

Role of small RNAs in DNA damage repair

It has been previously reported that small RNAs play a role in establishing the DNA damage response Lee et al. (2009). We leveraged the discovery potential of small RNA sequencing to gain some insight into the potential interplay between small RNAs and DNA damage. Intriguingly, we discovered that small RNAs formed near the site of DNA damage. We considered alternative hypotheses that could explain the presence of these small RNAs such as RNA degradation or technical artefacts. We¹ characterised certain features of the DNA damage small RNAs (DDRNAs) to the population of sequenced small RNAs and observed that the bulk of the DDRNAs had a characteristic size and nucleotide profile, suggesting that they are not random degradation products. Furthermore, we performed experiments to suggest possible biogenesis pathways and the knock-down of Dicer and Drosha, which are enzymes involved with small RNA processing, affected the profile of DDRNAs and impaired the DNA damage response. This work has important implications to the observation that the genome is pervasively transcribed, as it offers a hypothesis that pervasive transcription is necessary for maintaining DNA integrity.

¹All the bioinformatic analysis was performed by Dave Tang.

Site-specific DICER and DROSHA RNA products control the DNA-damage response

Sofia Francia^{1,2}, Flavia Michelini¹, Alka Saxena³, Dave Tang³, Michiel de Hoon³, Viviana Anelli^{1†}, Marina Mione^{1†}, Piero Carninci³ & Fabrizio d'Adda di Fagagna^{1,4}

Non-coding RNAs (ncRNAs) are involved in an increasingly recognized number of cellular events¹. Some ncRNAs are processed by DICER and DROSHA RNases to give rise to small double-stranded RNAs involved in RNA interference (RNAi)². The DNA-damage response (DDR) is a signalling pathway that originates from a DNA lesion and arrests cell proliferation³. So far, DICER and DROSHA RNA products have not been reported to control DDR activation. Here we show, in human, mouse and zebrafish, that DICER and DROSHA, but not downstream elements of the RNAi pathway, are necessary to activate the DDR upon exogenous DNA damage and oncogene-induced genotoxic stress, as studied by DDR foci formation and by checkpoint assays. DDR foci are sensitive to RNase A treatment, and DICER- and DROSHA-dependent RNA products are required to restore DDR foci in RNase-A-treated cells. Through RNA deep sequencing and the study of DDR activation at a single inducible DNA double-strand break, we demonstrate that DDR foci formation requires site-specific DICER- and DROSHA-dependent small RNAs, named DDRNAs, which act in a MRE11–RAD50–NBS1-complex-dependent manner (MRE11 also known as MRE11A; NBS1 also known as NBN). DDRNAs, either chemically synthesized or *in vitro* generated by DICER cleavage, are sufficient to restore the DDR in RNase-A-treated cells, also in the absence of other cellular RNAs. Our results describe an unanticipated direct role of a novel class of ncRNAs in the control of DDR activation at sites of DNA damage.

Mammalian genomes are pervasively transcribed, with most transcripts apparently not associated with coding functions^{4,5}. An increasing number of ncRNAs have been shown to have a variety of relevant cellular functions, often with very low estimated expression levels^{6–8}. DICER and DROSHA are two RNase type III enzymes that process ncRNA hairpin structures to generate small double-stranded RNAs⁹ (see Supplementary Information).

Detection of a DNA double-strand break (DSB) triggers the kinase activity of ATM, which initiates a signalling cascade by phosphorylating the histone variant H2AX (γ H2AX) at the DNA-damage site and recruiting additional DDR factors. This establishes a local self-feeding loop that leads to accumulation of upstream DDR factors in the form of cytologically detectable foci at damaged DNA sites^{3,10}. The DDR has been considered to be a signalling cascade made up exclusively of proteins, with no direct contributions from RNA species to its activation.

Oncogene-induced senescence (OIS) is a non-proliferative state characterized by a sustained DDR¹¹ and senescence-associated heterochromatic foci (SAHF)¹². Because ncRNAs participate in heterochromatin formation¹³, we investigated whether they could control SAHF and OIS. We used small interfering RNAs (siRNAs) to knockdown DICER or DROSHA in OIS cells and monitored SAHF

and cell-cycle progression. Knockdown of either DICER or DROSHA, as well as ATM as control¹⁴, restored DNA replication and entry into mitosis (Supplementary Figs 1 and 2); we did not detect overt SAHF changes, however (Supplementary Fig. 3a, b). Instead, we observed that DICER or DROSHA inactivation significantly reduced the number of cells positive for DDR foci containing 53BP1, the autophosphorylated form of ATM (pATM) and the phosphorylated substrates of ATM and ATR (pS/TQ), but not γ H2AX, without decreasing the expression of proteins involved in the DDR (Supplementary Fig. 3a–c). Importantly, the simultaneous inactivation of all three GW182-like proteins, TNRC6A, B and C, essential for the translational inhibition mediated by microRNAs (miRNAs; canonical DICER and DROSHA products involved in RNAi)¹⁵, does not affect DDR foci formation (Supplementary Fig. 4).

We next asked whether DICER or DROSHA inactivation also affects ionizing-radiation-induced DDR activation. We transiently inactivated DICER or DROSHA by siRNA in human normal fibroblasts (HNFs), exposed cells to ionizing radiation, and monitored DDR foci. We observed that a few hours after exposure to ionizing radiation, DICER or DROSHA inactivation impairs the formation of pATM, pS/TQ and MDC1, but not γ H2AX, foci without decreasing their protein levels (Fig. 1a, b and Supplementary Fig. 5). Furthermore, at an earlier time point (10 min) after ionizing radiation, 53BP1 foci were significantly reduced (Supplementary Fig. 6a). Using an RNAi-resistant form of DICER in DICER knockdown cells, we observed that re-expression of wild-type DICER, but not of a DICER endonuclease mutant (DICER44ab)¹⁶, rescues DDR foci formation (Supplementary Fig. 6b–d). The simultaneous knockdown of TNRC6A, B and C, or DICER has a comparable impact on a reporter system specific for miRNA-dependent translational repression¹⁷, but only DICER inactivation reduces DDR foci formation (Supplementary Fig. 7). To confirm further the involvement of DICER in DDR activation, we used a cell line carrying a hypomorphic allele of *DICER* (*DICER*^{exon5}) defective in miRNA maturation¹⁸. In *DICER*^{exon5}-irradiated cells, pATM, pS/TQ and MDC1, but not γ H2AX, foci formation is impaired without a decrease in their protein levels, and 53BP1 foci formation is delayed compared to the DICER wild-type parental cell line (Supplementary Fig. 8). These defects could be reversed by the re-expression of wild-type DICER but not of the mutant form DICER44ab (Supplementary Fig. 9). By immunoblotting, we confirmed that ATM autophosphorylation is reduced in DICER or DROSHA knockdown HNFs, and in *DICER*^{exon5} cell lines (Supplementary Fig. 10). These results indicate that DICER and DROSHA RNA products control DDR activation and act independently from canonical miRNA-mediated translational repression mechanisms.

DDR signalling enforces cell-cycle arrest at the G1/S and G2/M checkpoints³. We observed that DNA-damage-induced checkpoints were impaired in DICER- or DROSHA-inactivated cells and that

¹IFOM Foundation - FIRC Institute of Molecular Oncology Foundation, Via Adamello 16, 20139 Milan, Italy. ²Center for Genomic Science of IIT@SEMM, Istituto Italiano di Tecnologia, at the IFOM-IEO Campus, Via Adamello 16, 20139 Milan, Italy. ³Oomics Science Center, RIKEN Yokohama Institute, 1-7-22 Suehiro-cho, Tsurumi-ku, Yokohama, Kanagawa 230-0045, Japan. ⁴Istituto di Genetica Molecolare, Consiglio Nazionale delle Ricerche, Pavia 27100, Italy. [†]Present addresses: Departments of Surgery and Medicine, Weill Cornell Medical College and New York Presbyterian Hospital, 1300 York Avenue, New York, New York 10065, USA (V.A.); Institute of Toxicology and Genetics, Karlsruhe Institute of Technology, 76344 Karlsruhe, Germany (M.M.).

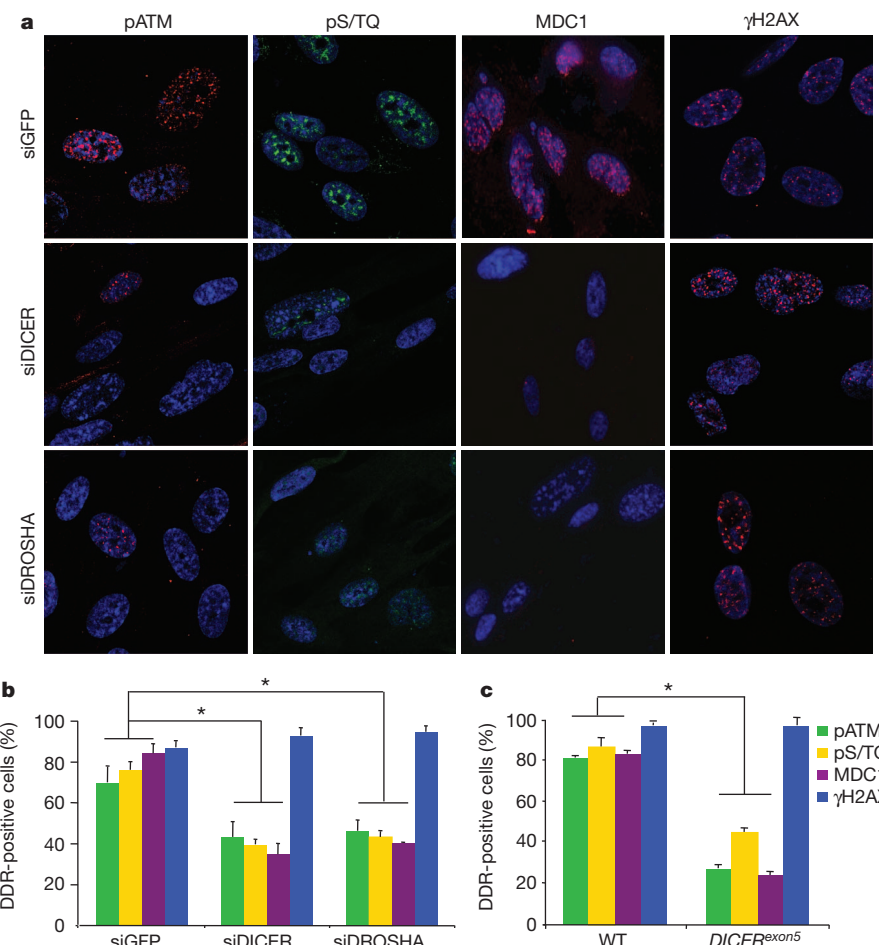


Figure 1 | DICER or DROSHA inactivation impairs DDR foci formation in irradiated cells. **a**, DICER or DROSHA knockdown WI-38 cells were irradiated (10 Gy) and fixed 7 h later. Original magnification, $\times 250$. **b**, Histogram shows the percentage of cells positive for pATM, pS/TQ, MDC1

and γ H2AX foci. **c**, Wild-type (WT) and $DICER^{exon5}$ cells were irradiated (2 Gy) and fixed 2 h later. Histogram shows the percentage of cells positive for pATM, pS/TQ, MDC1 and γ H2AX foci. Error bars indicate s.e.m. ($n \geq 3$). Differences are statistically significant (* P value < 0.01).

wild-type DICER re-expression in $DICER^{exon5}$ cells restores checkpoint functions whereas two independent mutant forms of DICER fail to do so (Supplementary Figs 11–13). Thus, DICER and DROSHA are required for DNA-damage-induced checkpoint enforcement.

To test the role of DICER in DDR activation in a living organism, we inactivated it by morpholino antisense oligonucleotide injection in *Danio rerio* (zebrafish) larvae¹⁹. Such Dicer inactivation results in a marked impairment of pAtm and zebrafish γ H2AX accumulation in irradiated larvae as detected both by immunostaining and immunoblotting of untreated or Dicer morpholino-injected larvae and of chimaeric animals (Supplementary Figs 14 and 15).

Previous reports have shown that mammalian cells can withstand transient membrane permeabilization and RNase A treatment, enabling investigation of the contribution of RNA to heterochromatin organization and 53BP1 association to chromatin^{20,21}. We used this approach to address the direct contribution of DICER and DROSHA RNA products in DDR activation. Irradiated HeLa cells were permeabilized and treated with RNase A, leading to degradation of all RNAs, without affecting protein levels (Supplementary Fig. 16a). We observed that 53BP1, pATM, pS/TQ and MDC1 foci become markedly reduced in number and intensity upon RNA degradation whereas, similarly to DICER- or DROSHA-inactivated cells, γ H2AX is unaffected (Fig. 2a and Supplementary Fig. 16b). Notably, 53BP1, MDC1 and γ H2AX triple staining shows that RNA degradation reduces 53BP1 and MDC1 accumulation at unperturbed γ H2AX foci

(Supplementary Fig. 16c). When RNase A is inhibited, DDR foci progressively reappear within minutes and α -amanitin prevents this (Supplementary Fig. 17a, b), suggesting that DDR foci stability is RNA polymerase II dependent.

We tested whether DDR foci can reform upon addition of exogenous RNA to RNase-A-treated cells. We observed that DDR foci robustly reform in RNase-A-treated cells following their incubation with total RNA purified from the same cells, but not with transfer RNA (tRNA) control (Fig. 2b–d). Similar conclusions were reached using an inducible form of Ppol and AsISI site-specific endonucleases^{22,23} (data not shown).

Next, we attempted to characterize the length of the RNA species involved in DDR foci reformation, which we refer to as DDRRNAs. We observed that an RNA fraction enriched by chromatography for species < 200 nucleotides was sufficient to restore DDR foci (Supplementary Fig. 17c–e). To attain better size separation, we resolved total RNA on a polyacrylamide gel and recovered RNA fractions of different lengths (Supplementary Fig. 17f, g). Using equal amounts of each fraction, we observed that only the 20–35-nucleotide fraction could restore DDR foci (Fig. 2b), consistent with the size range of DICER and DROSHA RNA products.

To test the hypothesis that DDRRNAs are DICER and DROSHA products, we tested DDR foci restoration with total RNA extracted from wild-type or $DICER^{exon5}$ cells. Although RNA extracted from wild-type cells restores pATM, pS/TQ and 53BP1 foci, RNA from $DICER^{exon5}$ cells does not (Fig. 2c, d). Importantly, RNA from

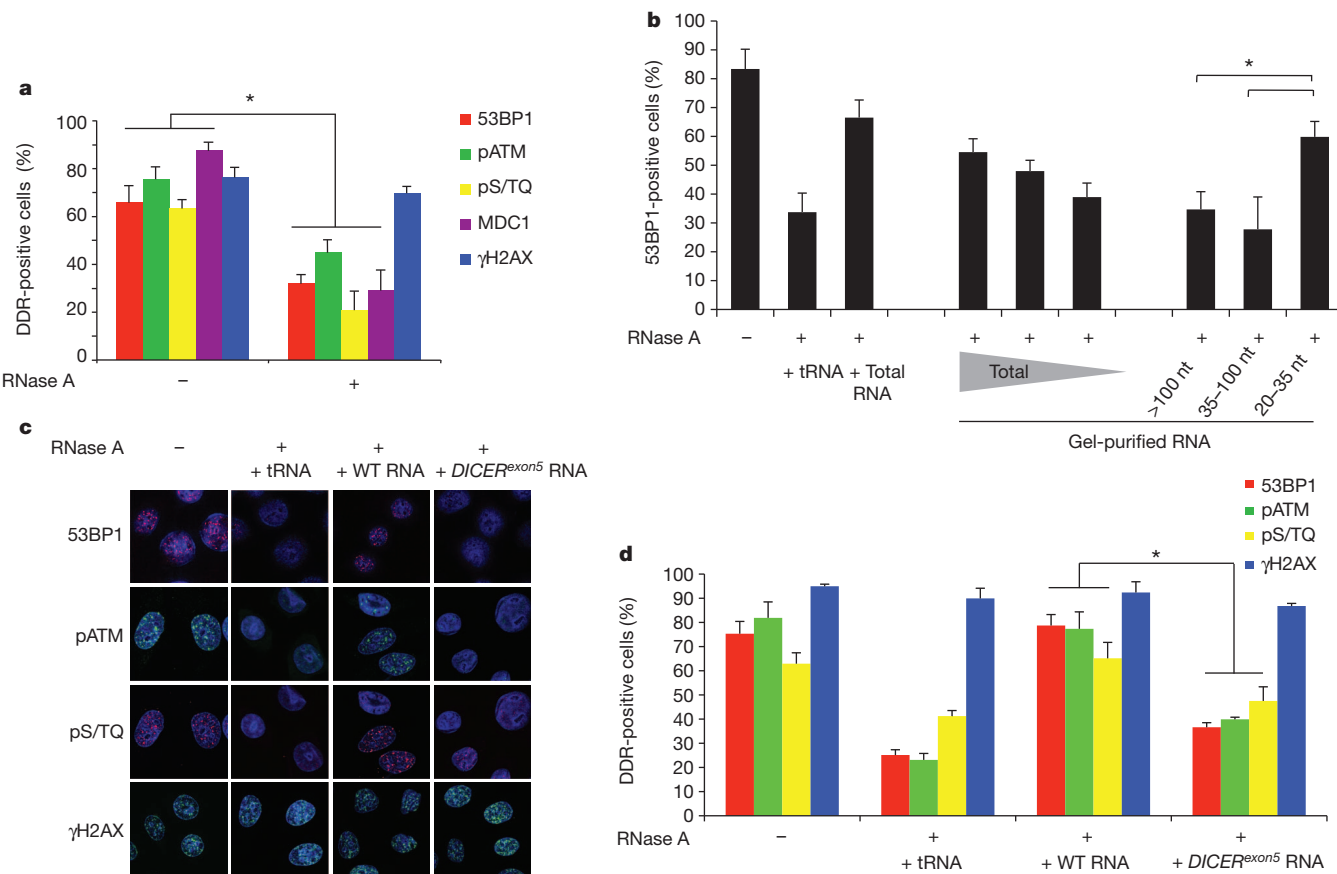


Figure 2 | Irradiation-induced DDR foci are sensitive to RNase A treatment and are restored by small and DICER-dependent RNAs. **a**, Irradiated HeLa cells (2 Gy) were treated with PBS (−) or RNase A (+) and probed for 53BP1, pATM, pS/TQ, MDC1 and γH2AX foci. Histogram shows the percentage of cells positive for DDR foci. **b**, 100, 50 or 20 ng of gel-extracted total RNA and 50 ng of RNA extracted from each gel fraction (>100, 35–100 and 20–35

nucleotides (nt)) were used for DDR foci reconstitution after RNase treatment. **c**, 53BP1, pS/TQ and pATM foci are restored in RNase-treated cells when incubated with RNA of wild-type cells but not with RNA of *DICER^{exon5}* cells or tRNA. Original magnification, $\times 350$. **d**, Histogram shows the percentage of cells positive for DDR foci. Error bars indicate s.e.m. ($n \geq 3$). Differences are statistically significant (* P value < 0.01).

DICER^{exon5} cells re-expressing wild-type, but not endonuclease-mutant, DICER allows DDR foci reformation (Supplementary Fig. 18a, b). These results were reproduced using RNA extracted from cells transiently knocked down for DICER or DROSHA (Supplementary Fig. 18c–f).

Ionizing radiation induces DNA lesions that are heterogeneous in nature and random in their genomic location. To reduce this complexity, we studied a single DSB at a defined and traceable genomic locus. We therefore took advantage of NIH2/4 mouse cells carrying an integrated copy of the I-SceI restriction site flanked by arrays of Lac- or Tet-operator repeats at either sites²⁴. In this cell line, the expression of the I-SceI restriction enzyme together with the fluorescent protein Cherry-Lac-repressor allows the visualization of a site-specific DDR focus that overlaps with a focal Cherry-Lac signal (cut NIH2/4 cells). No DDR focus formation is observed overlapping with the Cherry-Lac signal in the absence of I-SceI expression (uncut NIH2/4 cells). Also in this system, RNase A treatment causes the disappearance of the 53BP1, but not the γH2AX, focus at the I-SceI-induced DSB; total RNA addition from cut cells restores 53BP1 focus formation in a dose-dependent manner (Fig. 3a, b). Therefore, a DDR focus generated on a defined DSB can disassemble and reassemble in an RNA-dependent manner.

To determine whether DDRNA are generated at the damaged locus or elsewhere in the genome, we took advantage of the fact that the I-SceI-induced DSB is generated within an integrated exogenous sequence, which is not present in the parental cell line. As RNAs extracted from NIH2/4 or parental cells are expected to differ only in the potential presence of RNA transcripts generated at the locus, we used these two RNA preparations to attempt to restore 53BP1

focus formation at the I-SceI-induced DSB in RNase-A-treated cells. The formation of the 53BP1 focus was efficiently recovered only by RNA purified from NIH2/4 cells and not from parental cells (Fig. 3c), indicating that DDRNA originate from the damaged genomic locus.

The MRE11–RAD50–NBS1 (MRN) complex is necessary for ATM activation²⁵, and pATM and MRE11 foci formation is sensitive to RNase A treatment in the NIH2/4 cell system (Supplementary Fig. 19a, b). To probe the molecular mechanisms by which RNA modulates DDR focus formation, we used a specific MRN inhibitor²⁶, mirin, which prevents ATM activation also in the NIH2/4 system (Supplementary Fig. 19d). In the presence of mirin, NIH2/4 RNA is unable to restore 53BP1 or pATM focus formation (Fig. 3d, e), indicating that DDRNA act in a MRN-dependent manner.

To detect potential short RNAs originating from the integrated locus, we deep-sequenced libraries generated from short (<200 nucleotides) nuclear RNAs of cut or uncut NIH2/4 cells, as well as from parental cells expressing I-SceI as negative control. Sequencing revealed short transcripts arising from the exogenous locus (Supplementary Fig. 20a–e), 47 reads in cut cells, 20 reads in uncut cells and none in parental cells, indicating that even an exogenous integrated locus lacking mammalian transcriptional regulatory elements is transcribed and can generate small RNAs.

To test whether the identified locus-specific small RNAs are biologically active and have a causal role in DDR activation, we chemically synthesized four potential pairs among the sequences obtained and used them to attempt to restore the DDR focus in RNase-A-treated

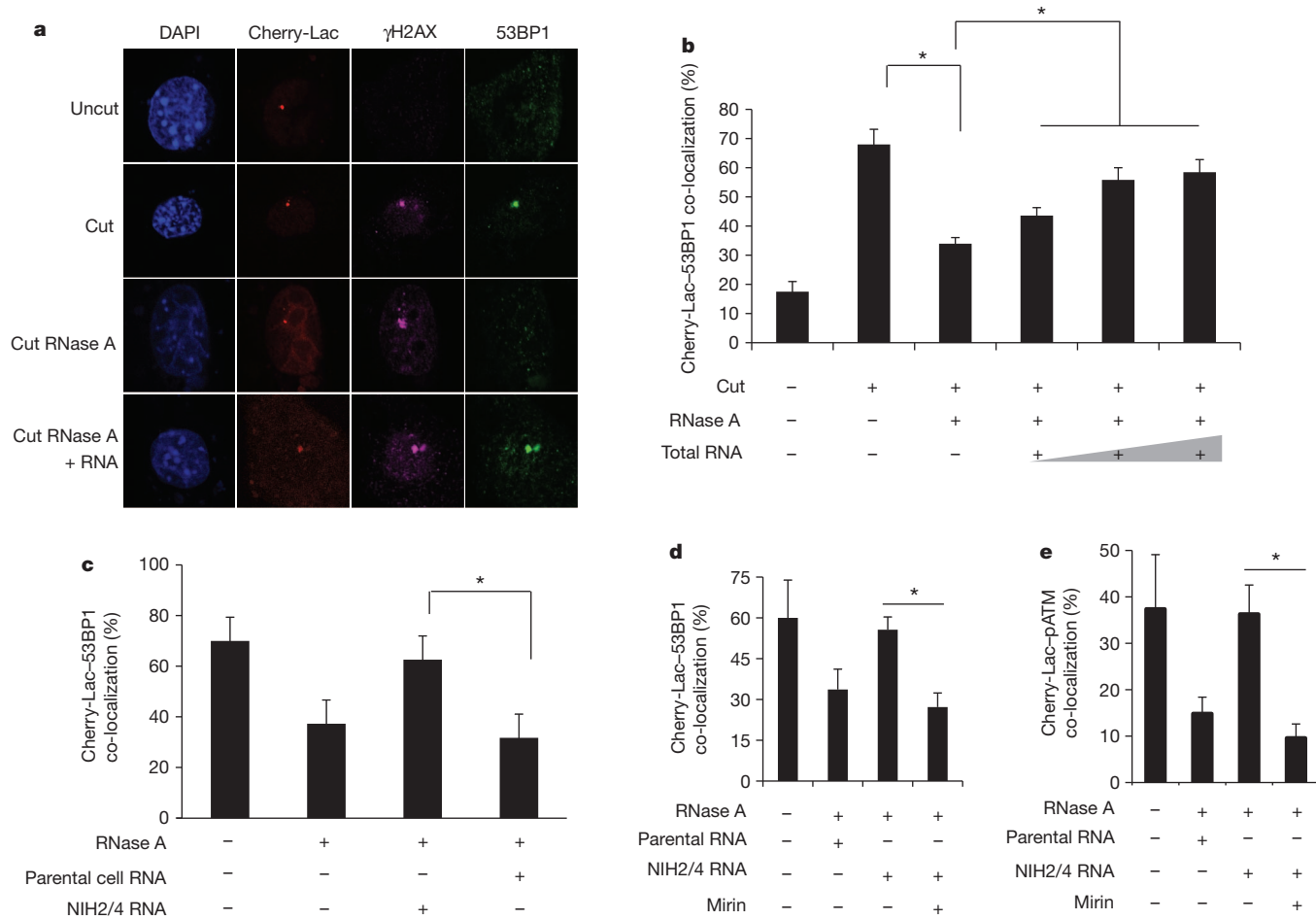


Figure 3 | Site-specific DDR focus formation is RNase A sensitive and can be restored by site-specific RNA in a MRN-dependent manner. **a**, Cut NIH2/4 cells display a 53BP1 and γH2AX focus co-localizing with a Cherry-Lac focus. 53BP1, but not γH2AX, focus is sensitive to RNase A and is restored by incubation with total RNA. DAPI, 4',6-diamidino-2-phenylindole. Original magnification, $\times 450$. **b**, Histogram shows the percentage of cells in which 53BP1 and Cherry-Lac foci co-localize. Addition of 50, 200 or 800 ng of RNA purified from cut NIH2/4 rescues 53BP1 foci formation in a dose-dependent

manner. **c**, RNA purified from cut NIH2/4 restores 53BP1 focus whereas RNA from parental cells expressing I-SceI does not. **d**, **e**, RNase-A-treated cut NIH2/4 cells were incubated with RNA from cut NIH2/4 cells, or parental ones, to test 53BP1 or pATM focus reformation in the presence of the MRN inhibitor mirin (100 μ M). Histogram shows the percentage of cells positive for a DDR focus. Error bars indicate s.e.m. ($n \geq 3$). Differences are statistically significant (* P value < 0.05).

cells. Notably, we observed that addition of locus-specific synthetic RNAs, but not equal amounts of control RNAs, triggers site-specific 53BP1 focus reformation over a large range of concentrations in the presence, but also in the absence, of total RNA from parental cells (Fig. 4a and Supplementary Fig. 20f). To show further the biological activity of RNAs processed by DICER, we *in vitro* transcribed both strands of the sequence spanning the locus, or a control one, and processed the resulting RNAs with recombinant DICER. *In vitro*-generated locus-specific DICER RNA products, but not control RNAs, allowed DDR focus reformation in RNase-A-treated cells even in the absence of parental RNA (Fig. 4b and Supplementary Fig. 20g, h). Overall, these results indicate that DDRRNAs are small RNAs with the sequence of the damaged locus, which have a direct role in DDR activation.

To investigate the biogenesis of such RNAs *in vivo*, we performed deeper sequencing of small nuclear RNAs from cut and uncut wild-type as well as DICER or DROSHA knockdown NIH2/4 cells (Supplementary Fig. 21). As expected, DICER or DROSHA knockdown significantly reduced reads mapping to the known miRNAs (Supplementary Fig. 22). Our statistical analyses revealed that the percentage of 22–23-nucleotide RNAs arising from the locus significantly

increases in the wild-type cut sample compared to the uncut one and that DICER inactivation significantly reduces it (Supplementary Fig. 23a, b); the detectable decrease in DROSHA-inactivated cells did not reach statistical significance. Because the fraction of 22–23-nucleotide RNAs from the locus is significantly higher with respect to that of non-miRNA genomic loci, the RNAs detected are very unlikely to be random degradation products (Supplementary Fig. 23c). Finally, 22–23-nucleotide RNAs at the locus tend to have an A/U at their 5' and a G at their 3' end (Supplementary Fig. 23d), a nucleotide bias significantly different from the originating locus and from the rest of the genome.

In summary, we demonstrate that different sources of DNA damage, including oncogenic stress, ionizing radiation and site-specific endonucleases, activate the DDR in a manner dependent on DDRRNAs, which are DICER- and DROSHA-dependent RNA products with the sequence of the damaged site. DDRRNAs control DDR foci formation and maintenance, checkpoint enforcement and cellular senescence in cultured human and mouse cells and in different cell types in living zebrafish larvae. They act differently from canonical miRNAs, as inferred by their demonstrated biological activity independent of other RNAs and of GW182-like proteins.

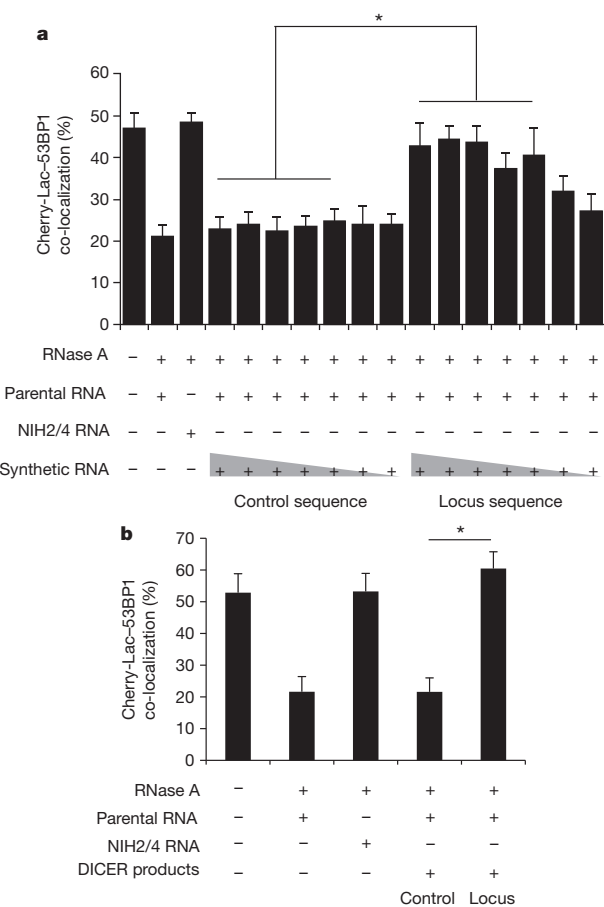


Figure 4 | Chemically synthesized small RNAs and *in vitro*-generated DICER RNA products are sufficient to restore DDR focus formation in RNase-A-treated cells in a sequence-specific manner. **a**, Chemically synthesized RNA oligonucleotides were annealed and were tested to restore DDR focus formation in RNase-A-treated cut NIH2/4 cells. Mixed with a constant amount (800 ng) of parental cell RNA, a concentration range (1 ng μ l $^{-1}$ to 1 fg μ l $^{-1}$, tenfold dilution steps) of locus-specific or GFP RNAs was used. Locus-specific synthetic RNAs (down to 100 fg μ l $^{-1}$) allow site-specific DDR activation. **b**, Small double-stranded RNAs generated by recombinant DICER were tested to restore DDR focus formation in RNase-A-treated cut NIH2/4 cells. 1 ng μ l $^{-1}$ RNA was tested mixed with 800 ng of parental cell RNA. Locus-specific DICER RNAs, but not control RNAs, allow site-specific DDR activation. Histograms show the percentage of cells positive for DDR focus. Error bars indicate s.e.m. ($n \geq 3$). Differences are statistically significant (* P value < 0.05).

METHODS SUMMARY

Details of cell cultures, plasmids, siRNAs and antibodies used, as well as descriptions of methods for immunofluorescence, immunoblotting, checkpoint assays, real-time quantitative polymerase chain reaction (PCR), zebrafish injection and transplantation, RNase A treatment, small RNA extraction and purification from gel, RNA sequencing and statistical analyses are provided in Methods.

Full Methods and any associated references are available in the online version of the paper.

Received 8 February 2010; accepted 4 May 2012.

Published online 23 May 2012.

- Esteller, M. Non-coding RNAs in human disease. *Nature Rev. Genet.* **12**, 861–874 (2011).
- Krol, J., Loedige, I. & Filipowicz, W. The widespread regulation of microRNA biogenesis, function and decay. *Nature Rev. Genet.* **11**, 597–610 (2010).
- Jackson, S. P. & Bartek, J. The DNA-damage response in human biology and disease. *Nature* **461**, 1071–1078 (2009).
- Clark, M. B. et al. The reality of pervasive transcription. *PLoS Biol.* **9**, e1000625 (2011).
- Wilusz, J. E., Sunwoo, H. & Spector, D. L. Long noncoding RNAs: functional surprises from the RNA world. *Genes Dev.* **23**, 1494–1504 (2009).

- Wang, X. et al. Induced ncRNAs allosterically modify RNA-binding proteins *in cis* to inhibit transcription. *Nature* **454**, 126–130 (2008).
- Zhao, J., Sun, B. K., Erwin, J. A., Song, J. J. & Lee, J. T. Polycomb proteins targeted by a short repeat RNA to the mouse X chromosome. *Science* **322**, 750–756 (2008).
- Mercer, T. R., Dinger, M. E. & Mattick, J. S. Long non-coding RNAs: insights into functions. *Nature Rev. Genet.* **10**, 155–159 (2009).
- Kim, V. N., Han, J. & Siomi, M. C. Biogenesis of small RNAs in animals. *Nature Rev. Mol. Cell Biol.* **10**, 126–139 (2009).
- Lukas, J., Lukas, C. & Bartek, J. More than just a focus: the chromatin response to DNA damage and its role in genome integrity maintenance. *Nature Cell Biol.* **13**, 1161–1169 (2011).
- d'Adda di Fagagna, F. Living on a break: cellular senescence as a DNA-damage response. *Nature Rev. Cancer* **8**, 512–522 (2008).
- Narita, M. et al. Rb-mediated heterochromatin formation and silencing of E2F target genes during cellular senescence. *Cell* **113**, 703–716 (2003).
- White, S. A. & Allshire, R. C. RNAi-mediated chromatin silencing in fission yeast. *Curr. Top. Microbiol. Immunol.* **320**, 157–183 (2008).
- Di Micco, R. et al. Oncogene-induced senescence is a DNA damage response triggered by DNA hyper-replication. *Nature* **444**, 638–642 (2006).
- Tritschler, F., Huntzinger, E. & Izaurralde, E. Role of GW182 proteins and PABPC1 in the miRNA pathway: a sense of déjà vu. *Nature Rev. Mol. Cell Biol.* **11**, 379–384 (2010).
- Zhang, H., Kolb, F. A., Jaskiewicz, L., Westhof, E. & Filipowicz, W. Single processing center models for human Dicer and bacterial RNase III. *Cell* **118**, 57–68 (2004).
- Nicolli, S. et al. MicroRNA-mediated integration of haemodynamics and Vgef signalling during angiogenesis. *Nature* **464**, 1196–1200 (2010).
- Cummins, J. M. et al. The colorectal microRNAome. *Proc. Natl Acad. Sci. USA* **103**, 3687–3692 (2006).
- Wienholds, E. et al. MicroRNA expression in zebrafish embryonic development. *Science* **309**, 310–311 (2005).
- Maison, C. et al. Higher-order structure in pericentric heterochromatin involves a distinct pattern of histone modification and an RNA component. *Nature Genet.* **30**, 329–334 (2002).
- Pryde, F. et al. 53BP1 exchanges slowly at the sites of DNA damage and appears to require RNA for its association with chromatin. *J. Cell Sci.* **118**, 2043–2055 (2005).
- Berkovich, E., Monnat, R. J. Jr & Kastan, M. B. Roles of ATM and NBS1 in chromatin structure modulation and DNA double-strand break repair. *Nature Cell Biol.* **9**, 683–690 (2007).
- Iacoboni, J. S. et al. High-resolution profiling of γ H2AX around DNA double strand breaks in the mammalian genome. *EMBO J.* **29**, 1446–1457 (2010).
- Soutoglou, E. et al. Positional stability of single double-strand breaks in mammalian cells. *Nature Cell Biol.* **9**, 675–682 (2007).
- Stracker, T. H. & Petri, J. H. The MRE11 complex: starting from the ends. *Nature Rev. Mol. Cell Biol.* **12**, 90–103 (2011).
- Dupré, A. et al. A forward chemical genetic screen reveals an inhibitor of the Mre11-Rad50-Nbs1 complex. *Nature Chem. Biol.* **4**, 119–125 (2008).

Supplementary Information is linked to the online version of the paper at www.nature.com/nature.

Acknowledgements We thank E. Soutoglou, W. C. Hahn, M. Kastan, V. Orlando, R. Shiekhattar, J. Amatruda, T. Halazonetis, E. Dejana, P. Ng and F. Nicassio for sharing reagents, M. Fumagalli and F. Rossiello for reading the manuscript, M. Dobrava, V. Matti and F. Pezzimenti for technical support, G. D'Ari for help with statistical analyses, B. Amati, M. Foiani, V. Costanzo and F.d.A.d.F. group members for help and discussions. The F.d.A.d.F. laboratory was supported by Fondazione Italiana Ricerca Sul Cancro (FIRC), Associazione Italiana Ricerca sul Cancro (AIRC) European Community's 7th Framework Programme (FP7/2007–2013) under grant agreement no. 202230, acronym "GENINCA", HFSP, AIRC, the EMBO Young Investigator Program. The initial part of this project was supported by Telethon grant no. GGP08183. P.C. was supported by 7th Framework of the European Union commission to the Dopaminet consortium, a Grant-in-Aids for Scientific Research (A) no. 20241047, Funding Program for the Next Generation World-Leading Researchers (NEXT Program) to P.C. and a Research Grant to RIKEN Omics Science Center from MEXT. S.F. is supported by Center for Genomic Science of IIT@SEMM (Scuola Europea di Medicina Molecolare) and AIRC. M.M. was supported by Cariplo (grant no. 2007–5500) and AIRC. A.S. is supported by a JSPS fellowship P09745 and grant in aid by JSPS, and D.T. is supported by the European Union 7th Framework Programme under grant agreement FP7-People-ITN-2008-238055 ("BrainTrain" project) to P.C.

Author Contributions A.S., D.T. and P.C. planned, generated and analysed the genomics data presented in Supplementary Figs 20a–e, 21, 22b and 23. M.d.H. performed statistical analysis of the genomics data. A.S. and P.C. also edited the manuscript. M.M. and V.A. generated the data presented in Supplementary Figs 14 and 15. F.M. generated the data shown in Figs 2b, 3d, e, 4b and Supplementary Figs 2b, e, 3e, 4b, 5f, g, 6b–d, 7d, 9, 13d–f, 14d, f, 17f, g, 18a, b, 19, 20g, h and 22a and generated RNA for deep sequencing; contributed to: Supplementary Figs 16a, 5d, e, 11c, d and edited the manuscript. S.F. generated the data shown in remaining figures, contributed to experimental design and edited the manuscript. F.d.A.d.F. conceived the study, designed the experiments and wrote the manuscript.

Author Information Sequence data have been deposited in the DNA Data Bank of Japan under accession code DRA000540. Reprints and permissions information is available at www.nature.com/reprints. The authors declare no competing financial interests. Readers are welcome to comment on the online version of this article at www.nature.com/nature. Correspondence and requests for materials should be addressed to F.d.A.d.F. (fabrizio.dadda@ifom-ieo-campus.it).

METHODS

Cultured cells. Early-passage WI-38 cells (ATCC) were grown under standard tissue culture conditions (37°C , 5% CO₂) in MEM supplemented with 10% fetal bovine serum, 1% L-glutamine, 1% non-essential aminoacids, 1% Na pyruvate. HeLa, Phoenix ecotropic and HEK293T cell lines were grown under standard tissue culture conditions (37°C , 5% CO₂) in DMEM, supplemented with 10% fetal bovine serum, 1% glutamine, 1% penicillin/streptomycin. *DICER*^{exons 5} colon cancer cell lines¹⁸ were cultured in McCoy's 5A medium plus 10% fetal calf serum, 1% penicillin/streptomycin. NIH2/4 cells²⁴ were grown in DMEM, supplemented with 10% fetal bovine serum, 1% glutamine, gentamicine (40 µg ml⁻¹) and hygromycin (400 µg ml⁻¹).

H-RasV12-overexpressing senescent BJ cells were generated as described previously¹⁴. BrdU incorporation assays were carried out at least 1 week after cultures had fully entered the senescent state, as determined by ceased proliferation, DDR activation and SAHF formation. Ionizing radiation was induced by a high-voltage X-ray generator tube (Faxitron X-Ray Corporation). In general, WI-38 cells were exposed to 5 Gy and transformed cells (RKO, HCT116 and HeLa) to 2 Gy for the DDR foci formation studies. 5 Gy were used for the G2/M checkpoint assays and 10 Gy for the G1/S checkpoint assays.

Cherry-Lac and I-SceI-restriction endonuclease expressing vectors were transfected by lipofectamine 2000 (Invitrogen) in a ratio of 3:1. Sixteen hours after transfection around 70% of the cells were scored positive for DDR markers in the Lac array. For generation of DICER and DROSHA knockdown, NIH2/4 cells were infected with lentiviral particles carrying pLKO.1, shDICER or shDROSHA vectors. After 48 h cells were superinfected with Adeno Empty Vector (gift from E. Dejana) or Adeno I-SceI (gift from P. Ng). Nuclei were isolated the day after the adenoviral infection.

Antibodies. Mouse anti-γH2AX, anti-H3K9me3, rabbit polyclonal anti-pH3 (Upstate Biotechnology); anti-pS/TQ (Cell Signaling Technology); anti-H2AX, anti-H3 and anti-DICER (13D6) (Abcam); rabbit polyclonal anti-53BP1 (Novus Biological); mouse monoclonal anti-53BP1 (gift from T. Halazonetis); anti-MRE11 (gift from S. P. Jackson); anti-BrdU (Becton Dickinson); rabbit polyclonal anti-MCM2 (gift from M. Melixetian); anti-MRE11 rabbit polyclonal raised against recombinant MRE11; anti-pATM (Rockland); mouse monoclonal anti-ATM and anti-MDC1 (SIGMA); anti-Lamin A/C (Santa Cruz); anti-vinculin (clone hVIN-1), anti-β-tubulin (clone AA2) and anti-Flag M2 monoclonal antibodies (Sigma).

Indirect immunofluorescence. Cells were grown on poly-D-lysinated coverslips (poly-D-lysine was used at 50 µg ml⁻¹ final concentration) and plated (15–20 × 10³ cells per cover) 1 day before staining. DDR and BrdU staining was performed as described previously¹⁴. Cells were fixed in 4% paraformaldehyde or methanol:acetone 1:1. NIH2/4 mouse cells were fixed by 4% paraformaldehyde as described previously²⁴. Images were acquired using a wide field Olympus Biosystems Microscope BX71 and the analySIS or the MetaMorph software (Soft Imaging System GmbH). Comparative immunofluorescence analyses were performed in parallel with identical acquisition parameters; at least 100 cells were screened for each antigen. Cells with more than two DDR foci were scored positive. Confocal sections were obtained with a Leica TCS SP2 or AOBS confocal laser microscope by sequential scanning.

Plasmids. DICER-Flag, DICER44ab-Flag and DICER110ab-Flag were a gift from R. Shiekhattar. DICER110ab-Flag and DICER44ab-Flag double mutants carry two amino acid substitutions in the RNase III domains of DICER (Asp 1320 Ala and Asp 1709 Ala for 44ab, and Glu 1652 Ala and Glu 1813 Ala for 110ab mutant; both mutants were reported to be deficient in endonuclease activity¹⁶). pLKO.1 shDICER-expressing vector was a gift from W. C. Hahn. Short hairpin sequence for DICER is: CCGGCCACACATCTCAAGACTTAAGT CGAGTTAACGTCITGAAGATGTGGTTTTG. pRETROSUPER shp53 was as described previously¹⁴. Short hairpin sequence for p53 was: AGTAGATTAC CACTGGAGTCTT. Cherry-Lac-repressor and I-SceI-restriction endonuclease expressing vectors were gifts from E. Soutoglou²⁴. shRNA against mouse DICER- and DROSHA-expressing vectors were a gift from W. C. Hahn. shRNA for mouse DICER: CCGGGCCTCACITGACCTGAAGTATCTCGAGA TACTTCAGGTCAAGTGAGGCTTTT. shRNA for mouse DROSHA: CCGG CCTGAAATATGTCCACACTTCTCGAGAAAGTGTGGACATATTCCAGG TTTTG.

siRNA. The DHARMACON siGENOME SMARTpool siRNA oligonucleotide sequences for human 53BP1, ATM, DICER, DROSHA were as follows. 53BP1: GAGAGCAGAUGAUCCUUUA; GGACAAGUCUCAGCUAU; GAUAUC AGC UUAGACAAU; GGACAGAACCGCAGAUU. ATM: GAAUGUU GCUUUCUGAAU; AGACAGAAUUCCAAUAU; UUAUACACC UGUU UGUUAG; AGGAGGAGCUGGGCCUU. DICER: UAAAGUAGCUGGAA UGAUG; GGAAGAGGCUACUAUGAA; GAAUAUCGAUCCUAUGUUC; GAUCCUAUGUCAACUAA. DROSHA: CAACAUAGACUACACGAUU;

CCAACUCCCUCGAGGAUUA; GGCCAACUGUUUAAGAAUA; GAGUAG GCUUCGUGACUUA.

The DHARMACON siGENOME si RNA sequences for human TNRC6A, B and C were as follows. GW182/TNRC6A: GAAAUGCUCUGGUCCGCUA; GCCUAAAUAUUGGUGAUUA. TNRC6B: GCACUGCCCUGAUCCGAUA; GGAAUUAAGUCGUCGUCAU. TNRC6C: CUAAUAACCUCGCCAAUUA; GGUAAGGUCCAUUGAUG.

siRNA against human DICER 3' UTR: CCGUGAAAGUUUAACGUUU. siRNA against GFP: AACACUUGUCACUACUUCUC. siRNA against luciferase: CAUUCUAUCCCUAGAGGAUGdTdT; dTdTGAAGAUAGGAGAUC UCCUAC.

siRNAs were transfected by Oligofectamine or Lipofectamine RNAi Max (Invitrogen) at a final concentration of 200 nM in OIS cells and 100 nM in HNFs. In the siRNA titration experiment OIS cells were transfected in parallel with 20 nM and 200 nM siRNA oligonucleotides. For siRNA transfection with deconvolved siRNA oligonucleotides we used 50 nM for smart pools and 12.5 nM for deconvolved siRNAs.

Real-time quantitative PCR. Total RNA was isolated from cells using TRIzol (Invitrogen) or RNAeasy kit (Qiagen) according to the manufacturer's instructions, and treated with DNase before reverse transcription. For small RNA isolation we used the mirVana miRNA Isolation Kit (Ambion). cDNA was generated using the Superscript II Reverse Transcriptase (Invitrogen) and used as a template in real-time quantitative PCR analysis. TaqMan MicroRNA Assays (Applied Biosystems) were used for the evaluation of mature miR-21 and rnu44 and rnu19 expression levels (assay numbers 000397, 001094 and 001003). 18S or β-actin was used as a control gene for normalization. Real-time quantitative PCR reactions were performed on an Applied Biosystems ABI Prism 7900HT Sequence Detection System or on a Roche LightCycler 480 Sequence Detection System. The reactions were prepared using SyBR Green reaction mix from Roche. Ribosomal protein P0 (RPP0) was used as a human and mouse control gene for normalization.

Primer sequences for real-time quantitative PCR. RPP0: TTCTATTGTGGGAG CAGAC (forward), CAGCAGTTCTCCAGAGC (reverse); human endogenous DICER: AGCAACACAGAGATCTAACATT (forward), GCAAAGCAGG GCTTTTCAT (reverse); human endogenous and overexpressed DICER: TGTTCCAGGAAGACCAGGTT (forward), ACTATCCCTCAAACACTCT GGAA (reverse); human DROSHA: GGCCCCGAGAGCCTTTATAG (forward), TGCACACGCTTAACCTTCCAC (reverse); human GW182: CAGCCAGTCA GAAAGCAGT (forward), TGTGAGTCCAGGATCTGCTACTT (reverse); mouse DICER: GCAAGGAATGGACTCTGAGC (forward), GGGGACTTCG ATATCCTCTTC (reverse); mouse DROSHA: CGTCTCTAGAAAGGTCTAC AAGAA (forward), GGCTCAGGAGCAACTGGTAA (reverse).

RNase A treatment and RNA complementation experiments. Cells were plated on poly-D-lysinated coverslips and irradiated with 2 Gy of ionizing radiation. One hour later HeLa cells were permeabilized with 2% Tween 20 in PBS for 10 min at room temperature while I-SceI-transfected NIH2/4 cells were permeabilized in 0.5% Tween 20 in PBS for 10 min at room temperature. RNase A treatment was carried out in 1 ml of 1 mg ml⁻¹ ribonuclease A from bovine pancreas (Sigma-Aldrich catalogue no. R5503) in PBS for 25 min at room temperature. After RNase A digestion, samples were washed with PBS, treated with 80 units of RNase inhibitor (RNaseOUT Invitrogen 40 units µl⁻¹) and 20 µg ml⁻¹ of α-amanitin (Sigma) for 15 min in a total volume of 70 µl. For experiments with mirin, NIH2/4 cells were incubated at this step also with 100 µM mirin (Sigma) or DMSO for 15 min. Then, RNase-A-treated cells were incubated with total, small or gel-extracted RNA, or the same amount of tRNA, for an additional 15 min at room temperature. If using mirin, NIH2/4 cells were incubated with total RNA in the presence of 100 µM mirin or DMSO for 25 min at room temperature. Cell were then fixed with 4% paraformaldehyde or methanol:acetone 1:1.

In complementation experiments with synthetic RNA oligonucleotides, eight RNA oligonucleotides with the potential to form four pairs were chosen among the sequences that map at the integrated locus in NIH2/4 cells, obtained by deep sequencing. Synthetic RNA oligonucleotides were generated by Sigma with a monophosphate modification at the 5' end. Sequences map to different regions of the integrated locus: two pairs map to a unique sequence flanking the I-SceI restriction site, one to the Lac-operator and one to the Tet-operator repetitive sequences. Two paired RNA oligonucleotides with the sequences of GFP were used as negative control. Sequences are reported below.

Oligonucleotide 1: 5'-AUUACAAUUGUGGAAUUCGGCGC-3', oligonucleotide 2: 5'-CGAAUUCACAAUUGUUAUC-3', oligonucleotide 3: 5'-AU UUGUGGAAUUCGGCCUUCAGAGUCGAGG-3', oligonucleotide 4: 5'-CC UCGACUCUAGAGGGC-3', oligonucleotide 5: 5'-AGCGGAUACAAUUA UGGGCCACAUGUGGA-3', oligonucleotide 6: 5'-UGUGGCCACAAUUG UU-3', oligonucleotide 7: 5'-ACUCCCUAUCAGUGAUAGAGAAAAGUGA

AAGU-3', oligonucleotide 8: 5'-CUUCACUUUCUCUAUCACUGAUAGG GAGUG-3'. GFP 1: 5'-GUUCAGCGUGUCCGGCGAGUU-3', GFP 2: 5'-CU CGCCGGACACGCUGAACUUU-3'.

RNAs were resuspended in 60 mM KCl, 6 mM HEPES, pH 7.5, 0.2 mM MgCl₂, at the stock concentration of 12 μM, denatured at 95 °C for 5 min and annealed for 10 min at room temperature.

DICER RNA products were generated as follows. A 550-bp DNA fragment carrying the central portion of the genomic locus studied (three Lac repeats, the I-SceI site and two Tet repeats) was flanked by T7 promoters at both ends and was used as a template for *in vitro* transcription with the TurboScript T7 transcription kit (AMSBIO). The 500-nucleotide-long RNAs obtained were purified and incubated with human recombinant DICER enzyme (AMSBIO) to generate 22–23-nucleotide RNAs. RNA products were purified, quantified and checked on gel. As a control, the same procedure was followed with a 700-bp construct containing the RFP DNA sequence. Equal amounts of DICER RNA products generated in this way were used in a complementation experiment in NIH2/4 cells following RNase A treatment.

Small RNA preparation. Total RNA was isolated from cells using TRIzol (Invitrogen) according to the manufacturer's instructions. To generate small RNA-enriched fraction and small RNA-devoid fraction we used the *mir*Vana microRNA Isolation Kit (Ambion) according to the manufacturer's instructions. The *mir*Vana microRNA isolation kit uses an organic extraction followed by immobilization of RNA on glass-fibre (silica-fibres) filters to purify either total RNA, or RNA enriched for small species. For total RNA extraction ethanol is added to samples, and they are passed through a filter cartridge containing a glass-fibre filter, which immobilizes the RNA. The filter is then washed a few times and the RNA is eluted with a low ionic-strength solution. To isolate RNA that is highly enriched for small RNA species, ethanol is added to bring the samples to 25% ethanol. When this lysate/ethanol mixture is passed through a glass-fibre filter, large RNAs are immobilized, and the small RNA species are collected in the filtrate. The ethanol concentration of the filtrate is then increased to 55%, and it is passed through a second glass-fibre filter where the small RNAs become immobilized. This RNA is washed a few times, and eluted in a low ionic strength solution. Using this approach consisting of two sequential filtrations with different ethanol concentrations, an RNA fraction highly enriched in RNA species ≤200 nucleotides can be obtained^{18,27}.

RNA extraction from gel. Total RNA samples (15 ng) were heat denatured, loaded and resolved on a 15% denaturing acrylamide gel (1× TBE, 7 M urea, 15% acrylamide (29:1 acryl:bis-acryl)). Gel was run for 1 h at 180 V and stained in GelRed solution. Gel slices were excised according to the RNA molecular weight marker, moved to a 2 ml clean tube, smashed and RNA was eluted in 2 ml of ammonium acetate 0.5 M, EDTA 0.1 M in RNase-free water, rocking overnight at 4 °C. Tubes were then centrifuged 5 min at top speed, the aqueous phase was recovered and RNA was precipitated and resuspended in RNase free water.

G1/S checkpoint assay. WI-38 cells were irradiated with 10 Gy and 1 h afterwards incubated with BrdU (10 μg ml⁻¹) for 7 h; HCT116 cells were irradiated at 2 Gy and incubated with BrdU for 2 h. Cells were fixed with 4% paraformaldehyde and probed for BrdU immunostaining. At least 100 cells per condition were analysed.

G2/M checkpoint assay. HEK 293 calcium phosphate transfected cells were irradiated with 5 Gy and allowed to respond to ionizing-radiation-induced DNA damage in a cell culture incubator for 12, 24 or 36 h. Then, at these three time points after irradiation, together with non-irradiated cells, 1 × 10⁶ cells were collected for fluorescence activated cell sorting (FACS) analysis, fixed in 75% ethanol in PBS, 30 min on ice. Afterwards, cells were treated 12 h with 250 μg ml⁻¹ of RNase A and incubated for at least 1 h with propidium iodide (PI). FACS profiles were obtained by the analysis of at least 5 × 10⁵ cells. In the complementation experiments HEK 293 cells were transfected using Lipofectamine RNAi Max (Invitrogen) and 48 h later irradiated with 5 Gy. Cells were then treated as explained above.

Immunoblotting. Cells were lysed in sample buffer and 50–100 μg of whole cell lysates were resolved by SDS-PAGE, transferred to nitrocellulose and probed as previously described¹⁴.

For zebrafish immunoblotting protein analysis, 72 h post-fertilization (hpf) larvae were deyolked in Krebs Ringer's solution containing 1 mM EDTA, 3 mM PMSF and protease inhibitor (Roche complete protease inhibitor cocktail). Embryos were then homogenized in SDS sample buffer containing 1 mM EDTA with a pestle, boiled for 5 min and centrifuged at 13,000 r.p.m. for 1 min. Protein concentration was measured with the BCA method (Pierce) and proteins (50–900 μg) were loaded in an SDS-12% (for γH2AX and H3) and SDS-6% polyacrylamide gel (for pATM and ATM), transferred to a nitrocellulose membrane, and incubated with anti-γH2AX (1:2,000, a gift from J. Amatruda²⁸), H3 (1:10,000, Abcam), pATM (1:1,000, Rockland), ATM (1:1,000, Sigma). Immunoreactive bands were detected with horseradish-peroxidase-conjugated

anti-rabbit or anti-mouse IgG and an ECL detection kit (Pierce). Protein loading was normalized to equal amounts of total ATM and H3.

Zebrafish embryo injection, cell transplantation and staining. Zebrafish embryos at the stage of 1–2 cells were injected with a morpholino against Dicer¹⁹ diluted in Danieau buffer. The morpholino oligonucleotide was injected at a concentration of 5 ng nl⁻¹, and a volume of 2 nl per embryo. To assess the efficiency of the morpholino to block miRNA maturation, we co-injected the morpholino with *in vitro* synthesized mRNA, encoding for red fluorescent protein (RFP) and carrying three binding sites for miR126 in the 3' UTR¹⁷. The oligonucleotides carrying the binding sites for miR126 used for construction of the pCS2:RFPmiR126 sensor are: 5'-GCATTATTACTCACGGTACGAATAAGG CATTATTACTCACGGTACGAATAAGCATTATTACTCACGGTACGA-3' and 5'-CGTAATAATGAGTGCCATGCCATGCTTATTCGTAATAATGAGTGCCA TGCTTATTCGTAATAATGAGTGCCATGCT-3'. The construct was verified by sequencing and used to synthesize mRNA *in vitro* using the mMessage Kit (Ambion). mRNA encoding for RFPmiR126 sensor was injected alone or in combination with Dicer1 morpholino at a concentration of 10 pg nl⁻¹. For cell transplantation experiments, we injected donor embryos with a mixture of *dicer* morpholino and mRNA encoding for GFP (5 pg nl⁻¹). Approximately 20 cells were transplanted from donor embryos at dome stage (5 hpf) to uninjected host at the same stage. Successfully transplanted larvae (displaying GFP+ cells) were irradiated as described below. Mature miRNAs were reverse transcribed to produce six different cDNAs for TaqMan MicroRNA assay (30 ng of total mRNA for each reaction; Applied Biosystems). Real-time PCR reactions based on TaqMan reagent chemistry were performed in duplicate on ABI PRISM 7900HT Fast Real-Time PCR System (Applied Biosystems). The level of miRNA expression was measured using *C_T* (threshold cycle). Fold change was calculated as 2^{-ΔC_T}.

For immunofluorescence in zebrafish larvae, 72 hpf larvae were irradiated with 12 Gy, fixed in 2% paraformaldehyde for 2 h at room temperature. After equilibration in 10 and 15% sucrose in PBS, larvae were frozen in OCT compound on coverslips on dry ice. Sections were cut with a cryostat at a nominal thickness of 14 μm and collected on Superfrost slides (BDH). Antisera used were zebrafish γH2AX (gift from J. Amatruda²⁸) and pATM (Rockland). GFP fluorescence in transplanted embryos was still easily visible in fixed embryos. Images were acquired with a confocal (Leica SP2) microscope and ×63 oil immersion lens.

RNA sequencing. Nuclear RNA shorter than 200 nucleotides was purified using *mir*Vana microRNA Isolation Kit. RNA quality was checked on a small RNA chip (Agilent) before library preparation. For Illumina hi Seq Version3 sequencing, spike RNA was added to each RNA sample in the RNA: spike ratio of 10,000:1 before library preparation and libraries for Illumina GA IIx were prepared without spike. An improved small RNA library preparation protocol was used to prepare libraries³⁰. In brief, adenylated 3' adaptors were ligated to 3' ends of 3'-OH small RNAs using a truncated RNA ligase enzyme followed by 5' adaptor ligation to 5'-monophosphate ends using RNA ligase enzyme, ensuring specific ligation of non-degraded small RNAs. cDNA was prepared using a primer specific to the 3' adaptor in the presence of dimer eliminator and amplified for 12–15 PCR cycles using a special forward primer targeting the 5' adaptor containing additional sequence for sequencing and a reverse primer targeting the 3' adaptor. The amplified cDNA library was run on a 6% polyacrylamide gel and the 100 bp band containing cDNAs up to 33 nucleotides long was extracted using standard extraction protocols. Libraries were sequenced after quality check on a DNA high sensitivity chip (Agilent). Multiplexed barcode sequencing was performed on Illumina GA-IIx (35 bp single end reads) and Illumina Hi seq version3 (51 bp single end reads).

Statistical analyses. Results are shown as means ± s.e.m. *P* value was calculated by Chi-squared test. Quantitative PCR with reverse transcription results are shown as means of a triplicate ± standard deviation (s.d.) and *P* value was calculated by Student's *t*-test as indicated. *n* stands for number of independent biological experiments.

Statistical analysis of small RNA sequencing data. Statistical significance of downregulation of normalized miRNAs in DICER and DROSHA knockdown samples was calculated using the Wilcoxon signed-rank test.

The differences in the fraction of 22–23 nucleotides versus total small RNAs at the locus between the wild-type, DICER knockdown and DROSHA knockdown before and after cut were calculated by fitting a negative binomial model to the small RNAs count data and performing a likelihood ratio test, keeping the fraction of 22–23-nucleotide versus total small RNAs at the locus fixed across conditions under the null hypothesis and allowing it to vary between conditions under the alternative hypothesis.

27. Duchaine, T. F. et al. Functional proteomics reveals the biochemical niche of *C. elegans* DCR-1 in multiple small-RNA-mediated pathways. *Cell* **124**, 343–354 (2006).
28. Sidi, S. et al. Chk1 suppresses a caspase-2 apoptotic response to DNA damage that bypasses p53, Bcl-2, and caspase-3. *Cell* **133**, 864–877 (2008).

29. Wienholds, E., Koudijs, M. J., van Eeden, F. J., Cuppen, E. & Plasterk, R. H. The microRNA-producing enzyme Dicer1 is essential for zebrafish development. *Nature Genet.* **35**, 217–218 (2003).
30. Kawano, M. et al. Reduction of non-insert sequence reads by dimer eliminator LNA oligonucleotide for small RNA deep sequencing. *Biotechniques* **49**, 751–755 (2010).

Chapter 4

Rett syndrome and piRNAs

Mutations in the gene methyl CpG binding protein 2 (MECP2) are the cause of most cases of Rett syndrome (RTT), a neurodevelopmental disorder that affects girls almost exclusively. Given that the MECP2 protein contains a methyl-CpG binding domain (MBD) and can recruit histone deacetylases, they are largely considered as transcriptional repressors. In rodents, the absence of MeCP2 leads to an increase in long interspersed nuclear elements-1 (L1) neuronal transcription and retrotransposition (Muotri et al., 2010). Furthermore, by analysing neuronal progenitor cells (derived from fibroblasts using induced pluripotent stem cell technology) and post mortem human tissues from patients with RTT, it was revealed elevated L1 activity compared (Muotri et al., 2010). MeCP2 chromatin immuno-precipitation sequencing in mice whole brain also suggested that MeCP2 may play a role in silencing retrotransposons (Skene et al., 2010). A class of small RNAs called piwi-interacting RNAs (piRNAs), can be derived from L1 elements, and are involved in silencing transposons, by forming the piRNA-induced silencing complex (piRISC). In this work, we¹ analysed a short RNA library prepared from cerebellum of mice with a Mecp2 knock-out (Wu et al., 2010). Our analyses revealed that hundreds of piRNAs are expressed in the cerebellum, including previously characterised brain-specific piRNAs. Furthermore, we found that in the Mecp2 knock-out mice, a large number of piRNAs were over-expressed, suggesting that piRNA expression levels may also be affected by the absence of Mecp2. While piRNAs are thought to function mainly as silencers for transposons in germ cells, this study suggests that a subset of piRNAs may have other roles in gene regulation.

¹All the bioinformatic analysis was performed by Dave Tang.

piRNAs warrant investigation in Rett Syndrome: An omics perspective

Alka Saxena*, Dave Tang and Piero Carninci
RIKEN Omics Science Center, Yokohama, Japan

Abstract. Mutations in the *MECP2* gene are found in a large proportion of girls with Rett Syndrome. Despite extensive research, the principal role of MeCP2 protein remains elusive. Is MeCP2 a regulator of genes, acting in concert with co-activators and co-repressors, predominantly as an activator of target genes or is it a methyl CpG binding protein acting globally to change the chromatin state and to suppress transcription from repeat elements? If MeCP2 has no specific targets in the genome, what causes the differential expression of specific genes in the *Mecp2* knockout mouse brain? We discuss the discrepancies in current data and propose a hypothesis to reconcile some differences in the two viewpoints. Since transcripts from repeat elements contribute to piRNA biogenesis, we propose that piRNA levels may be higher in the absence of MeCP2 and that increased piRNA levels may contribute to the mis-regulation of some genes seen in the *Mecp2* knockout mouse brain. We provide preliminary data showing an increase in piRNAs in the *Mecp2* knockout mouse cerebellum. Our investigation suggests that global piRNA levels may be elevated in the *Mecp2* knockout mouse cerebellum and strongly supports further investigation of piRNAs in Rett syndrome.

Keywords: Rett Syndrome, MeCP2, piRNAs, LINE 1, short RNAs

Rett Syndrome (RTT), a severe neurodevelopmental disorder, leads to intellectual disability in girls. After a normal prenatal and postnatal period, patients usually present with developmental delay between 6 and 18 months of age, followed by the development of stereotypic hand movements and loss of acquired skills including voluntary hand use, language and communication. This regression is characteristic of Rett Syndrome which, in 97% of clinically diagnosed classic cases and 70% of atypical cases, is caused by mutations in the methyl CpG binding protein 2 gene, (*MECP2*) [1]. In some patients with atypical Rett Syndrome, where some but not all clinical features are seen, mutations in *CDKL5* [2] or *FOXP1* [3] are found, albeit infrequently. Diagnosis of Rett Syndrome is based on clinical criteria [4] and confirmed upon detection of a mutation in *MECP2*, *CDKL5* or *FOXP1*. However, in approximately 20% of girls clinically diagnosed with classic or atypical Rett syndrome, mutations cannot be detected in either of these genes.

MECP2 gene undergoes X chromosome inactivation (XCI) [5], which means that in any cell with two

X chromosomes, RNA transcripts arise only from the *MECP2* gene on the active X chromosome. This is because the *MECP2* gene on the inactive X chromosome has been silenced. Chaumeil et al. demonstrated, through in-situ hybridization in mouse ES cells, that the *Mecp2* gene moves inside the silencing compartment of *Xist* on the 4th day after differentiation [6]. Although some genes are known to escape X inactivation in humans and mouse [7–10], Carrel et al. showed using rodent/human somatic hybrid cell lines that in humans *MECP2* transcripts are not expressed from the inactive X chromosome [7]. Due to the random nature of X inactivation, part of the clinical variability in RTT is attributed to the differences in the X inactivation status of patients [11–13], however more recent data suggest X inactivation status may not adequately explain the phenotypic variations [14].

MECP2 gene is composed of 4 exons and generates two transcripts which encode two nearly identical protein isoforms [15,16]. MeCP2_e1, which commences translation from exon 1, is encoded from a transcript encompassing exons 1, 3 and 4; and MeCP2_e2, which starts translation from the end of exon 2, is generated from a transcript arising from exons 1, 2, 3 and 4, where exon 1 and most of exon 2 form the 5'UTR [15,

*Corresponding author: Alka Saxena, RIKEN Omics Science Center, Yokohama, Japan. E-mail: alka@gsc.riken.jp.

16]. Although *MECP2* is expressed in all tissues, semi-quantitative PCR analysis has shown that *Mecp2_e1* may have a higher expression level over *Mecp2_e2* in the brain [16]. Mutations in exons 3 and 4 affect both protein isoforms and are frequently found in Rett patients. Mutations in exon 1 can cause Rett syndrome despite the fact that mutations in exon 1 do not affect the coding region of the MeCP2_e2 protein. Interestingly, mutations in exon 2 of the gene, which have the potential to affect the MeCP2_e2 isoform alone, have so far not been found in patients. While earlier work on an Australian patient with a recurrent deletion in exon 1 of *MECP2* gene demonstrated the absence of MeCP2_e2 protein correlated with X inactivation status, suggesting translational interference from the mutation [17], a recent publication found no evidence of loss of MeCP2_e2 protein in a Canadian patient with a similar mutation indicating that some patients may present with clinical features of Rett syndrome even in the presence of a fully functional MeCP2_e2 isoform [18]. Interestingly, this data also suggests that despite high sequence similarities there is no functional redundancy between the two protein isoforms.

Due to its property to bind methylated DNA with high affinity and its association with repressor complexes consisting of HDAC1/2 and Sin3A, MeCP2 was believed to function as a transcriptional repressor [19, 20]. The MeCP2-DNA interaction was shown to result in chromatin compaction, which is also correlated with silencing of chromatin [21]. Subsequent studies revealed that MeCP2 had binding affinity to methylated DNA as well as non-methylated DNA [22]. Absence of MeCP2 in mouse brains also results in an increase in H3Ac levels, suggesting a role for MeCP2 in chromatin modification [23,24]. Recent data suggest that MeCP2 protein may be a regulator of transcription, acting in concert with activators as well as repressors to regulate gene expression. Yasui et al. first reported that promoter occupancy by MeCP2 may not result in gene silencing [25]. Using a custom tiling array of selected chromosomal regions totalling 26.3 Mb, they performed ChIP-chip analysis on SH-SY5Y cells with antibodies against MeCP2 and RNA polymerase II. The data revealed co-occupancy of MeCP2 and RNA Polymerase II at selected promoters suggesting that MeCP2 binding may not be correlated to gene repression [25]. Using ChIP-chip assays for 24,275 promoters, they demonstrated that only 2600–4300 promoters were occupied by MeCP2, of which 1534 promoters showed strongest enrichment. Comparison with gene expression arrays in the same cell lines revealed

that almost 63% of the “strongest” promoters were expressed in SH-SY5Y cells. Subsequent MeDIP-ChIP analysis revealed that just 2.2% of methylated promoters were occupied by MeCP2 [25]. These data were supported in part by Chahrour et al. who used microarrays to determine differentially expressed genes in the hypothalamus of 6 week old *Mecp2* knockout (KO) mouse and in the hypothalamus of a mouse model that overexpressed *Mecp2* under its endogenous promoter (Tg) [26]. Combining their data from the KO and Tg models, they identified 2561 genes as direct targets of MeCP2, of which ~85% were activated by MeCP2 and ~ 15% were repressed by MeCP2 [26]. Using mass spectrometry on proteins co-immunoprecipitated with an anti-MeCP2 antibody, they identified CREB1 as a co-activator associated with MeCP2 and demonstrated co-occupancy of the two proteins at an activated target *Sst* [26]. Together, these data established MeCP2 as an activator of transcription [25,26]. Thus transcriptional mis-regulation is believed to underlie the phenotype seen in patients with mutations in the *MECP2* gene. In view of the fact that FOXG1 is a member of the forkhead family of transcription regulators, it is likely that in patients carrying mutations in *FOGX1*, mis-regulation of genes may contribute to the phenotypic features. The molecular pathology leading to the clinical phenotype of Rett Syndrome in mutation negative patients remains unknown. While much has been reported on the mis-regulation of specific genes after MeCP2 knockdown (KD) or KO, such studies have not yet been reported for FOXG1. Other studies reveal subtle changes in the expression levels of specific genes after MeCP2 KD or in the *Mecp2* KO mouse brain rather than genome wide transcriptional mis-regulation [27–29].

However, a recent report suggests that the absence of a functional MeCP2 may result widespread mis-regulation of repeat elements. Skene et al. investigated MeCP2 binding on selected loci in the mature mouse brain using ChIP-qPCR and demonstrated that MeCP2 was enriched all across the loci, but the enrichment was reduced over CpG islands, which are generally methylation free [24]. With bisulfite modification and sequencing of selected loci they demonstrated the recovery of predominantly methylated chromatin from the MeCP2 ChIP, re-emphasizing the role of MeCP2 as a methyl CpG binding protein [24]. Based on their investigation of the histone acetylation status by Western blotting and H3Ac ChIP-qPCR at 100 loci, they concluded that the association of MeCP2 with chromatin causes a genome-wide decrease in histone acetylation [24]. To investigate the binding sites of MeCP2

genome wide, Skene et al. performed MeCP2-ChIP-sequencing on the whole brain. Despite deep sequencing, they did not find peaks of MeCP2 occupancy, but found reads which coincided with methylated regions of the genome. Since they did not uncover specific binding targets of MeCP2 in the genome, they hypothesized that MeCP2 may act at a global level, most likely to suppress transcription from the repeat regions of the genome [24]. Using qPCR, they demonstrated a 1.6 fold increase in transcripts arising from repeat sequences such as LINE-1, intra-cisternal A particles (IAPs) and major satellite DNA in the nuclear fraction of the *Mecp2* KO mouse brain. Based on their data they proposed that MeCP2 functions to repress spurious transcription of repeat elements [24] rather than to activate specific gene targets. An earlier investigation into the association between MeCP2 and LINE-1 and Alus had revealed that MeCP2 repressed LINE-1 expression and transposition, but activated Alu expression [30]. The role of MeCP2 in repressing transcription and transposition of LINE-1 elements was also corroborated by independent studies from the Gage Lab that showed that LINE-1 is over expressed in neuron progenitor cells after KD of MeCP2 and in neurons derived from Rett patients [31]. The data from Yasui et al. suggests that MeCP2 displays limited binding to methylated sites [25] and from Chahrour et al. proposes that MeCP2 acts as a transcriptional activator of specific targets [26]. In contrast, the data from Skene et al. suggests that MeCP2 binds methylated DNA, is a modulator of global chromatin state and may not have specific gene targets [24]. We note that some of these studies were conducted using microarrays or custom tiling arrays, which are generally limited to gene specific probes and exclude repeat sequences. Despite contradictory inferences on MeCP2 function, the fact remains that specific genes are mis-expressed and repeat elements are over-expressed in *Mecp2* KO mice. To reconcile the two opposing views, an alternative model would suggest that the key role of MeCP2 is to silence LINEs and similar repeat elements globally and that the observed mis-expression of genes is a downstream consequence of mis-expressed repeat elements.

Several recent reports suggest that non-coding RNAs play a role in the regulation of transcription through epigenetic modifications, [for a review see [32]]. Repeat elements, particularly LINEs, are known to participate in the silencing of genes on the X chromosome [33]. Expression of LINEs in the vicinity of genes is instrumental for their inclusion into the Xist silencing compartment [33]. It is not yet known whether transcripts

from LINE elements are associated with chromatin remodelling complexes to mediate epigenetic changes and fine-tune gene transcription, but we note that the elevated repeat elements were found in the nuclear compartment of the *Mecp2* KO mouse brain cells [24] and there is emerging evidence of enrichment of LINEs in nuclear and chromatin fraction of cells [34]. A recent report using a retrotransposon capture sequencing technique (RC-seq) reveals that somatic transposition of LINE-1 (L1) in the hippocampus results in insertions, predominantly in exons and introns of protein coding genes [35]. Comparing microarray data with their RC-seq data, Baillie et al. reported that intronic L1 insertions are likely to cause overexpression of such genes in the brain, suggesting a regulatory role for L1 [35]. It is not clear if the increase in retrotransposon expression in the *Mecp2* KO brain leads to their active transposition even in post mitotic neurons. Random integration of transposons is suppressed in differentiated somatic cells by transcriptional [36] and post-transcriptional mechanisms [37]. It would be interesting to investigate if somatic retrotransposition is increased in the *Mecp2* KO brain and whether overexpressed genes identified in *Mecp2* KO mouse show novel intronic L1 insertion events.

Retrotransposons such as LINEs can be further processed into short 21–24 nucleotide double stranded siRNAs [38] or into single stranded 24–31 nucleotide long piRNAs [39,40]. Watanabe et al. described in mouse oocytes dicer dependent double stranded endogenous siRNAs mapping exclusively to retrotransposons or expressed mRNA transcripts [38]. While the presence of endogenous siRNAs has not been demonstrated in the mouse brain, given that such short RNAs are shown to regulate the expression levels of specific genes and specific retrotransposons [38,41], and that dysfunctional MeCP2 may result in the overexpression of LINE-1 [24,31], it would be interesting to investigate the presence of endogenous siRNAs in the MeCP2 KO mouse brain.

piRNAs are germ line specific short RNAs of size 24 to 31 nucleotides generated through dicer independent processing of long single strand RNA transcripts. piRNAs interact with the PIWI proteins (MILI, MIWI and MIWI2 in mouse) [39,40] and their function, though not fully understood, appears to relate to silencing of transposons especially LINE-1 [39,40,42] intracisternal A particles [39,40] and specific genes through DNA hypermethylation [43]. In mouse testis, 17% of piRNAs bound to the MIWI protein map to repeats including LINEs, SINEs and LTRs [40]. In addition, through

a unique ping-pong cycle, piRNAs are amplified from existing retrotransposon transcripts, mostly LINE-1 elements [44,45]. This amplification cycle also results in the depletion of LINE-1 in germ line cells and is believed to deplete the levels of retrotransposon transcripts after differentiation [42]. Thus piRNAs regulate expression of LINEs and Intracisternal A particles both transcriptionally and post transcriptionally. Interestingly, piRNAs have recently been shown to regulate expression of a single imprinted gene in an imprinted locus in mouse spermatogonia via DNA methylation by piRNA targeting of a non coding RNA (pi-tRNA) arising from the locus [43]. It is as yet not known if such specific targeting by piRNAs is a widespread phenomenon, nevertheless it highlights a mechanism through which piRNAs may regulate expression of specific genes.

Until recently, piRNAs and their associated proteins were presumed to be germ line specific in mouse, but a report published last year confirmed the presence of MIWI and its associated piRNAs in the mouse hippocampus through sequencing, RIP-qPCR, northern blots, western blots and in situ hybridization studies [46]. Through bioinformatics analysis, Lee et al. identified specific piRNAs expressed in the brain and showed through piRNA inhibition studies, that one piRNA in the brain, DQ541777, may play a role in regulating the size of dendritic spines [46]. It appears plausible that in the absence of MeCP2, over expression of repeat elements, particularly LINE-1 may result in an increase in piRNA amplification from transposons. It would be interesting to investigate whether akin to germ line cells, in brain also, the increase in piRNAs result in depletion of retrotransposon transcript levels through transcriptional and post transcriptional silencing. The mechanism of transcriptional silencing by piRNAs through DNA methylation may require recruitment of repressor complexes by proteins that bind methylated DNA, including MeCP2, thus highlighting a feedback loop for MeCP2 requirement.

To investigate our hypothesis that piRNAs may be overexpressed in the *Mecp2* KO mouse brain, we analysed a short RNA library made from mouse cerebellum [47]. To identify miRNAs differentially expressed in the cerebellum, Wu et al. performed short RNA sequencing of pooled 6 week old pre-symptomatic wild-type and *Mecp2* KO cerebellum ($n = 4$ in each pool) using the SOLiD version 2 sequencer [47]. We downloaded the pooled libraries from the DDBJ database (DDBJ accession number SRP005132). ncRNAs were downloaded from NONCODE version 3 [48] and a to-

tal of 75,814 mouse piRNAs were extracted from this database. As the SOLiD reads correspond to the 5' ends of small RNAs, we directly mapped the respective reads from the pooled WT and KO libraries, using SHRiMP version 2.2.2 [49] with the default parameters, to the mouse piRNAs. After mapping we corrected tag numbers for reads multi-mapping to more than one piRNA, so that if a read mapped equally well to 2 or more individual piRNA sequences, the tag numbers were divided by the number of times it multi mapped, followed by equal assignment to all the piRNAs. For expression analysis we did not take into consideration multi mapped reads that mapped to 5 or more piRNAs and also filtered out reads that had less than 5 tags in the KO samples. The tag numbers were normalized by tags per million before comparison between wildtype and KO samples. Our very preliminary analysis of piRNAs in the cerebellum reveals 357 piRNAs in the cerebellum libraries (Supplementary Table 1). While 81% (287) of the individual piRNAs found in the cerebellum have a higher expression in KO, 59% (208) piRNAs show an expression change of over 1.5 fold in the KO cerebellum compared with the wildtype (Fig. 1B and supplementary Table 1). Overall, we found a striking 1.9 fold increase in the total piRNAs in the KO cerebellum in comparison with the wildtype cerebellum (Table 1 and Fig. 1A) suggesting a global increase in piRNAs in the *Mecp2* KO sample. We next investigated whether the 20 most abundant piRNAs identified by Lee et al. in the mouse hippocampus were represented in the mouse cerebellum [46]. We found 19 out of the 20 piRNAs reported by Lee et al. in the cerebellum libraries (Table 2) including DQ 541777 (the piRNA implicated in regulating the size of dendritic spines) and of these, 12 piRNAs (60%) revealed a fold change of over 1.5 in the KO cerebellum (Table 2). Interestingly, DQ541777 is the 5th most abundant piRNA in the cerebellum libraries, the two most highly abundant piRNAs in the cerebellum libraries map to rRNA loci, which were incidentally excluded in the hippocampal analysis [46].

Based on our preliminary findings, we suggest a model for Rett Syndrome where, in the absence of a functional MeCP2, the over-expressed repeat elements lead to an increase in the total piRNAs. The over-represented piRNAs may function, not only to deplete the load of repeat transcripts in cells, but also to fine-tune the expression level of specific genes. Thus piRNA mis-regulation may contribute to some of the differences in gene expression seen in the *Mecp2* KO mouse brain.

While our analyses provide preliminary evidence of genome wide piRNA over-expression in the *Mecp2*

Table 1

piRNA analysis in the short RNA libraries made from 6 week old pooled cerebellum from the wildtype mouse and the *Mecp2* knockout mouse [38] (DDBJ accession number SRP005132)

	WT cerebellum	KO cerebellum
Read ID	SRR089647	SRR089648
Total sRNA reads	3660124	2789136
Total reads mapped to piRNAs (no filter)	362089	522238
Reads mapped to piRNAs (filter out < 5 reads in KO)	356283	518589
piRNA mapped tags normalized by TPM	97341.74762	185931.8441
Fold change (tpm normalized piRNAs over WT)	1	1.910093548

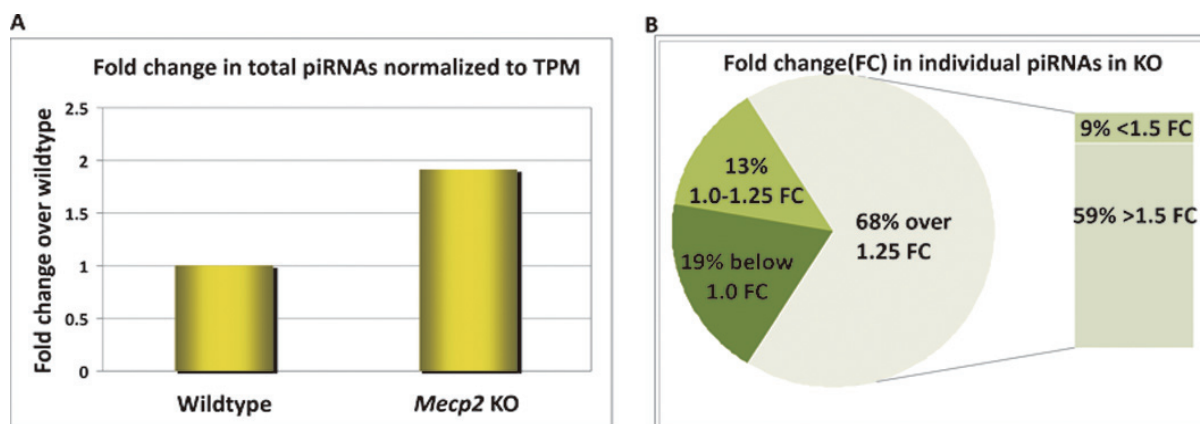


Fig. 1. piRNA levels are elevated in *Mecp2* KO cerebellum. Read numbers for individual piRNAs found in the wildtype (WT) and *Mecp2* knockout (KO) samples were normalized to tags per million as described in the text. After filtering out the piRNAs with less than 5 reads in the KO sample, the total piRNA reads were summed up. The histogram in panel A shows that the total numbers of piRNAs are almost doubled (1.9 fold) in the KO sample suggesting a global rise in piRNAs. The fold change relative to WT was calculated for each individual piRNA in KO. The pie chart in panel B reveals that 81% of piRNAs show a higher expression level in the KO sample. Of these, 59% have a fold change of over 1.5 in the KO sample (see supplementary Table 1). (Colours are visible in the online version of the article; <http://dx.doi.org/10.3233/DMA-2012-0932>)

KO cerebellum, this data was generated from libraries without replicates. Thus additional detailed investigations are warranted to affirm the over-representation of piRNAs and gain insights into the extent of their contribution to the gene mis-regulation seen in the Rett mouse model. We did not venture into the identification of gene targets of mis-regulated piRNAs and their intersection with the known mis-regulated genes or repeats. Such data may provide insights into the mis-regulation of some genes and the biogenesis of the over-represented piRNAs. Notably, in humans and mouse, an absence of MeCP2 results in fewer dendritic spines when compared with wildtype neurons [50,51]. While inhibition of DQ541777 was reported to cause a decrease in spine density, whether the overexpression of piRNAs, including DQ541777, can cause such morphological changes in the brain is not yet known. Further, recent reports have demonstrated that unlike mRNAs, miRNAs are stable in extracellular environments including blood serum [52,53]. Although such analyses have not been conducted for piRNAs, if piRNAs are found to be stable in extracellular fluids, differential-

ly expressed piRNAs may potentially represent clinical biomarkers for the diagnosis and prognosis of Rett Syndrome.

There is overwhelming complexity in unravelling the molecular pathogenesis of the phenotype seen in Rett syndrome. Although the miRNA repertoire of *Mecp2* KO cerebellum has been investigated using next generation sequencing approaches, the field would benefit in re-identifying mis-regulated transcripts through deep, long and short (to identify sRNAs other than miRNAs), RNA sequencing of specific brain regions. Additionally, RC-seq conducted to identify somatic integration events would reveal whether the overexpressed genes are correlated with intronic LINE-1 insertion events. And while it has been established for the *Mecp2* KO mouse model, that investigating a specific brain region is more fruitful than investigating the whole brain [26], analysis of neuronal subtypes would be even more insightful. Until now, the isolation of neuronal subtypes from adult mouse brain using high throughput techniques such as FACS sorting was challenging, yielding few nuclei and poor quality RNA. A recently pub-

Table 2
Comparison of the top twenty piRNAs reported in the hippocampus [38] with the piRNAs found in the cerebellum

Top 20 piRNAs in hippocampus	WT hippocampus tag numbers	WT cerebellum tag numbers	KO cerebellum tag numbers	WT cerebellum TPM	KO cerebellum TPM	FC KO/WT
DQ541777	16130	1995.50	2411.00	545.20	864.43	1.59
DQ705026	6257	154.00	377.00	42.08	135.17	3.21
DQ555094	3439	202.00	140.00	55.19	50.19	0.91
DQ719597	2459	168.00	306.00	45.90	109.71	2.39
DQ689086	1514	65.00	78.00	17.76	27.97	1.57
DQ540285	1433	457.40	548.23	124.97	196.56	1.57
DQ540981	1360	126.50	124.00	34.56	44.46	1.29
DQ720186	849	336.00	251.00	91.80	89.99	0.98
DQ555093	775	189.50	129.50	51.77	46.43	0.90
DQ540862	639	21.50	33.50	5.87	12.01	2.04
DQ540284	635	456.90	548.23	124.83	196.56	1.57
DQ541506	580	523.90	627.40	143.14	224.94	1.57
DQ539915	304	35.50	28.00	9.70	10.04	1.04
DQ540861	252	20.50	31.50	5.60	11.29	2.02
DQ715526	207	20.00	20.00	5.46	7.17	1.31
DQ543676	182	438.90	518.70	119.91	185.97	1.55
DQ722288	175	2.00	13.00	0.55	4.66	8.53
DQ551351	168	Not found	Not found	Not found	Not found	Not found
DQ550765	118	10.75	9.50	2.94	3.41	1.16
DQ708131	115	3.00	6.00	0.82	2.15	2.62

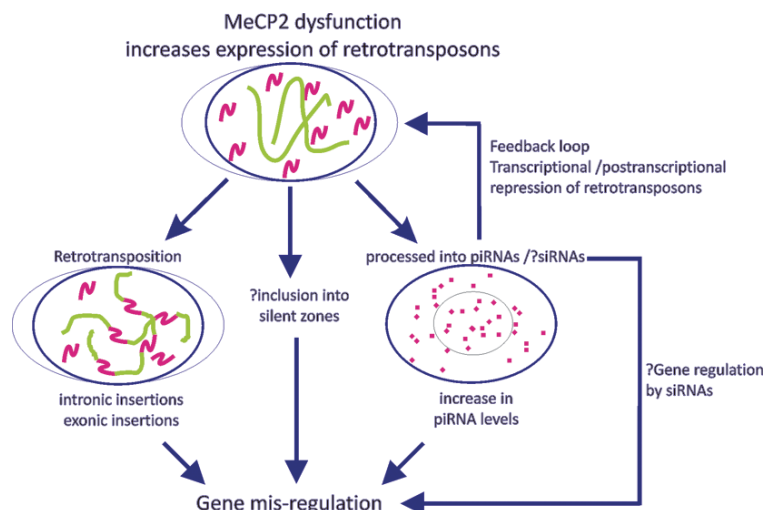


Fig. 2. Schematic of the proposed model showing that changes in the expression level of some genes may be a consequence of the increase in expression of retrotransposons. DNA is depicted in green, retrotransposon transcripts in pink and piRNAs as pink dots. See text for details. (Colours are visible in the online version of the article; <http://dx.doi.org/10.3233/DMA-2012-0932>)

lished trehalose enhanced technique for FACS sorting individual neuronal subtypes could help isolate high quality RNA from *Mecp2* null neuronal subtypes for transcriptome sequencing [54].

In conclusion, we propose that overexpression of LINE-1 may contribute to the mis-regulation of some genes in Rett syndrome, mediated through insertional events or by an increase in piRNAs (Fig. 2). Our preliminary data suggests that piRNA expression levels may be altered globally in the absence of MeCP2. Appli-

cation of next generation sequencing technologies may resolve some key questions regarding MeCP2 function and the downstream consequences of a dysfunctional MeCP2.

Acknowledgements

A.S. is supported by the Funding Program for Next Generation World-Leading Researchers by MEXT to

P.C and a MEXT Grant-in-Aid 321-EA-O-77; D.T. is supported by the European Union 7th Framework Programme under grant agreement FP7-People-ITN-2008-238055 (“BrainTrain” project) to P.C. and a Research Grant for RIKEN Omics Science Center from MEXT.

References

- [1] Amir, R.E., et al., Rett syndrome is caused by mutations in X-linked MECP2, encoding methyl-CpG-binding protein 2. *Nat Genet*, 1999. **23**(2): 185-8.
- [2] Weaving, L.S., et al., Mutations of CDKL5 cause a severe neurodevelopmental disorder with infantile spasms and mental retardation. *Am J Hum Genet*, 2004. **75**(6): 1079-93.
- [3] Ariani, F., et al., FOXG1 is responsible for the congenital variant of Rett syndrome. *Am J Hum Genet*, 2008. **83**(1): 89-93.
- [4] Neul, J.L., et al., Rett syndrome: revised diagnostic criteria and nomenclature. *Ann Neurol*, 2010. **68**(6): 944-50.
- [5] Adler, D.A., et al., The X-linked methylated DNA binding protein, MeCP2, is subject to X inactivation in the mouse. *Mamm Genome*, 1995. **6**(8): p. 491-2.
- [6] Chaumeil, J., et al., A novel role for Xist RNA in the formation of a repressive nuclear compartment into which genes are recruited when silenced. *Genes Dev*, 2006. **20**(16): 2223-37.
- [7] Carrel, L. and H.F. Willard, X-inactivation profile reveals extensive variability in X-linked gene expression in females. *Nature*, 2005. **434**(7031): 400-4.
- [8] Lingenfelter, P.A., et al., Escape from X inactivation of Smcx is preceded by silencing during mouse development. *Nat Genet*, 1998. **18**(3): 212-3.
- [9] Xu, J., X. Deng and C.M. Disteche, Sex-specific expression of the X-linked histone demethylase gene Jarid1c in brain. *PLoS One*, 2008. **3**(7): e2553.
- [10] Yang, F., et al., Global survey of escape from X inactivation by RNA-sequencing in mouse. *Genome Res*, 2010. **20**(5): 614-22.
- [11] Hoffbuhr, K.C., et al., Associations between MeCP2 mutations, X-chromosome inactivation, and phenotype. *Ment Retard Dev Disabil Res Rev*, 2002. **8**(2): 99-105.
- [12] Weaving, L.S., et al., Effects of MECP2 mutation type, location and X-inactivation in modulating Rett syndrome phenotype. *Am J Med Genet A*, 2003. **118A**(2): 103-14.
- [13] Huppke, P., et al., Very mild cases of Rett syndrome with skewed X inactivation. *J Med Genet*, 2006. **43**(10): 814-6.
- [14] Xinhua, B., et al., X chromosome inactivation in Rett Syndrome and its correlations with MECP2 mutations and phenotype. *J Child Neurol*, 2008. **23**(1): 22-5.
- [15] Kriaucionis, S. and A. Bird, The major form of MeCP2 has a novel N-terminus generated by alternative splicing. *Nucleic Acids Res*, 2004. **32**(5): 1818-23.
- [16] Mnatzakanian, G.N., et al., A previously unidentified MECP2 open reading frame defines a new protein isoform relevant to Rett syndrome. *Nat Genet*, 2004. **36**(4): 339-41.
- [17] Saxena, A., et al., Lost in translation: translational interference from a recurrent mutation in exon 1 of MECP2. *J Med Genet*, 2006. **43**(6): 470-7.
- [18] Gianakopoulos, P.J., et al., Mutations in MECP2 exon 1 in classical Rett patients disrupt MECP2_e1 transcription, but not transcription of MECP2_e2. *Am J Med Genet B Neuropsychiatr Genet*, 2012. **159B**(2): 210-6.
- [19] Nan, X., et al., Transcriptional repression by the methyl-CpG-binding protein MeCP2 involves a histone deacetylase complex. *Nature*, 1998. **393**(6683): 386-9.
- [20] Jones, P.L., et al., Methylated DNA and MeCP2 recruit histone deacetylase to repress transcription. *Nat Genet*, 1998. **19**(2): 187-91.
- [21] Georgel, P.T., et al., Chromatin compaction by human MeCP2. Assembly of novel secondary chromatin structures in the absence of DNA methylation. *J Biol Chem*, 2003. **278**(34): 32181-8.
- [22] Nikitina, T., et al., Multiple modes of interaction between the methylated DNA binding protein MeCP2 and chromatin. *Mol Cell Biol*, 2007. **27**(3): 864-77.
- [23] Shahbazian, M., et al., Mice with truncated MeCP2 recapitulate many Rett syndrome features and display hyperacetylation of histone H3. *Neuron*, 2002. **35**(2): 243-54.
- [24] Skene, P.J., et al., Neuronal MeCP2 is expressed at near histone-octamer levels and globally alters the chromatin state. *Mol Cell*, 2010. **37**(4): 457-68.
- [25] Yasui, D.H., et al., Integrated epigenomic analyses of neuronal MeCP2 reveal a role for long-range interaction with active genes. *Proc Natl Acad Sci U S A*, 2007. **104**(49): 19416-21.
- [26] Chahrour, M., et al., MeCP2, a key contributor to neurological disease, activates and represses transcription. *Science*, 2008. **320**(5880): 1224-9.
- [27] Urdinguo, R.G., et al., Mecp2-null mice provide new neuronal targets for Rett syndrome. *PLoS One*, 2008. **3**(11): e3669.
- [28] Yakabe, S., et al., MeCP2 knockdown reveals DNA methylation-independent gene repression of target genes in living cells and a bias in the cellular location of target gene products. *Genes Genet Syst*, 2008. **83**(2): 199-208.
- [29] Smrt, R.D., et al., Mecp2 deficiency leads to delayed maturation and altered gene expression in hippocampal neurons. *Neurobiol Dis*, 2007. **27**(1): 77-89.
- [30] Yu, F., et al., Methyl-CpG-binding protein 2 represses LINE-1 expression and retrotransposition but not Alu transcription. *Nucleic Acids Res*, 2001. **29**(21): 4493-501.
- [31] Muotri, A.R., et al., L1 retrotransposition in neurons is modulated by MeCP2. *Nature*, 2010. **468**(7322): 443-6.
- [32] Saxena, A. and P. Carninci, Long non-coding RNA modifies chromatin: epigenetic silencing by long non-coding RNAs. *Bioessays*, 2011. **33**(11): 830-9.
- [33] Chow, J.C., et al., LINE-1 activity in facultative heterochromatin formation during X chromosome inactivation. *Cell*, 2010. **141**(6): 956-69.
- [34] Djebali S, et al., Landscape of transcription in human cells. *Nature*, 2012. doi:10.1038/nature11233.
- [35] Baillie, J.K., et al., Somatic retrotransposition alters the genetic landscape of the human brain. *Nature*, 2011. **479**(7374): 534-7.
- [36] Slotkin, R.K. and R. Martienssen, Transposable elements and the epigenetic regulation of the genome. *Nat Rev Genet*, 2007. **8**(4): 272-85.
- [37] Yang, N. and H.H. Kazazian, Jr., L1 retrotransposition is suppressed by endogenously encoded small interfering RNAs in human cultured cells. *Nat Struct Mol Biol*, 2006. **13**(9): 763-71.
- [38] Watanabe, T., et al., Endogenous siRNAs from naturally formed dsRNAs regulate transcripts in mouse oocytes. *Nature*, 2008. **453**(7194): 539-43.
- [39] Aravin, A., et al., A novel class of small RNAs bind to MILI protein in mouse testes. *Nature*, 2006. **442**(7099): 203-7.
- [40] Girard, A., et al., A germline-specific class of small RNAs

- binds mammalian Piwi proteins. *Nature*, 2006. **442** (7099): 199-202.
- [41] Chen, L., et al., Naturally occurring endo-siRNA silences LINE-1 retrotransposons in human cells through DNA methylation. *Epigenetics*, 2012. **7**(7): 758-71.
- [42] Reuter, M., et al., Miwi catalysis is required for piRNA amplification-independent LINE1 transposon silencing. *Nature*, 2011. **480**(7376): 264-7.
- [43] Watanabe, T., et al., Role for piRNAs and noncoding RNA in de novo DNA methylation of the imprinted mouse Rasgrf1 locus. *Science*, 2011. **332**(6031): 848-52.
- [44] Brennecke, J., et al., Discrete small RNA-generating loci as master regulators of transposon activity in Drosophila. *Cell*, 2007. **128**(6): 1089-103.
- [45] Gunawardane, L.S., et al., A slicer-mediated mechanism for repeat-associated siRNA 5' end formation in Drosophila. *Science*, 2007. **315**(5818): 1587-90.
- [46] Lee, E.J., et al., Identification of piRNAs in the central nervous system. *RNA*, 2011. **17**(6): 1090-9.
- [47] Wu, H., et al., Genome-wide analysis reveals methyl-CpG-binding protein 2-dependent regulation of microRNAs in a mouse model of Rett syndrome. *Proc Natl Acad Sci U S A*, 2010. **107**(42): 18161-6.
- [48] Bu, D., et al., NONCODE v3.0: integrative annotation of long noncoding RNAs. *Nucleic Acids Res*, 2012. **40** (Database issue): D210-5.
- [49] David, M., et al., SHRiMP2: sensitive yet practical SHort Read Mapping. *Bioinformatics*, 2011. **27**(7): 1011-2.
- [50] Belichenko, P.V., et al., Widespread changes in dendritic and axonal morphology in MeCP2-mutant mouse models of Rett syndrome: evidence for disruption of neuronal networks. *J Comp Neurol*, 2009. **514**(3): 240-58.
- [51] Chapleau, C.A., et al., Dendritic spine pathologies in hippocampal pyramidal neurons from Rett syndrome brain and after expression of Rett-associated MECP2 mutations. *Neurobiol Dis*, 2009. **35**(2): 219-33.
- [52] Wang, K., et al., Export of microRNAs and microRNA-protective protein by mammalian cells. *Nucleic Acids Res*, 2010. **38**(20): 7248-59.
- [53] Turchinovich, A., et al., Characterization of extracellular circulating microRNA. *Nucleic Acids Res*, 2011. **39**(16): 7223-33.
- [54] Saxena, A., et al., Trehalose-enhanced isolation of neuronal sub-types from adult mouse brain. *Biotechniques*, 2012. **52**(6): 381-5.

Chapter 5

Regulated expression of repetitive elements

It is well established that the human genome is pervasively transcribed and this has been attributed to a “leaky” transcriptional system. Our observation that small RNAs are formed near the vicinity of DNA damaged sites and are required for establishing the DNA damage response, implies that all RNAs are potentially useful, since any site in the genome is vulnerable to DNA damage. A class of RNA that is often neglected from study are those that form from the repetitive portion of the genome. It is estimated that at least half of the human genome is made up of repetitive elements (REs) and transcription initiation has been observed within these elements (Faulkner et al., 2009). However, the general impression is that these elements are non-functional and are simply transcriptional noise. Motivated by the hypothesis that all RNAs could be potentially useful, we quantified and catalogued expression signal from REs using the FANTOM5 atlas.

The regulated expression of repetitive elements across human cell types and tissues

Dave Tang^{*1}, the FANTOM5 consortium, and Piero Carninci^{†1}

¹*RIKEN Center for Life Science Technologies (Division of
Genomic Technologies)*

November 12, 2014

Abstract

A large fraction of the human genome is composed of repetitive elements (REs), many of which are transposable elements (TEs). Most of these TEs are molecular fossils that have long lost the ability to transpose. However, transcription can initiate from these elements as they contain requisite signals necessary for transcription. However, it is unclear whether these transcriptional products have any functional purpose or are just transcriptional by-products. In order to address this question, we performed the most comprehensive survey of transcriptional events arising from TEs by using the FANTOM5 human atlas of Cap Analysis Gene Expression (CAGE) libraries, which consists of a large panel of human cell and tissues types (totalling 988 samples). We observed that TEs were lowly expressed on average compared to protein-coding genes, have restrictive expression patterns, overlap enhancer sequences, serve as precursors to small RNAs, and drive the transcription of long noncoding RNA. Furthermore, based on the expression patterns of TEs, we could associate families of TEs to specific sample ontologies that have been ascribed to the FANTOM5 samples. This hints at the fact that characteristics of certain families of TEs, such as their sequence composition, may be associated to factors that are specific to particular cell types. These lines of evidence support the hypothesis that various TEs have become exapted and have a functional role in the human genome.

^{*}Email: dave.tang@riken.jp

[†]Email: carninci@riken.jp; Corresponding author

1 Introduction

Roughly half of the human genome is made up of repetitive elements (REs), consisting mainly of completely inactive transposable elements (TEs) (Lander et al., 2001). The estimated number of active TEs in the human genome is less than 0.05% (Mills et al., 2007), which is as expected given that TEs are a major factor in causing mutations that lead to human disease (Callinan and Batzer, 2006). However, despite the detrimental effects of TEs, their ability to move around has shaped the evolution of the genomes in which they reside (Cordaux and Batzer, 2009). For example, TEs have been found to contribute transcription factor binding sites (TFBSs) to various mammalian transcription factors (Wang et al., 2007; Bourque et al., 2008; Kunarso et al., 2010) and it has been suggested that TEs have played a major part in wiring and re-wiring regulatory networks (Feschotte, 2008). This phenomenon has been observed in both humans and mice, where transcription factors pervasively bound to TEs (Kunarso et al., 2010). However the TEs that served as “repeatassociated binding sites” in human and mouse were from different families of endogenous retroviruses, suggesting the convergent evolution of TEs as binding sites. In addition to TFBSs, a recent study demonstrated that methylation patterns in TEs were hypomethylated in a tissue-specific manner and displayed enhancer hallmarks (Xie et al., 2013). TEs also promote transcript diversity by providing alternative promoters for extant genes. A genome-wide study examining transcription initiation events arising within TEs observed that TEs were used as alternative promoters in normal tissues and contributed to tissue-specific expression profiles (Faulkner et al., 2009). These studies suggest that TEs are developmentally regulated and may have contributed to driving the large diversity of cell types observed in humans.

With the advent of high-throughput sequencing, numerous RNA sequencing studies have revealed a large set of long non-coding RNAs (lncRNAs) in the human genome (Cabili et al., 2011; Khalil et al., 2009; Guttman et al., 2011). TEs have been suggested to have contributed to the biogenesis of many lncRNAs (Kapusta and Feschotte, 2014) and it was demonstrated that lncRNAs are enriched with TE sequences (Kapusta et al., 2013). The distribution of TEs within lncRNAs was also found to be positioned and orientated in a biased with respect to the transcription start site (TSS), suggesting that TEs provided the initial spark that gave rise to the lncRNA (Kelley and Rinn, 2012). As TEs naturally contain transcriptional regulatory signals, this is not surprising; for example, the long terminal repeats (LTRs) of retrotransposons have been found to drive the expression of nearby genes (Cohen et al., 2009). The TSS of the lncRNAs *BANCR*, *lnc-RoR*, and *lncRNA-ES3* all overlap the LTR sequence of separate endogenous retroviruses (Kapusta et al., 2013). In addition, these lncRNAs only exist in the genomes of organisms that descended from the last common ancestor which contains the retrovirus, clearly supporting the idea that these lncRNAs arose from TEs (Kapusta et al., 2013). Furthermore, a specific TE family was found to drive the expression of stem cell specific lncRNAs (Kelley and Rinn, 2012) and a large number of “non-annotated stem transcripts”

(Fort et al., 2014), suggesting that TEs are able confer tissue-specificity possibly by associating with specific regulatory signals.

The consideration that TEs may be functional products of the genome is generally met with scepticism due to historical views that TEs are simply selfish elements that serve no purpose apart from propagating itself (Doolittle and Sapienza, 1980) and therefore provide little to no selective advantage to organisms (Orgel and Crick, 1980). Furthermore, the elaborate silencing systems that repress the transposition of mobile genetic elements in the human genome suggest that they molecular pests that need to be silenced (Yang and Kazazian, 2006). However, in their original paper, Orgel and Crick suggested at the hypothesis that these selfish DNA sequences may become exapted for control purposes (Orgel and Crick, 1980). Indeed, there have been an increasing number of studies reporting the exaptation of TE insertions, however it has been suggested that many studies are not conclusive and more work in this area is required (de Souza et al., 2013). One reason for the limited number of studies is due to the technical difficulties associated with REs. During the era of microarray technologies, cross-hybridisation issues made it difficult to study the expression of REs. High-throughput sequencing technology has made it possible to quantify the expression of REs, however the short read nature of these technologies has made it difficult to map reads to REs.

It has been previously reported that 75% of reads that are 25 nucleotides long can be mapped uniquely to the human genome and at 60 nucleotides long 95% uniqueness can be achieved (Whiteford et al., 2005). However, this estimate assumes an equal distribution of reads in a given library, which is typically not the case. When dealing with a read that maps to multiple places, there are usually three choices on what to do: a) Discard the read, b) Take the best alignment and if there are multiple best hits, take one randomly, and c) Report all alignments or report up to a certain number (Treangen and Salzberg, 2012). The third choice can also be incorporated with a strategy that uses uniquely mapped reads to probabilistically weight multi-mapping reads (Faulkner et al., 2008). This strategy is based on the basic premise that a region that is transcriptional active is more likely to have given rise to a read than a transcriptional inert region. Other strategies for dealing with multi-mapping reads include mapping to a consensus database of REs, such as RepBase Update (Jurka et al., 2005), or mapping to regions of a genome that has been annotated as being repetitive (Xie et al., 2013), or combining reference genome mapping with consensus sequence mapping (Day et al., 2010). These strategies aim to utilise as many reads as possible to obtain a more representative expression profile.

In this study, we processed over two billion reads from 988 FANTOM5 CAGE libraries and overlaid them to REs annotated using profile hidden Markov models. We found that various REs are expressed in a tissue-specific manner and expression signal from REs can be used to produce biologically meaningful clusters. Furthermore, expression profiles of specific REs can be associated to specific sample ontologies, suggesting that specific families of REs may be associated to tissue-types. Lastly, by examining the genomic locality of expressed REs, we observed that they overlapped genomic regions known to produce small RNAs

and lncRNAs, as well as enhancer regions, more often than expected by chance.

2 Methods

2.1 Annotating repeats in the human genome

RepeatMasker (Smit et al., 2004) is a program that screens DNA sequences for repetitive elements (REs); the tool relies on a search algorithm and a database of RE profiles. Traditionally, homology-based tools such as cross_match and variants of BLAST have been used to screen DNA sequence against RE consensus sequences, the most commonly used database being Repbase Update (Jurka et al., 2005). Recently a database of REs based on profile hidden Markov models was developed, called Dfam (Wheeler et al., 2013), which allowed screening of REs using a hidden Markov model search tool, called nhmmer (Wheeler and Eddy, 2013). It has been reported that screening for REs using nhmmer and Dfam is more sensitive and specific than consensus sequence based approaches (Wheeler et al., 2013). For this reason, we annotated REs in the human genome (hg19) using RepeatMasker (4.0.3), nhmmer (hmmer-3.1b1), and Dfam (1.2). Specifically, we ran the command `RepeatMasker -e hmmer -species human -s -xsmall -pa 8 chr.fa`, for each assembled chromosome. REs were classified by class, family, and individual element names.

2.2 Aggregating CAGE reads to repetitive elements

The details describing the preparation of the Cap Analysis Gene Expression (CAGE) libraries for the FANTOM5 project are described elsewhere (Kanamori-Katayama et al., 2011). Briefly, a CAGE protocol optimised for the HeliScope Genetic Analysis System was developed and used to prepare 988 FANTOM5 libraries. A high-throughput short read sequence alignment program called Delve (Djebali et al., 2012) was used to map the CAGE reads to the human genome (hg19). Delve is able to recognise sequencing biases or increased error rates in homopolymer stretches, which makes it suitable for the HeliScope sequencer. Mapping qualities following the Phred scale were provided for each mapped read, where the qualities are probabilities that a mapped read is incorrect (Li et al., 2008).

To aggregate CAGE reads to REs, the coordinates of the mapped reads were intersected with the RE coordinates using intersectBed from the BEDTools suite (Quinlan and Hall, 2010); parallelisation of the computations was achieved using GNU parallel (Tange, 2011). For each repeat class (1087 in total), we tallied the number of reads that intersected that class; thus for each FANTOM5 library, a tally was produced for each repeat class resulting in a 1087×988 matrix. We performed this aggregation step using reads thresholded at various mapping qualities (0, ..., 10). Finally, tallies for each library were normalised by tags per million (TPM); library size was the total number of reads that intersected the repeat classes.

2.3 Markov clustering

We calculated the Spearman’s rank correlation coefficient between all repeat classes (590,241 pairwise calculations) and all libraries (487,578 pairwise calculations) using the matrix of aggregated CAGE reads. Correlations between REs and libraries were represented as a graph, where the nodes or vertices represented a single RE class and the edges or connections represented a correlation between the two nodes. We used the Markov clustering (MCL) algorithm (Enright et al., 2002) to reveal natural groups within the graphs using only nodes that had a correlation of 0.96 or better to another node. The algorithm simulates flow within a graph and promotes flow in a highly connected region and demotes less connected regions. The MCL algorithm takes one parameter, the inflation parameter, which adjusts the granularity of the clusters. We tested various inflation parameters between two to ten, and used four as this was a good compromise between the number of clusters and cluster sizes. The graphs were visualised using the Cytoscape software (Shannon et al., 2003).

2.4 FANTOM5 sample ontology enrichment analysis

Structured sample ontologies were used to annotate the FANTOM5 libraries, allowing the identification of enriched biological properties based on CAGE expression profiles (Forrest et al., 2014). Specifically, samples were annotated using the The Open Biological and Biomedical Ontologies (<http://www.obofoundry.org/>) and the structured ontologies, were grouped into hierarchical cellular, anatomical, disease and experimental ontologies. Each ontology can be used to separate libraries in a binary manner, where a library either has membership (x) or no membership (y) to a particular ontology. To test for ontology enrichment, the TPM expression of libraries in x were compared to the expression of libraries in y using a Mann-Whitney-Wilcoxon test; this was performed on all 845 sample ontologies and for all all repeat classes (1,087). The p-values were adjusted following the Benjamini & Hochberg method (Benjamini and Hochberg, 1995) and resulted in a 1087×845 matrix of adjusted p-values. Each element of this matrix corresponds to a p-value indicating whether the expression profile of a particular repeat class enriches a particular sample ontology.

2.5 Parametric tag clustering of CAGE reads

The FANTOM5 CAGE libraries were previously clustered using a decomposition-based peak identification (DPI) method that utilised a stringent mapping quality threshold of 20 (Forrest et al., 2014). This criteria removes signal arising from REs and is inappropriate for studying the expression of REs. We used a tag clustering method known as parametric clustering (Frith et al., 2008), which uses maximal scoring segments to clusters reads. Specifically for every maximal scoring segments, the minimum and maximum values of the density parameter, d , are reported and used to assess whether a cluster is robust and not formed due to random fluctuations in the data set. We kept tag clusters

with at least ten raw tags, a maximum density / minimum density ratio of at least two, and limited tag clusters to a length of 200 bps. We performed tag clustering using reads thresholded at various mapping qualities ($0, \dots, 10$) and to simplify the large number of tag clusters, we took the largest tag cluster that could encompass all other tag clusters, which we called non-overlapping tag clusters.

2.6 Tag cluster annotation

We used the intersectBed tool from the BEDTools suite to annotate tag clusters to GENCODE (v19) transcripts (Harrow et al., 2012), REs, FANTOM5 permissive enhancers (Andersson et al., 2014), FANTOM5 small RNAs, and long intergenic non-coding RNAs (Cabili et al., 2011). We separated the genome into 5 separate classes based on the GENCODE annotations and annotated each tag cluster hierarchically in the order: promoter, exon, intron, repetitive elements, and intergenic region. Genomic regions +/- 200 bp around the starting site of a GENCODE transcript was considered the promoter region of that transcript. Exonic regions were defined as regions overlapping the exons of GENCODE transcripts. Intronic regions were defined as the region remaining from the subtraction (using subtractBed) between a GENCODE gene model and the exonic regions. Intergenic regions were defined as the remaining region from the subtraction between gene models and the genome sequence. FANTOM5 small RNA libraries were clustered in the same manner as the CAGE data (see section 2.5).

We used the GenometriCorr package (Favorov et al., 2012) to calculate potential correlations between two sets of genomic features: a query and a reference set. Relative and absolute distances between query and reference features are tested against a uniform distribution of distances. The significance of overlap between two sets of features is tested using a projection test, using a binomial test, where the probability of overlap is based on the coverage of reference features and by using the Jaccard index defined as:

$$J(A, B) = \frac{|A \cap B|}{|A \cup B|}$$

which measures the amount of overlap between two features. To test where observed intersections are statistically significant, a null distribution was created by measuring the Jaccard index of 1,000 permutations of the query features. A list of random coordinates was generated by using randomBed from the BEDTools suite running the following command `bedtools random -g hg19.genome -l 300 -n 100000 -seed 31`, where `hg19.genome` is a file containing the start and end coordinates of the assembled chromosomes ($n=25$) on hg19.

2.7 Measuring expression specificity

The Shannon entropy has been previously used as a metric to characterise the overall expression specificity of a gene amongst a panel of samples (Schug et al.,

2005). We used the Shannon entropy as a measure for expression specificity and calculated the metric as follows:

$$-\sum_{i=1}^n x_i \cdot \log_2 x_i$$

where i is the library index and x_i the expression of a feature in a particular library. In addition, we normalised the expression of a feature in a single library by the total expression of the features in all libraries. The Shannon entropy, measured in bits, ranges from zero for transcripts expressed only in a single sample to $\log_2 n$ for features that are expressed uniformly across all n samples.

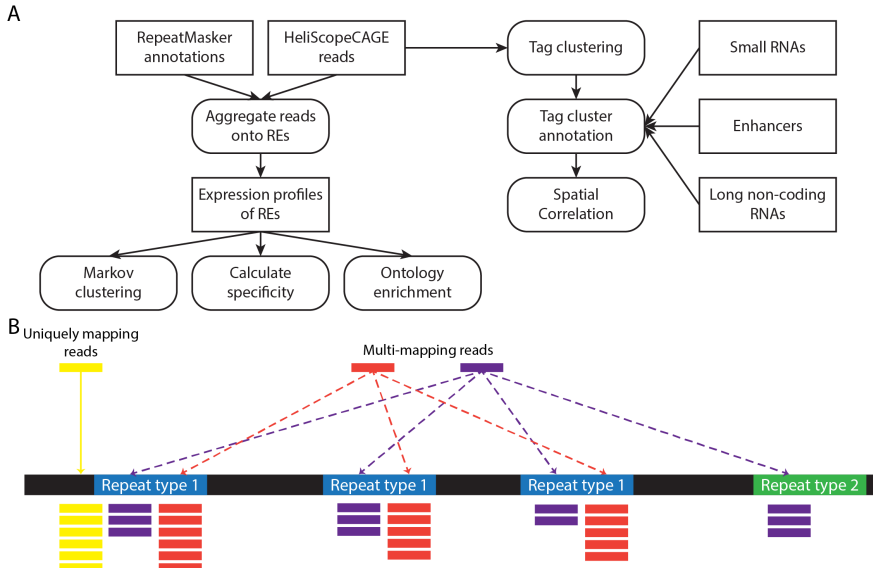


Figure 1: Summary of the methods. A) The pipeline of this study; rectangles show data sources and rounded rectangles show bioinformatic procedures. B) The aggregation strategy used to assign reads to repeat types. In the example above, 3 scenarios are shown: the first scenario shows the unambiguous assignment of reads to a repeat type, the second scenario shows how multi-mapping reads are all randomly assigned to the same repeat type, and the third scenario shows how multi-mapping reads can be randomly assigned to different repeat types, which can occur in repeats belonging to a similar class.

3 Results

3.1 Annotating repetitive elements

Repetitive elements (REs) make up a large fraction of the human genome, with estimates ranging from 50% using sequence homology based approaches to up to

two thirds based on *de novo* detection methods (de Koning et al., 2011). However, *de novo* detection methods are annotation agnostic, thus these approaches do not classify the repeats into classes and types. Accurate annotations of REs enables much more precise biological conclusions to be made. For this work, we used a recently developed database of RE called Dfam (Wheeler et al., 2013), which represents each element by a profile hidden Markov model (HMM), built from alignments generated using RepeatMasker (Smit et al., 2004) and Repbase Update (Jurka et al., 2005). Each profile-HMM contains much richer information than the consensus sequence built from multiple alignments of REs, such as those present in Repbase Update. Using the profile-HMMs with a HMM search tool called nhmmmer (Wheeler and Eddy, 2013), resulted in an increase in annotations (Wheeler et al., 2013). We compared RE annotations performed using consensus sequences to those based on profile-HMMs and found an 5.4% increase in annotations using profile-HMMs: 46.8% (1,448,043,873 / 3,095,693,983) versus 52.2% (1,614,955,505 / 3,095,693,983) of the human genome was annotated as repetitive using consensus sequences and profile-HMMs, respectively.

3.2 The robustness of aggregating reads

We quantified the expression of REs, in two independent ways: by aggregating reads onto REs and by tag clustering and intersection (Figure 1). In the first approach, CAGE reads were tallied across 1,087 RE classes (Figure 1B) to measure the overall expression strength of REs. This method relies solely on the overlap of a mapped read to a RE, which has its advantages and disadvantages. Positional information of a read with respect to a RE is lost and we cannot distinguish whether a RE is strongly expressed at one locus or weakly expressed at 100 loci. However, this method provides a bird's-eye view of REs across a large panel of samples and is robust to multi-mapping reads. To demonstrate the robustness of this method, we performed the aggregation step using reads filtered at various mapping qualities and compared the expression profiles (Figure 2). The Spearman correlations between the expression profiles were very high, with the lowest correlation (Spearman's rho = 0.83) between the expression profiles prepared using all reads against using reads thresholded with a mapping quality of 10 or better. The results suggest that multi-mapping reads were mapped back to the same RE class.

3.3 The expression specificity of repetitive elements

To measure the specificity of expression, we calculated the Shannon entropy of all REs using their expression profile across the FANTOM5 libraries. The distribution of Shannon entropies show that on an aggregated level, most REs are expressed in roughly the same amount across the libraries (Figure 3). This may be due to summing all genome-wide expression events of a RE class into one value; though it is interesting to note that on average most REs are expressed equally. However, even on this level, there are various classes of REs that are enriched in particular libraries. For example, the expression of LTR7 was

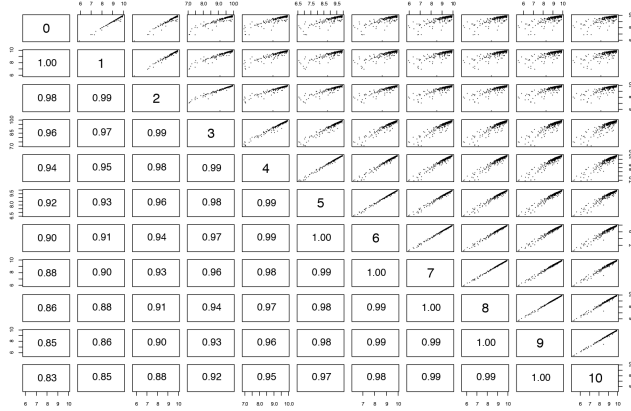


Figure 2: Correlation of repetitive element expression profiles aggregated using reads at different mapping qualities.

enriched in pluripotent and embryonic stem cells, the expression of MER74C was enriched in blood samples, the expression of an ultra-conserved element UCON15 is enriched in brain samples, and the expression of MER41E was enriched in placental samples.

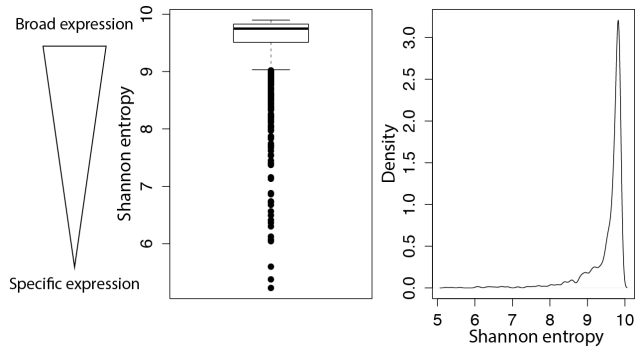


Figure 3: The distribution of Shannon entropies reveals that on an aggregated level, most repetitive elements are expressed at similar levels. However, a small subset shows a much more restrictive expression profile.

Motivated by the observation that some REs were expressed in a tissue-specific manner, we clustered the FANTOM5 libraries using correlations of aggregated RE expression profiles. We represented the correlations as a graph, whereby each node is a single library and nodes were connected if the two libraries had RE expression profiles that were correlated (Figure 4A). The graph showed that most libraries had a very similar RE expression profile. Next, we performed Markov clustering (MCL), an unsupervised clustering algorithm based on the simulation of stochastic flow in graphs, to reveal any natural groups within this graph. Impressively, the clusters formed by the MCL algorithm

grouped together libraries that were technically or biological related together (Figure 4B). For example, induced pluripotent stem cells clustered with human embryonic stem cells and embryoid bodies and whole blood samples taken from different donors clustered together (Table 1).

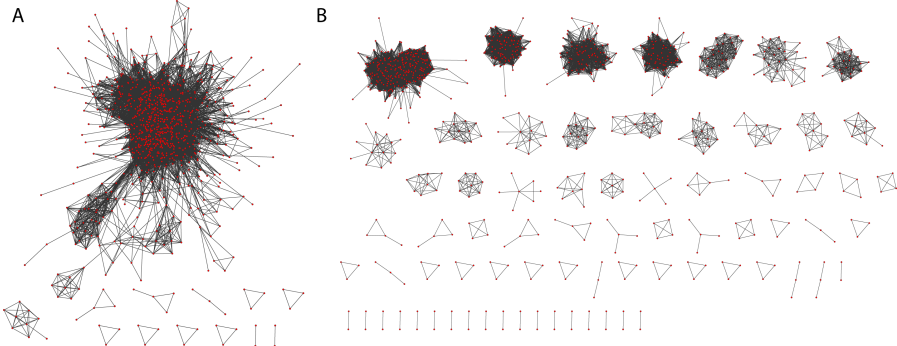


Figure 4: Representing the expression patterns of REs as graphs. A) Each red node represents a FANTOM5 library and each edge represents a Spearman’s correlation of 0.96 between two nodes B) Markov clustering revealed natural groups present in the correlation graph.

Markov cluster 1	Markov cluster 2
blood_adult_pool1	iPS_to_neuron.control.donor.day00.rep1
Whole_blood_ribopure_donor090612_1	iPS_to_neuron.control.donor.day00.rep2
Whole_blood_ribopure_donor090612_2	iPS_to_neuron.control.donor.day00.rep2
Whole_blood_ribopure_donor090612_3	H9_Embryoid_body_cells_rep1_H9EB_1_d0
Whole_blood_ribopure_donor090325_1	H9_Embryoid_body_cells_rep2_H9EB_2_d0
Whole_blood_ribopure_donor090325_2	H9_Embryoid_body_cells_rep3_H9EB_3_d0
Whole_blood_ribopure_donor090309_1	H9_Embryonic_Stem_cells_rep2_H9ES_2
Whole_blood_ribopure_donor090309_2	H9_Embryonic_Stem_cells_rep3_H9ES_3
Whole_blood_ribopure_donor090309_3	

Table 1: Two examples of the Markov clusters formed (out of ninety) using the correlation values calculated on the aggregated RE expression profiles. The samples names were slightly shorten from the full name used in the FANTOM5 project.

3.4 Sample ontology enrichment analysis

The FANTOM5 libraries have been associated to specific sample ontologies (Forrest et al., 2014), which allowed us to test whether the expression of specific REs enriched specific sample ontologies. Based on a particular ontology, libraries could be separated into two groups: those that are associated with the ontology and those that are not. Based on this separation, we tested whether the RE expression between the two groups was statistically different. We performed 919,602 enrichment tests and found 69,038 associations that were statistically significant (adjusted p-value <0.05) (Figure 5A). Many of the 845 sample ontologies are subtly different but typically associated to the same libraries, thus a RE may enrich several similar ontologies. For example, LTR7 had 80 sample ontologies that were significantly enriched including “embryonic stem cell”

and “H9 embryonic stem cell line” (adjusted p-value for both ~ 0.00693) (Figure 5B). MER74C had 59 ontologies that were significantly enriched including “blood” (adjusted p-value ~ 0.001952) and “whole blood” (adjusted p-value ~ 0.00012) (Figure 5C). UCON15 had 37 sample ontologies significantly enriched, including “regional part of brain” (adjusted p-value ~ 0.000169) and “nucleus of brain” (adjusted p-value ~ 0.016551). We can also lookup specific REs that are enriched to specific sample ontologies (Table 2).

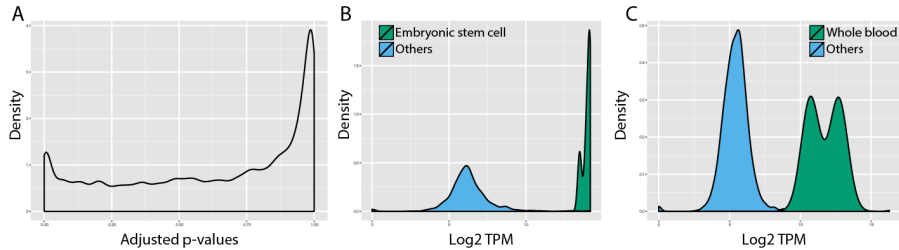


Figure 5: Sample ontology enrichment analysis. A) The distribution of adjusted p-values for the sample ontology enrichment analysis. B) The expression distribution, in tags per million, of LTR7 in samples annotated as “Embryonic stem cell” and those that are not, i.e. others. C) The expression distribution, in tags per million, of MER74C in samples annotated as “Whole blood” and those that are not, i.e. others.

HERV571-int	LTR28C	HERV4.1-int	MER110A	REP522
0.010	0.010	0.010	0.010	0.010
LTR70	MER4-int	MER67C	HERVH48-int	MSTB1
0.010	0.009	0.008	0.008	0.008
MER61-int	MER4CL34	LTR8A	LTR10D	MER51C
0.008	0.008	0.008	0.007	0.007
LTR1A2	MER4A1-v	MER41A	L1M7	L1M2b
0.007	0.007	0.007	0.007	0.007
LTR10B1	LTR17	LTR33A	LTR22C2	MER48
0.006	0.006	0.006	0.006	0.006
L1M2	MER11C	MER4A1	LTR7B	LTR6A
0.006	0.006	0.006	0.006	0.006
LTR29	LTR5	LTR7Y	LTR6B	Charlie21a
0.006	0.006	0.006	0.006	0.006
LTR27B	LTR48B	LTR7A	LTR49	MER4C
0.006	0.006	0.006	0.006	0.006
MER61D	LTR7	LTR5_Hs	MER61B	LTR9D
0.006	0.006	0.006	0.006	0.006
MER21B	LTR9B	MER61E	LTR26B	LTR7C
0.006	0.006	0.006	0.006	0.006
LTR49-int	MER74A	MER61C	HUERS-P1-int	LTR9C
0.006	0.006	0.006	0.006	0.006
HERVH-int	LTR16D2	MER61A		
0.006	0.006	0.006		

Table 2: Repetitive elements that are enriched in samples with the ontology “embryonic stem cells”; the adjusted p-values are sorted by the level of significance in descending order.

3.5 Repetitive elements overlap small RNAs, enhancers, and long non-coding RNAs

In the second approach of quantifying the expression of REs, we clustered all mapped FANTOM5 CAGE reads at various mapping qualities, using a parametric clustering methods (Frith et al., 2008). This tag clustering approach, as opposed to the aggregation method, allows REs to be put into context of other

genomic features. We first annotated tag clusters to GENCODE transcripts in a hierarchical manner to avoid confounding signal from known transcripts. The expression level of annotated GENCODE promoters is clearly higher much higher than any other genomic feature (Table 3). The median expression of intronic, RE, and intergenic regions are similar; however the mean expression of RE regions is higher, suggesting that a population of REs that are much higher expressed than transcripts arising within intronic and intergenic regions (Table 3).

Genomic feature	Tag cluster count	Mean expression	Median expression
Promoter	390162	9914	52
Exonic	937236	391	33
Intronic	2219891	87	20
Repetitive	410313	210	20
Intergenic	421534	126	21

Table 3: A summary of the number and raw expression levels of tag clusters with respect to their GENCODE annotations.

Next we performed statistical tests to determine whether these REs overlapped different various genomic features more often than by chance. The p-values of the projection and Jaccard index test are highly significant indicating that expressed REs overlap small RNAs, enhancer regions, and lncRNAs more often than by chance (Table 4). A random set of genomic features did not significantly overlap expressed REs.

	sRNAs	Enhancers	lncRNAs	Random
Number of genomic features	610,246	43,011	14,281	100,000
Projection test p-value	0	0	0.00264	0.2246452
Jaccard measure p-value	<0.001	<0.001	<0.001	0.391

Table 4: P-values for the projection and Jaccard index statistical tests for assessing the significance of overlap between RE tag clusters and various genomic features. P-values were calculated using 1,000 permutation tests in each case.

4 Discussion

One of the first genome-wide screenings of transcription events initiating within repetitive elements (REs) was based on roughly 42 million CAGE reads from across 80 human samples, which were clustered into 12 separate tissue types (Faulkner et al., 2009). This initial study revealed that retrotransposon-derived transcription events are generally tissue-specific and function as alternative promoters (Faulkner et al., 2009). This observation was supported by the fact that the human L1 retrotransposon contain internal promoter sequences, including an antisense promoter that can drive the expression of various human genes, even in normal cells (Nigumann et al., 2002; Speek, 2001). Furthermore, these L1 retrotransposon promoters were found to drive tissue-specific transcription of

genes (Matlik et al., 2006). In addition to L1, the long terminal repeats (LTRs) of endogenous retroviruses also have the capacity for driving the expression of human genes, especially in a tissue-specific manner (Cohen et al., 2009). In another large scale study examining the transcriptional landscape in 15 cell lines, it was demonstrated that repetitive elements exhibit cell type specific expression patterns and are enriched in the nucleus (Djebali et al., 2012). Deeply profiled nuclear and cytoplasmic transcriptomes of stem cells also revealed an enrichment of transcripts initiating from REs (Fort et al., 2014).

In this work, we examined the expression pattern of REs in 988 human samples, which included technical and biological replicates, using CAGE technology adopted onto a single molecule sequencing platform (Kanamori-Katayama et al., 2011). This expression atlas has been previously used to systematically study the cohort of genes (Forrest et al., 2014) and enhancers (Andersson et al., 2014) that are used in specific cell types. We leveraged the use of profile hidden Markov models (HMMs) as a replacement over the use of consensus sequences to more accurate RE annotations due to the richer information content contained within a profile (Wheeler et al., 2013). The use of profile-HMMs resulted in a 5.4% increase in annotations, allowing us to ascribe more transcription events to REs. Expression pattern of REs were studied in two independent manners: by aggregating reads onto REs and by tag clustering and annotation. The first approach aimed to quantify the expression of REs on the scale of samples to mitigate multi-mapping issues and to gain an overview of the expression of REs across samples. The second approach puts the expression of REs into the context of other genomic features to identify potential correlations between the expression of REs to nearby genomic features.

To measure the expression specificity of REs, we calculated the Shannon entropy using the expression profiles of REs. On an aggregated level, most REs were broadly expressed with a Shannon entropy near maximum ($\log_2(988)$); however, a subset of REs were more specifically expressed. Of the 20 REs with the lowest entropies, 15 corresponded to the long terminal repeats (LTRs), which are the control centres of gene expression for endogenous retroviruses, since they contain all the requisite signals for gene expression. This observation supports the notion that LTRs have become exapted as alternative promoters for driving tissue-specific expression patterns (Cohen et al., 2009). On closer examination of these 15 LTR sequences, we observed that they had enriched expression patterns in a specific cohort of biological samples. For example, the expression of LTR7 is enriched in human embryonic stem cells, induced pluripotent stem cells (iPCSSs), and germ line cancers compared to the other samples. LTR7, which is associated with human endogenous retrovirus H (HERVH), has been observed to be enriched in long intergenic non-coding RNAs that are expressed at much higher levels in stem-like cells (Kelley and Rinn, 2012). One potential mechanism by which LTR7 confers specificity to stem cells is the observation that the master transcriptional regulators of pluripotency NANOG, OCT4, and SOX2, were found to bind to LTR7 elements (Loewer et al., 2010). Furthermore, over-expression of LTR7 has been shown to lead to defective human induced pluripotent stem cell clones, suggesting that careful regulation of

LTR7 is required for maintaining pluripotency (Koyanagi-Aoi et al., 2013).

There are other examples of transcription factors (TFs) associating to specific RE sequences. One study discovered the pervasive association of several TFs to sequences in distinctive families of transposable elements (TEs) (Bourque et al., 2008). Since REs harbour sequences that resemble transcription factor binding sites (TFBSs), this may be one mechanism by which REs can confer tissue specificity. Indeed, we demonstrated that the FANTOM5 libraries could cluster biologically and technically similar libraries together, using just the aggregated expression signal from REs. Furthermore, in support of specific RE associating with specific cell types, our sample ontology enrichment analysis, showed that the expression pattern of many REs enriched particular sample ontologies. The enrichment analysis showed that LTR7 is enriched in “embryonic stem cell” samples and while this was observed prior to the enrichment analysis, the ontologies provide a structured manner to associate REs to samples. Furthermore, this analysis can be used to identify REs enriched in specific sample ontologies. For example, many other LTR families are enriched in “embryonic stem cell” samples and one of the most statistically significant LTRs, MER61A, has previously been reported to provide binding sites for p53 (Wang et al., 2007), a tumour suppressor gene that plays an important role in stem cells (Solozobova and Blattner, 2011). This large list of associations between samples and REs is a useful resource for generating hypotheses on the potential role of REs.

In addition to the role of REs in regulatory networks (Feschotte, 2008), REs have been found to be associated with long non-coding RNAs (lncRNAs) (Kelley and Rinn, 2012; Kapusta et al., 2013) and have been proposed to have played a major role in the origin and evolution of lncRNA (Kapusta and Feschotte, 2014). Furthermore, TEs are positioned and orientated in a biased manner at the transcription start site of lncRNAs, suggesting that they may play a role in regulating the expression of the lncRNA (Kelley and Rinn, 2012). In addition to lncRNAs, small regulatory RNAs, such as Piwi-interacting RNAs (piRNAs) and small interfering RNAs (siRNAs) are produced from the sequences of TEs (Cowley and Oakey, 2013). While these small RNAs, primarily function as a host defence mechanism to silence TEs, epigenetically and developmentally regulated bursts in expression of TEs resulted in the production of piRNAs that regulated the expression of messenger RNA (mRNA) by binding to the 3' UTR (McCue and Slotkin, 2012). The enrichment of TE sequences within the 3' UTR sequences of mRNAs (Faulkner et al., 2009) may suggest that this phenomenon may be more widespread. In addition to generating non-coding RNA, a recent study examining the methylation patterns of TEs, demonstrated that methylation patterns of TEs was tissue specific, and may act as enhancers (Xie et al., 2013). Another study found evidence of TEs acting as enhancer regions in stem cells (Fort et al., 2014). By examining the genomic locations of these three genomic features (lncRNAs, enhancers, and small RNAs) to expressed REs, we showed that they overlapped more often than by chance. Additional work needs to be carried out to better characterise the overlap between these features with the expressed REs.

It is becoming evident that TEs have had a major impact in the evolution of regulatory networks. Our work here, takes advantage of the large breath of samples provided by the FANTOM5 project, to illustrate the tissue-specific manner of REs. Given that the technical difficulties with analysing REs are now becoming less of a problem due to longer read lengths in high-throughput sequencers and various computational pipelines have been developed to analyse signal from REs, we may see additional studies in this exciting area of research.

5 Data deposition

All CAGE data has been deposited at DDBJ DRA under accession number DRA000991.

6 Acknowledgements

We would like to thank Dr. Alex Fort for reading an early version of this manuscript and for making suggestions.

7 Funding

FANTOM5 was made possible by a Research Grant for RIKEN Omics Science Center from MEXT to YH and a Grant of the Innovative Cell Biology by Innovative Technology (Cell Innovation Program) from the MEXT, Japan to YH. DT is supported by the European Union Seventh Framework Programme under grant agreement FP7-People-ITN-2008-238055 ("BrainTrain" project) to PC.

8 Authors' contributions

DT processed the data, designed the analyses, performed the analyses, interpreted the data, and wrote the manuscript. PC oversaw the project. All authors read and approved the final manuscript.

References

- Andersson, R., Gebhard, C., Miguel-Escalada, I., Hoof, I., Bornholdt, J., et al. (2014). An atlas of active enhancers across human cell types and tissues. *Nature*, 507(7493):455–461.
- Benjamini, Y. and Hochberg, Y. (1995). Controlling the False Discovery Rate: A Practical and Powerful Approach to Multiple Testing. *Journal of the Royal Statistical Society. Series B (Methodological)*, 57(1):289–300.
- Bourque, G., Leong, B., Vega, V. B., Chen, X., Lee, Y. L., Srinivasan, K. G., Chew, J. L., Ruan, Y., Wei, C. L., Ng, H. H., and Liu, E. T. (2008). Evolution of the mammalian transcription factor binding repertoire via transposable elements. *Genome Res.*, 18(11):1752–1762.
- Cabili, M. N., Trapnell, C., Goff, L., Koziol, M., Tazon-Vega, B., Regev, A., and Rinn, J. L. (2011). Integrative annotation of human large intergenic noncoding RNAs reveals global properties and specific subclasses. *Genes Dev.*, 25(18):1915–1927.
- Callinan, P. A. and Batzer, M. A. (2006). Retrotransposable elements and human disease. *Genome Dyn.*, 1:104–115.
- Cohen, C. J., Lock, W. M., and Mager, D. L. (2009). Endogenous retroviral LTRs as promoters for human genes: a critical assessment. *Gene*, 448(2):105–114.
- Cordaux, R. and Batzer, M. A. (2009). The impact of retrotransposons on human genome evolution. *Nat. Rev. Genet.*, 10(10):691–703.
- Cowley, M. and Oakey, R. J. (2013). Transposable elements re-wire and fine-tune the transcriptome. *PLoS Genet.*, 9(1):e1003234.
- Day, D. S., Luquette, L. J., Park, P. J., and Kharchenko, P. V. (2010). Estimating enrichment of repetitive elements from high-throughput sequence data. *Genome Biol.*, 11(6):R69.
- de Koning, A. P., Gu, W., Castoe, T. A., Batzer, M. A., and Pollock, D. D. (2011). Repetitive elements may comprise over two-thirds of the human genome. *PLoS Genet.*, 7(12):e1002384.
- de Souza, F. S., Franchini, L. F., and Rubinstein, M. (2013). Exaptation of transposable elements into novel cis-regulatory elements: is the evidence always strong? *Mol. Biol. Evol.*, 30(6):1239–1251.
- Djebali, S., Davis, C. A., Merkel, A., Dobin, A., Lassmann, T., et al. (2012). Landscape of transcription in human cells. *Nature*, 489(7414):101–108.
- Doolittle, W. F. and Sapienza, C. (1980). Selfish genes, the phenotype paradigm and genome evolution. *Nature*, 284(5757):601–603.

- Enright, A. J., Van Dongen, S., and Ouzounis, C. A. (2002). An efficient algorithm for large-scale detection of protein families. *Nucleic Acids Res.*, 30(7):1575–1584.
- Faulkner, G. J., Forrest, A. R., Chalk, A. M., Schroder, K., Hayashizaki, Y., Carninci, P., Hume, D. A., and Grimmond, S. M. (2008). A rescue strategy for multimapping short sequence tags refines surveys of transcriptional activity by CAGE. *Genomics*, 91(3):281–288.
- Faulkner, G. J., Kimura, Y., Daub, C. O., Wani, S., Plessy, C., et al. (2009). The regulated retrotransposon transcriptome of mammalian cells. *Nat. Genet.*, 41(5):563–571.
- Favorov, A., Mularoni, L., Cope, L. M., Medvedeva, Y., Mironov, A. A., Makeev, V. J., and Wheelan, S. J. (2012). Exploring massive, genome scale datasets with the GenometriCorr package. *PLoS Comput. Biol.*, 8(5):e1002529.
- Feschotte, C. (2008). Transposable elements and the evolution of regulatory networks. *Nat. Rev. Genet.*, 9(5):397–405.
- Forrest, A. R., Kawaji, H., Rehli, M., Baillie, J. K., de Hoon, M. J., et al. (2014). A promoter-level mammalian expression atlas. *Nature*, 507(7493):462–470.
- Fort, A., Hashimoto, K., Yamada, D., Salimullah, M., Keya, C. A., et al. (2014). Deep transcriptome profiling of mammalian stem cells supports a regulatory role for retrotransposons in pluripotency maintenance. *Nat. Genet.*, 46(6):558–566.
- Frith, M. C., Valen, E., Krogh, A., Hayashizaki, Y., Carninci, P., and Sandelin, A. (2008). A code for transcription initiation in mammalian genomes. *Genome Res.*, 18(1):1–12.
- Guttman, M., Donaghey, J., Carey, B. W., Garber, M., Grenier, J. K., et al. (2011). lncRNAs act in the circuitry controlling pluripotency and differentiation. *Nature*, 477(7364):295–300.
- Harrow, J., Frankish, A., Gonzalez, J. M., Tapanari, E., Diekhans, M., et al. (2012). GENCODE: the reference human genome annotation for The ENCODE Project. *Genome Res.*, 22(9):1760–1774.
- Jurka, J., Kapitonov, V. V., Pavlicek, A., Klonowski, P., Kohany, O., and Walichiewicz, J. (2005). Repbase Update, a database of eukaryotic repetitive elements. *Cytogenet. Genome Res.*, 110(1-4):462–467.
- Kanamori-Katayama, M., Itoh, M., Kawaji, H., Lassmann, T., Katayama, S., et al. (2011). Unamplified cap analysis of gene expression on a single-molecule sequencer. *Genome Res.*, 21(7):1150–1159.

- Kapusta, A. and Feschotte, C. (2014). Volatile evolution of long noncoding RNA repertoires: mechanisms and biological implications. *Trends Genet.*, 30(10):439–452.
- Kapusta, A., Kronenberg, Z., Lynch, V. J., Zhuo, X., Ramsay, L., Bourque, G., Yandell, M., and Feschotte, C. (2013). Transposable elements are major contributors to the origin, diversification, and regulation of vertebrate long noncoding RNAs. *PLoS Genet.*, 9(4):e1003470.
- Kelley, D. and Rinn, J. (2012). Transposable elements reveal a stem cell-specific class of long noncoding RNAs. *Genome Biol.*, 13(11):R107.
- Khalil, A. M., Guttman, M., Huarte, M., Garber, M., Raj, A., Rivea Morales, D., Thomas, K., Presser, A., Bernstein, B. E., van Oudenaarden, A., Regev, A., Lander, E. S., and Rinn, J. L. (2009). Many human large intergenic noncoding RNAs associate with chromatin-modifying complexes and affect gene expression. *Proc. Natl. Acad. Sci. U.S.A.*, 106(28):11667–11672.
- Koyanagi-Aoi, M., Ohnuki, M., Takahashi, K., Okita, K., Noma, H., Sawamura, Y., Teramoto, I., Narita, M., Sato, Y., Ichisaka, T., Amano, N., Watanabe, A., Morizane, A., Yamada, Y., Sato, T., Takahashi, J., and Yamanaka, S. (2013). Differentiation-defective phenotypes revealed by large-scale analyses of human pluripotent stem cells. *Proc. Natl. Acad. Sci. U.S.A.*, 110(51):20569–20574.
- Kunarso, G., Chia, N. Y., Jeyakani, J., Hwang, C., Lu, X., Chan, Y. S., Ng, H. H., and Bourque, G. (2010). Transposable elements have rewired the core regulatory network of human embryonic stem cells. *Nat. Genet.*, 42(7):631–634.
- Lander, E. S., Linton, L. M., Birren, B., Nusbaum, C., Zody, M. C., et al. (2001). Initial sequencing and analysis of the human genome. *Nature*, 409(6822):860–921.
- Li, H., Ruan, J., and Durbin, R. (2008). Mapping short DNA sequencing reads and calling variants using mapping quality scores. *Genome Res.*, 18(11):1851–1858.
- Loewer, S., Cabili, M. N., Guttman, M., Loh, Y. H., Thomas, K., Park, I. H., Garber, M., Curran, M., Onder, T., Agarwal, S., Manos, P. D., Datta, S., Lander, E. S., Schlaeger, T. M., Daley, G. Q., and Rinn, J. L. (2010). Large intergenic non-coding RNA-RoR modulates reprogramming of human induced pluripotent stem cells. *Nat. Genet.*, 42(12):1113–1117.
- Matlik, K., Redik, K., and Speek, M. (2006). L1 antisense promoter drives tissue-specific transcription of human genes. *J. Biomed. Biotechnol.*, 2006(1):71753.
- McCue, A. D. and Slotkin, R. K. (2012). Transposable element small RNAs as regulators of gene expression. *Trends Genet.*, 28(12):616–623.

- Mills, R. E., Bennett, E. A., Iskow, R. C., and Devine, S. E. (2007). Which transposable elements are active in the human genome? *Trends Genet.*, 23(4):183–191.
- Nigumann, P., Redik, K., Matlik, K., and Speek, M. (2002). Many human genes are transcribed from the antisense promoter of L1 retrotransposon. *Genomics*, 79(5):628–634.
- Orgel, L. E. and Crick, F. H. (1980). Selfish DNA: the ultimate parasite. *Nature*, 284(5757):604–607.
- Quinlan, A. R. and Hall, I. M. (2010). BEDTools: a flexible suite of utilities for comparing genomic features. *Bioinformatics*, 26(6):841–842.
- Schug, J., Schuller, W. P., Kappen, C., Salbaum, J. M., Bucan, M., and Stoeckert, C. J. (2005). Promoter features related to tissue specificity as measured by Shannon entropy. *Genome Biol.*, 6(4):R33.
- Shannon, P., Markiel, A., Ozier, O., Baliga, N. S., Wang, J. T., Ramage, D., Amin, N., Schwikowski, B., and Ideker, T. (2003). Cytoscape: a software environment for integrated models of biomolecular interaction networks. *Genome Res.*, 13(11):2498–2504.
- Smit, A. F. A., Hubley, R., and Green, P. (1996-2004). RepeatMasker Open-3.0.
- Solozobova, V. and Blattner, C. (2011). p53 in stem cells. *World J Biol Chem*, 2(9):202–214.
- Speek, M. (2001). Antisense promoter of human L1 retrotransposon drives transcription of adjacent cellular genes. *Mol. Cell. Biol.*, 21(6):1973–1985.
- Tange, O. (2011). Gnu parallel - the command-line power tool. *;login: The USENIX Magazine*, 36(1):42–47.
- Treangen, T. J. and Salzberg, S. L. (2012). Repetitive DNA and next-generation sequencing: computational challenges and solutions. *Nat. Rev. Genet.*, 13(1):36–46.
- Wang, T., Zeng, J., Lowe, C. B., Sellers, R. G., Salama, S. R., Yang, M., Burgess, S. M., Brachmann, R. K., and Haussler, D. (2007). Species-specific endogenous retroviruses shape the transcriptional network of the human tumor suppressor protein p53. *Proc. Natl. Acad. Sci. U.S.A.*, 104(47):18613–18618.
- Wheeler, T. J., Clements, J., Eddy, S. R., Hubley, R., Jones, T. A., Jurka, J., Smit, A. F., and Finn, R. D. (2013). Dfam: a database of repetitive DNA based on profile hidden Markov models. *Nucleic Acids Res.*, 41(Database issue):70–82.
- Wheeler, T. J. and Eddy, S. R. (2013). nhmmer: DNA homology search with profile HMMs. *Bioinformatics*, 29(19):2487–2489.

- Whiteford, N., Haslam, N., Weber, G., Prugel-Bennett, A., Essex, J. W., Roach, P. L., Bradley, M., and Neylon, C. (2005). An analysis of the feasibility of short read sequencing. *Nucleic Acids Res.*, 33(19):e171.
- Xie, M., Hong, C., Zhang, B., Lowdon, R. F., Xing, X., et al. (2013). DNA hypomethylation within specific transposable element families associates with tissue-specific enhancer landscape. *Nat. Genet.*, 45(7):836–841.
- Yang, N. and Kazazian, H. H. (2006). L1 retrotransposition is suppressed by endogenously encoded small interfering RNAs in human cultured cells. *Nat. Struct. Mol. Biol.*, 13(9):763–771.

Chapter 6

General discussion

The work carried out as part of this thesis had the underlying goal of interpreting the transcriptional output from different biological systems. In the various studies, different transcriptome profiling methods employing the use of high-throughput sequencers were used to catalogue and quantify the expression of transcripts. While the genome is largely static, the transcriptome is highly dynamic and the cohort of expressed transcripts at a specific development stage or physiological condition will allow us to understand development and disease on a molecular level. However, two problems complicate the study of transcriptomes: 1) the presence of artefacts and biases and 2) pervasive transcription. In order to properly interpret transcriptional output, it is necessary to filter out the noise from the biological signal.

6.0.3 Artefacts and biases in high-throughput sequencing

Transcriptome profiling falls under the category of functional genomics, in which the aim is to identify functional elements in the genome by evidence of transcription. The "read out" from such experiments represents the expression of transcripts, which by itself is not entirely informative. The raw signal needs to be annotated or in other words, put into perspective, usually with respect to the genome. In the case of transcriptome profiling via high-throughput sequencing, the raw signal, i.e. sequenced reads, are first processed and mapped back to the genome. The processing step involves quality control steps that remove reads with missing features, ambiguously called bases, and reads that are composed of the primer or adaptor sequences used in the library preparation. Furthermore, different thresholds are usually implemented after read mapping to remove potentially spurious events; these thresholds can be based on the mapping confidence or mapping quality, and expression strength. The mapped reads are then annotated to genomic features, such as protein-coding genes and repetitive elements, or to genomic properties, such as sequence conservation to other genomes and the nucleotide composition of a region. Finally, the annotated data is interpreted with respect to the experiment design; "sanity checks", which are basic tests that can quickly assess the validity of the results, are commonly performed.

The identification of artefacts and biases is important prior to the analysis of data; while tools (Lassmann et al., 2009) are available for performing quality

control steps, they are unable to deal with idiosyncratic biases from specific protocols. In chapter 2, we demonstrated a particular type of bias that was introduced with the use of molecular barcodes. DNA barcodes are used to allow different RNA sources to be pooled at an early stage of sample preparation and are easily introduced by modifying the sequences of primers or linkers. This has two main benefits in that the starting material is increased and different samples can be sequenced on a single flowcell, increasing the cost-effectiveness of the experiment. In our study, we observed that the efficiency of primer annealing was dependent on the barcode sequence (Tang et al., 2013), thus creating a barcode bias. Furthermore, we noticed a particular type of artefact that was artificially produced during the template-switching step of the experimental protocol (Tang et al., 2013). Specifically, these template-switching artefact, which are a result of strand invasion, interrupted the process of reverse transcription when the cDNA has increased sequence complementary to the template-switching primer. The bias was identified when libraries prepared with the same or similar barcodes clustered together, regardless of the biological origin of the library. We mitigated this bias by introducing a spacer sequencer into the template-switching primer, which standardised the template-switching efficiency.

6.0.4 Pervasive transcription and functional RNA products

Another complication with interpreting transcriptional output is pervasive transcription. There have been two surprises in the genomics field since the completion of the draft human genome sequence (Lander et al., 2001, Venter et al., 2001). The first was the number of genes in the human genome, which many genome biologists had over-estimated prior to the sequencing of the human genome. This came as a surprise, as it was thought that organismal complexity was a consequence of the number of genes; however, humans have roughly the same number of genes as *Caenorhabditis elegans*. The next surprise was the observation that most of the human genome was transcribed (Kapranov et al., 2002, Birney et al., 2007), i.e. pervasive transcription. This phenomenon was first observed using tiling arrays (Kapranov et al., 2007) and later by various transcriptome profiling methods (Djebali et al., 2012). However, whether pervasive transcription consists mainly of background transcriptional noise or is of functional importance has been a matter of debate. The low fidelity of RNA polymerase II (Struhl, 2007) and promiscuous binding of transcription factors (Spitz and Furlong, 2012) may give rise to “leaky” transcription. Furthermore, the existence of various systems that suppress pervasive transcription (Jensen et al., 2013) also raises the question of whether these products of pervasive transcription are functional.

Despite questions over their functionality, pervasive transcription is known to produce various classes of non-coding RNAs (ncRNAs) with characteristic features. These include various classes of small RNAs that are associated to promoters (Jacquier, 2009), long non-coding RNAs (lncRNAs) (Yang et al., 2014), and long intergenic non-coding RNAs (lincRNA) (Hangauer et al., 2013). Evidence of context-specific transcription, e.g. transcription at a specific developmental stage, tissue type, or against a particular stimulus, has been observed in these classes of ncRNA. In chapter 3, we profiled the small RNA population of cells that were induced for DNA damage, as a role for small RNAs in

the DNA damage response (DDR) had been previously observed in *Neurospora crassa* (Lee et al., 2009). Our work and the work of an independent group, demonstrated that small RNAs would form in the vicinity of the double strand break (Francia et al., 2012, Wei et al., 2012). Furthermore, these RNAs, which we named as DDRNAs, had specific size and nucleotide profiles that differed from other classes of small RNAs. While it is unclear what role these DDRNAs serve in the DDR, knock-down of Dicer and Drosha (Francia et al., 2012) and mutations in *Ago2* (Wei et al., 2012) impaired the DNA repair efficiency. As a signalling cascade is initiated from the site of DNA damage (Jackson and Bartek, 2009), it was hypothesised that AGO2, which are known to bind to different classes of small RNAs, recruits the DNA damage repair complex (Wei et al., 2012).

“Many small RNA classes possess specific sequence biases at the 5’ end, and it has become clear that Argonaute proteins are able to sense the 5’-terminal nucleotide of the small RNA. A rigid loop in the MID domain of human AGO2 allows specific contacts to a 5’-terminal uridine or adenine.”

The guiding and recruitment of various complexes to specific genomic loci is becoming an emerging theme when discussing the potential role of various ncRNAs. Apart from the classical example of miRNAs being associated with the RNA-induced silencing complex, many lincRNAs were shown to be bound to chromatin-modifying complexes and may function to guide these complexes to regions that need to undergo epigenetic regulation (Saxena and Carninci, 2011, Khalil et al., 2009). Intriguingly, many enzymatic members of chromatin remodelling complexes do not contain DNA binding domains but possess RNA binding domains. For example, *Xist* has been shown to recruit chromatin silencing proteins within the Polycomb complex to induce gene silencing via histone methylation (Wutz and Gribnau, 2007). Other ncRNAs including *RepA*, *Air*, *Kcnq1ot1*, and *Hotair* have also been shown to be associated with Polycomb and direct the complex to specific loci (Saxena and Carninci, 2011). Another mode by which ncRNAs can regulate chromatin is through the act of transcription, whereby RNA Pol II activity causes nucleosome rearrangements and local chromatin remodelling (Chakalova et al., 2005). Thus while the transcriptional product may be inert, it serves its purpose by maintaining a open chromatin conformation. An extreme case of this mode of function is a study that suggests that non-coding transcription can send “ripples of transcription”, which causes remodelling of the expression landscape and thereby influences the expression of neighbouring loci (Ebisuya et al., 2008).

6.0.5 The repetitive human genome

One of the major points that argues against ascribing function to products of pervasive transcription is because the human genome is largely occupied by repetitive DNA sequences, made up of mainly transposable elements (TEs). These elements have been historically considered as simply selfish products that have propagated themselves very successfully (Doolittle and Sapienza, 1980, Orgel and Crick, 1980). However, it has been demonstrated that transcripts derived from TEs are able to regulate chromatin structure in centromeres and neocentromeres (Chueh et al., 2009). In a recent study, it was demonstrated that interspersed repeat sequences, such as LINE-1, are associated with euchromatin and loss of these repeat sequences caused aberrant chromatin distribution and

condensation (Hall et al., 2014). Furthermore, a large number of transcriptional events was shown to be initiated within TEs and served as alternative promoters (Faulkner et al., 2009). In addition, TEs have been observed to be part of many lncRNAs (Kelley and Rinn, 2012), which led to the Repeat Insertion Domains of LncRNAs (RIDLs) hypothesis (Johnson and Guigo, 2014), whereby TEs act in a manner similar to structural domains in proteins. Furthermore, it has been suggested that TEs have contributed to the origin of many lncRNAs (Kapusta et al., 2013, Kapusta and Feschotte, 2014).

In chapter 5, we profiled the expression of TEs in a large panel of samples (988 libraries), given the many potential functional roles of TEs. As previously reported, we observed that on average, expression from TEs are more tissue-specific and lowly expressed compared with protein-coding transcripts. The relatively low expression strength of pervasively transcribed products has been used to support the claim that these products are the consequence of degradation or background noise. However, it should be pointed out that unlike mRNAs, which require a longer half-life in order to be exported into the cytoplasm for translation, ncRNA exert their function immediately in the nucleus. Many transcriptome profiling methods do not enrich for nuclear fraction, where many transcripts arising from TEs exist (Fort et al., 2014). Furthermore, in the case that ncRNA are expressed in small quantities, like transcription factors, they are still able to trigger an amplified cascade of downstream events. However, despite their lower expression patterns, we were able to cluster biologically similar libraries together using the expression profiles from TEs. We also showed that transcriptional events initiating within TEs are overlap small RNAs, enhancers, and lincRNAs more often than chance. These lines of evidence support the notion that some TEs have become exapted in the human genome.

Acknowledgements

“Twenty years from now you will be more disappointed by the things that you didn’t do than by the ones you did do. So throw off the bowlines. Sail away from the safe harbor. Catch the trade winds in your sails. Explore. Dream. Discover.”

— Mark Twain

The culmination of work presented in this thesis would not have been possible without the guidance and support of many friends and colleagues. But my involvement in this PhD project would not have even begun if not for my supervisor who accepted me into the program and a former colleague who forwarded the opening to me. I still remember the predicament I faced over 4 years ago when I had to decide whether or not I would commit to the idea of potentially working in Japan. I had already brushed off the idea once but in the end I was convinced that it was a tremendous opportunity and I would have regretted it if I let it slip by. In the end, I decided to set my sails to explore an entirely new world.

To this day, I have absolutely no regrets for embarking on this journey and it has been the best experience of my life (thus far). I had to leave behind close friends of many years but I still remember their responses when I asked for their advice regarding the opportunity in Japan. Their answers were unanimous; clearly, they had had enough of me. I’ve made many new friends in Japan and I’d like to think that they know who they are. Thanks guys and gals for enduring me! I would also like to acknowledge the Good Samaritans who answer questions on discussion forums and mailing lists; where would I be without them.

(This acknowledgements page will be updated.)

Bibliography

- Dave T. P. Tang, Charles Plessy, Md Salimullah, Ana Maria Suzuki, Raffaella Calligaris, Stefano Gustincich, and Piero Carninci. Suppression of artifacts and barcode bias in high-throughput transcriptome analyses utilizing template switching. *Nucleic Acids Research*, 41(3):e44, 2013. doi: 10.1093/nar/gks1128.
- Sofia Francia, Flavia Michelini, Alka Saxena, Dave Tang, Michiel de Hoon, Viviana Anelli, Marina Mione, Piero Carninci, and Fabrizio d'Adda di Fagagna. Site-specific DICER and DROSHA RNA products control the DNA-damage response. *Nature*, 488(7410):231–235, 2012.
- Alka Saxena, Dave Tang, and Piero Carninci. piRNAs warrant investigation in rett syndrome: An omics perspective. *Disease markers*, 33(5):261–275, 2012.
- Dave Tang and Piero Carninci. The regulated expression of repetitive elements across human cell types and tissues. *In preparation*, 2014.
- Yuki Hasegawa, Dave Tang, Naoko Takahashi, Yoshihide Hayashizaki, Alistair R. R. Forrest, the FANTOM consortium, and Harukazu Suzuki. Ccl2 enhances pluripotency of human induced pluripotent stem cells by activating hypoxia related genes. *Sci. Rep.*, 4, Jun 2014.
- Dave Tang, Ana Maria Suzuki, Raffaella Calligaris, Stefano Gustincich, and Piero Carninci. Deep transcriptome sequencing of whole blood samples from Parkinson's disease patients. *In preparation*, 2014.
- Ralf Dahm. Discovering dna: Friedrich miescher and the early years of nucleic acid research. *Human genetics*, 122(6):565–581, 2008.
- Fred Griffith. The significance of pneumococcal types. *Journal of Hygiene*, 27 (02):113–159, 1928.
- Oswald T Avery, Colin M MacLeod, and Maclyn McCarty. Studies on the chemical nature of the substance inducing transformation of pneumococcal types induction of transformation by a desoxyribonucleic acid fraction isolated from pneumococcus type iii. *The Journal of experimental medicine*, 79(2): 137–158, 1944.
- Alfred D Hershey and Martha Chase. Independent functions of viral protein and nucleic acid in growth of bacteriophage. *The Journal of general physiology*, 36(1):39–56, 1952.

- E. Chargaff, R. Lipshitz, and C. Green. Composition of the desoxypentose nucleic acids of four genera of sea-urchin. *J. Biol. Chem.*, 195(1):155–160, Mar 1952.
- D. Elson and E. Chargaff. On the desoxyribonucleic acid content of sea urchin gametes. *Experientia*, 8(4):143–145, Apr 1952.
- J. D. Watson and F. H. C. Crick. Molecular structure of nucleic acids: A structure for deoxyribose nucleic acid. *Nature*, 171(4356):737–738, Apr 1953. ISSN 0028-0836. doi: 10.1038/171737a0.
- Francis H Crick. On protein synthesis. In *Symposia of the Society for Experimental Biology*, volume 12, page 138, 1958.
- H. M. Temin and S. Mizutani. RNA-dependent DNA polymerase in virions of Rous sarcoma virus. *Nature*, 226(5252):1211–1213, Jun 1970.
- D. Baltimore. RNA-dependent DNA polymerase in virions of RNA tumour viruses. *Nature*, 226(5252):1209–1211, Jun 1970.
- Francis Crick. Central Dogma of Molecular Biology. *Nature*, 227(5258):561–563, Aug 1970. doi: 10.1038/227561a0.
- Giles Newton. The Crick Papers: 1955 From DNA to protein. http://genome.wellcome.ac.uk/doc_WTD022319.html, 2013.
- M. B. Hoagland, M. L. Stephenson, J. F. Scott, L. I. Hecht, and P. C. Zamecnik. A soluble ribonucleic acid intermediate in protein synthesis. *J. Biol. Chem.*, 231(1):241–257, Mar 1958.
- S. Brenner, F. Jacob, and M. Meselson. An unstable intermediate carrying information from genes to ribosomes for protein synthesis. *Nature*, 190(4776): 576–581, May 1961. doi: 10.1038/190576a0.
- J. H. Matthaei, O. W. Jones, R. G. Martin, and M. W. Nirenberg. Characteristics and composition of RNA coding units. *Proc. Natl. Acad. Sci. U.S.A.*, 48:666–677, Apr 1962.
- M. Nirenberg, P. Leder, M. Bernfield, R. Brimacombe, J. Trupin, F. Rottman, and C. O’Neal. RNA codewords and protein synthesis, VII. On the general nature of the RNA code. *Proc. Natl. Acad. Sci. U.S.A.*, 53(5):1161–1168, May 1965.
- T. I. Lee and R. A. Young. Transcription of eukaryotic protein-coding genes. *Annu. Rev. Genet.*, 34:77–137, 2000.
- K.E. Van Holde, C.G. Sahasrabuddhe, and Barbara Ramsay Shaw. A model for particulate structure in chromatin. *Nucleic Acids Research*, 1(11):1579–1586, 1974. doi: 10.1093/nar/1.11.1579.
- M. D. Young, T. A. Willson, M. J. Wakefield, E. Trounson, D. J. Hilton, M. E. Blewitt, A. Oshlack, and I. J. Majewski. ChIP-seq analysis reveals distinct H3K27me3 profiles that correlate with transcriptional activity. *Nucleic Acids Res.*, 39(17):7415–7427, Sep 2011.

- T. Jenuwein and C. D. Allis. Translating the histone code. *Science*, 293(5532):1074–1080, Aug 2001.
- B. E. Bernstein, E. Birney, I. Dunham, E. D. Green, C. Gunter, et al. An integrated encyclopedia of DNA elements in the human genome. *Nature*, 489(7414):57–74, Sep 2012.
- F. Sanger, S. Nicklen, and A. R. Coulson. DNA sequencing with chain-terminating inhibitors. *Proc. Natl. Acad. Sci. U.S.A.*, 74(12):5463–5467, Dec 1977.
- A. M. Maxam and W. Gilbert. A new method for sequencing DNA. *Proc. Natl. Acad. Sci. U.S.A.*, 74(2):560–564, Feb 1977.
- L. M. Smith, J. Z. Sanders, R. J. Kaiser, P. Hughes, C. Dodd, C. R. Connell, C. Heiner, S. B. Kent, and L. E. Hood. Fluorescence detection in automated DNA sequence analysis. *Nature*, 321(6071):674–679, 1986.
- M. L. Metzker. Sequencing technologies - the next generation. *Nat. Rev. Genet.*, 11(1):31–46, Jan 2010.
- D. Dressman, H. Yan, G. Traverso, K. W. Kinzler, and B. Vogelstein. Transforming single DNA molecules into fluorescent magnetic particles for detection and enumeration of genetic variations. *Proc. Natl. Acad. Sci. U.S.A.*, 100(15):8817–8822, Jul 2003.
- M. Fedurco, A. Romieu, S. Williams, I. Lawrence, and G. Turcatti. BTA, a novel reagent for DNA attachment on glass and efficient generation of solid-phase amplified DNA colonies. *Nucleic Acids Res.*, 34(3):e22, 2006.
- E. E. Schadt, S. Turner, and A. Kasarskis. A window into third-generation sequencing. *Hum. Mol. Genet.*, 19(R2):R227–240, Oct 2010.
- I. Braslavsky, B. Hebert, E. Kartalov, and S. R. Quake. Sequence information can be obtained from single DNA molecules. *Proc. Natl. Acad. Sci. U.S.A.*, 100(7):3960–3964, Apr 2003.
- Eric S Lander, Lauren M Linton, Bruce Birren, Chad Nusbaum, Michael C Zody, Jennifer Baldwin, Keri Devon, Ken Dewar, Michael Doyle, William FitzHugh, et al. Initial sequencing and analysis of the human genome. *Nature*, 409(6822):860–921, 2001.
- NHGRI. <http://www.genome.gov/11006943/>, 2010. Accessed: 2014-05-21.
- Lex Nederbragt. developments in NGS. <http://dx.doi.org/10.6084/m9.figshare.100940>, 12 2012.
- J. C. Alwine, D. J. Kemp, and G. R. Stark. Method for detection of specific RNAs in agarose gels by transfer to diazobenzyloxymethyl-paper and hybridization with DNA probes. *Proc. Natl. Acad. Sci. U.S.A.*, 74(12):5350–5354, Dec 1977.
- K. J. Livak and T. D. Schmittgen. Analysis of relative gene expression data using real-time quantitative PCR and the 2(-Delta Delta C(T)) Method. *Methods*, 25(4):402–408, Dec 2001.

- M. Schena, D. Shalon, R. W. Davis, and P. O. Brown. Quantitative monitoring of gene expression patterns with a complementary DNA microarray. *Science*, 270(5235):467–470, Oct 1995.
- J. L. DeRisi, V. R. Iyer, and P. O. Brown. Exploring the metabolic and genetic control of gene expression on a genomic scale. *Science*, 278(5338):680–686, Oct 1997.
- M. J. Okoniewski and C. J. Miller. Hybridization interactions between probesets in short oligo microarrays lead to spurious correlations. *BMC Bioinformatics*, 7:276, 2006.
- V. E. Velculescu, L. Zhang, B. Vogelstein, and K. W. Kinzler. Serial analysis of gene expression. *Science*, 270(5235):484–487, Oct 1995.
- S. Brenner, M. Johnson, J. Bridgham, G. Golda, D. H. Lloyd, D. Johnson, S. Luo, S. McCurdy, M. Foy, M. Ewan, R. Roth, D. George, S. Eletr, G. Albrecht, E. Vermaas, S. R. Williams, K. Moon, T. Burcham, M. Pallas, R. B. DuBridge, J. Kirchner, K. Fearon, J. Mao, and K. Corcoran. Gene expression analysis by massively parallel signature sequencing (MPSS) on microbead arrays. *Nat. Biotechnol.*, 18(6):630–634, Jun 2000.
- P. Ng, C. L. Wei, W. K. Sung, K. P. Chiu, L. Lipovich, C. C. Ang, S. Gupta, A. Shahab, A. Ridwan, C. H. Wong, E. T. Liu, and Y. Ruan. Gene identification signature (GIS) analysis for transcriptome characterization and genome annotation. *Nat. Methods*, 2(2):105–111, Feb 2005.
- T. Shiraki, S. Kondo, S. Katayama, K. Waki, T. Kasukawa, et al. Cap analysis gene expression for high-throughput analysis of transcriptional starting point and identification of promoter usage. *Proc. Natl. Acad. Sci. U.S.A.*, 100(26):15776–15781, Dec 2003.
- P. Carninci, C. Kvam, A. Kitamura, T. Ohsumi, Y. Okazaki, M. Itoh, M. Kamiya, K. Shibata, N. Sasaki, M. Izawa, M. Muramatsu, Y. Hayashizaki, and C. Schneider. High-efficiency full-length cDNA cloning by biotinylated CAP trapper. *Genomics*, 37(3):327–336, Nov 1996.
- P. Carninci, A. Westover, Y. Nishiyama, T. Ohsumi, M. Itoh, S. Nagaoka, N. Sasaki, Y. Okazaki, M. Muramatsu, C. Schneider, and Y. Hayashizaki. High efficiency selection of full-length cDNA by improved biotinylated cap trapper. *DNA Res.*, 4(1):61–66, Feb 1997.
- H. Matsumura, S. Reich, A. Ito, H. Saitoh, S. Kamoun, P. Winter, G. Kahl, M. Reuter, D. H. Kruger, and R. Terauchi. Gene expression analysis of plant host-pathogen interactions by SuperSAGE. *Proc. Natl. Acad. Sci. U.S.A.*, 100(26):15718–15723, Dec 2003.
- Hazuki Takahashi, Timo Lassmann, Mitsuyoshi Murata, and Piero Carninci. 5' end-centered expression profiling using cap-analysis gene expression and next-generation sequencing. *Nature Protocols*, 7(3):542–561, Feb 2012. doi: 10.1038/nprot.2012.005.
- Z. Wang, M. Gerstein, and M. Snyder. RNA-Seq: a revolutionary tool for transcriptomics. *Nat. Rev. Genet.*, 10(1):57–63, Jan 2009.

- H. Kawaji, M. Lizio, M. Itoh, M. Kanamori-Katayama, A. Kaiho, H. Nishiyori-Sueki, J. W. Shin, M. Kojima-Ishiyama, M. Kawano, M. Murata, N. Ninomiya-Fukuda, S. Ishikawa-Kato, S. Nagao-Sato, S. Noma, Y. Hayashizaki, A. R. Forrest, and P. Carninci. Comparison of CAGE and RNA-seq transcriptome profiling using clonally amplified and single-molecule next-generation sequencing. *Genome Res.*, 24(4):708–717, Apr 2014.
- J. Kawai, A. Shinagawa, K. Shibata, M. Yoshino, M. Itoh, et al. Functional annotation of a full-length mouse cDNA collection. *Nature*, 409(6821):685–690, Feb 2001.
- Y. Okazaki, M. Furuno, T. Kasukawa, J. Adachi, H. Bono, et al. Analysis of the mouse transcriptome based on functional annotation of 60,770 full-length cDNAs. *Nature*, 420(6915):563–573, Dec 2002.
- S. Katayama, Y. Tomaru, T. Kasukawa, K. Waki, M. Nakanishi, et al. Antisense transcription in the mammalian transcriptome. *Science*, 309(5740):1564–1566, Sep 2005.
- P. Carninci, T. Kasukawa, S. Katayama, J. Gough, M. C. Frith, et al. The transcriptional landscape of the mammalian genome. *Science*, 309(5740):1559–1563, Sep 2005.
- P. Bertone, V. Stolc, T. E. Royce, J. S. Rozowsky, A. E. Urban, X. Zhu, J. L. Rinn, W. Tongprasit, M. Samanta, S. Weissman, M. Gerstein, and M. Snyder. Global identification of human transcribed sequences with genome tiling arrays. *Science*, 306(5705):2242–2246, Dec 2004.
- P. Kapranov, S. E. Cawley, J. Drenkow, S. Bekiranov, R. L. Strausberg, S. P. Fodor, and T. R. Gingeras. Large-scale transcriptional activity in chromosomes 21 and 22. *Science*, 296(5569):916–919, May 2002.
- J. Cheng, P. Kapranov, J. Drenkow, S. Dike, S. Brubaker, et al. Transcriptional maps of 10 human chromosomes at 5-nucleotide resolution. *Science*, 308 (5725):1149–1154, May 2005.
- P. Kapranov, J. Cheng, S. Dike, D. A. Nix, R. Duttagupta, et al. RNA maps reveal new RNA classes and a possible function for pervasive transcription. *Science*, 316(5830):1484–1488, Jun 2007.
- H. van Bakel, C. Nislow, B. J. Blencowe, and T. R. Hughes. Most "dark matter" transcripts are associated with known genes. *PLoS Biol.*, 8(5):e1000371, May 2010.
- E. Birney, J. A. Stamatoyannopoulos, A. Dutta, R. Guigo, T. R. Gingeras, et al. Identification and analysis of functional elements in 1human genome by the ENCODE pilot project. *Nature*, 447(7146):799–816, Jun 2007.
- G. W. Beadle and E. L. Tatum. Genetic control of biochemical reactions in neurospora. *Proceedings of the National Academy of Sciences*, 27(11):499–506, 1941.
- L. T. Chow, J. M. Roberts, J. B. Lewis, and T. R. Broker. A map of cytoplasmic RNA transcripts from lytic adenovirus type 2, determined by electron microscopy of RNA:DNA hybrids. *Cell*, 11(4):819–836, Aug 1977.

- A. J. Berk and P. A. Sharp. Sizing and mapping of early adenovirus mRNAs by gel electrophoresis of S1 endonuclease-digested hybrids. *Cell*, 12(3):721–732, Nov 1977.
- M. B. Gerstein, C. Bruce, J. S. Rozowsky, D. Zheng, J. Du, J. O. Korbel, O. Emanuelsson, Z. D. Zhang, S. Weissman, and M. Snyder. What is a gene, post-ENCODE? History and updated definition. *Genome Res.*, 17(6):669–681, Jun 2007.
- R. C. Lee, R. L. Feinbaum, and V. Ambros. The *C. elegans* heterochronic gene lin-4 encodes small RNAs with antisense complementarity to lin-14. *Cell*, 75 (5):843–854, Dec 1993.
- A. A. Aravin, N. M. Naumova, A. V. Tulin, V. V. Vagin, Y. M. Rozovsky, and V. A. Gvozdev. Double-stranded RNA-mediated silencing of genomic tandem repeats and transposable elements in the *D. melanogaster* germline. *Curr. Biol.*, 11(13):1017–1027, Jul 2001.
- C. P. Ponting, P. L. Oliver, and W. Reik. Evolution and functions of long noncoding RNAs. *Cell*, 136(4):629–641, Feb 2009.
- J. Wang, J. Zhang, H. Zheng, J. Li, D. Liu, H. Li, R. Samudrala, J. Yu, and G. K. Wong. Mouse transcriptome: neutral evolution of 'non-coding' complementary DNAs. *Nature*, 431(7010):1 p following 757; discussion following 757, Oct 2004.
- A. Huttenhofer, P. Schattner, and N. Polacek. Non-coding RNAs: hope or hype? *Trends Genet.*, 21(5):289–297, May 2005.
- J. T. Kung, D. Colognori, and J. T. Lee. Long noncoding RNAs: past, present, and future. *Genetics*, 193(3):651–669, Mar 2013.
- P. Preker, J. Nielsen, S. Kammler, S. Lykke-Andersen, M. S. Christensen, C. K. Mapendano, M. H. Schierup, and T. H. Jensen. RNA exosome depletion reveals transcription upstream of active human promoters. *Science*, 322(5909):1851–1854, Dec 2008.
- M. N. Cabili, C. Trapnell, L. Goff, M. Koziol, B. Tazon-Vega, A. Regev, and J. L. Rinn. Integrative annotation of human large intergenic noncoding RNAs reveals global properties and specific subclasses. *Genes Dev.*, 25(18):1915–1927, Sep 2011.
- I. Ulitsky, A. Shkumatava, C. H. Jan, H. Sive, and D. P. Bartel. Conserved function of lincRNAs in vertebrate embryonic development despite rapid sequence evolution. *Cell*, 147(7):1537–1550, Dec 2011.
- N. L. Kedersha and L. H. Rome. Isolation and characterization of a novel ribonucleoprotein particle: large structures contain a single species of small RNA. *J. Cell Biol.*, 103(3):699–709, Sep 1986.
- E. Valen, P. Preker, P. R. Andersen, X. Zhao, Y. Chen, C. Ender, A. Dueck, G. Meister, A. Sandelin, and T. H. Jensen. Biogenic mechanisms and utilization of small RNAs derived from human protein-coding genes. *Nat. Struct. Mol. Biol.*, 18(9):1075–1082, Sep 2011.

- T. K. Kim, M. Hemberg, J. M. Gray, A. M. Costa, D. M. Bear, et al. Widespread transcription at neuronal activity-regulated enhancers. *Nature*, 465(7295):182–187, May 2010.
- W. Wei, Z. Ba, M. Gao, Y. Wu, Y. Ma, S. Amiard, C. I. White, J. M. Rendtlew Danielsen, Y. G. Yang, and Y. Qi. A role for small RNAs in DNA double-strand break repair. *Cell*, 149(1):101–112, Mar 2012.
- Y. Tay, J. Rinn, and P. P. Pandolfi. The multilayered complexity of ceRNA crosstalk and competition. *Nature*, 505(7483):344–352, Jan 2014.
- R. J. Taft, E. A. Glazov, N. Cloonan, C. Simons, S. Stephen, et al. Tiny RNAs associated with transcription start sites in animals. *Nat. Genet.*, 41(5):572–578, May 2009.
- M. Kertesz, Y. Wan, E. Mazor, J. L. Rinn, R. C. Nutter, H. Y. Chang, and E. Segal. Genome-wide measurement of RNA secondary structure in yeast. *Nature*, 467(7311):103–107, Sep 2010.
- J. G. Underwood, A. V. Uzilov, S. Katzman, C. S. Onodera, J. E. Mainzer, D. H. Mathews, T. M. Lowe, S. R. Salama, and D. Haussler. FragSeq: transcriptome-wide RNA structure probing using high-throughput sequencing. *Nat. Methods*, 7(12):995–1001, Dec 2010.
- R. J. Britten and D. E. Kohne. Repeated sequences in dna. *Science*, 161(3841):529–540, Aug 1968. doi: 10.1126/science.161.3841.529.
- R. H. Waterston, K. Lindblad-Toh, E. Birney, J. Rogers, J. F. Abril, et al. Initial sequencing and comparative analysis of the mouse genome. *Nature*, 420(6915):520–562, Dec 2002.
- J. Craig Venter, Mark D Adams, Eugene W Myers, Peter W Li, Richard J Mural, Granger G Sutton, Hamilton O Smith, Mark Yandell, Cheryl A Evans, Robert A Holt, et al. The sequence of the human genome. *Science*, 291(5507):1304–1351, 2001.
- J. Jurka. Repeats in genomic DNA: mining and meaning. *Curr. Opin. Struct. Biol.*, 8(3):333–337, Jun 1998.
- Casey M. Bergman and Hadi Quesneville. Discovering and detecting transposable elements in genome sequences. *Briefings in Bioinformatics*, 8(6):382–392, 2007. doi: 10.1093/bib/bbm048.
- M. Tarailo-Graovac and N. Chen. Using RepeatMasker to identify repetitive elements in genomic sequences. *Curr Protoc Bioinformatics*, Chapter 4:Unit 4.10, Mar 2009.
- J. Jurka, V. V. Kapitonov, A. Pavlicek, P. Klonowski, O. Kohany, and J. Walichiewicz. Repbase Update, a database of eukaryotic repetitive elements. *Cytogenet. Genome Res.*, 110(1-4):462–467, 2005.
- T. J. Wheeler, J. Clements, S. R. Eddy, R. Hubley, T. A. Jones, J. Jurka, A. F. Smit, and R. D. Finn. Dfam: a database of repetitive DNA based on profile hidden Markov models. *Nucleic Acids Res.*, 41(Database issue):70–82, Jan 2013.

- A. P. de Koning, W. Gu, T. A. Castoe, M. A. Batzer, and D. D. Pollock. Repetitive elements may comprise over two-thirds of the human genome. *PLoS Genet.*, 7(12):e1002384, Dec 2011.
- W Ford Doolittle and Carmen Sapienza. Selfish genes, the phenotype paradigm and genome evolution. *Nature*, 284(5757):601–3, 1980.
- Leslie E Orgel and Francis H Crick. Selfish dna: the ultimate parasite. *Nature*, 284(5757):604–607, 1980.
- S. Ohno. So much "junk" DNA in our genome. *Brookhaven Symp. Biol.*, 23: 366–370, 1972.
- A. F. Palazzo and T. R. Gregory. The case for junk DNA. *PLoS Genet.*, 10(5): e1004351, May 2014.
- Elizabeth Pennisi. Encode project writes eulogy for junk dna. *Science*, 337 (6099):1159–1161, 2012. doi: 10.1126/science.337.6099.1159.
- D. Graur, Y. Zheng, N. Price, R. B. Azevedo, R. A. Zufall, and E. Elhaik. On the immortality of television sets: "function" in the human genome according to the evolution-free gospel of ENCODE. *Genome Biol Evol*, 5(3):578–590, 2013.
- W. F. Doolittle. Is junk DNA bunk? A critique of ENCODE. *Proc. Natl. Acad. Sci. U.S.A.*, 110(14):5294–5300, Apr 2013.
- Sean R. Eddy. The c-value paradox, junk dna and encode. *Current Biology*, 22 (21):R898–R899, Nov 2012. doi: 10.1016/j.cub.2012.10.002.
- T. R. Gregory. Coincidence, coevolution, or causation? DNA content, cell size, and the C-value enigma. *Biol Rev Camb Philos Soc*, 76(1):65–101, Feb 2001.
- M. G. Kidwell. Transposable elements and the evolution of genome size in eukaryotes. *Genetica*, 115(1):49–63, May 2002.
- S. Aparicio, J. Chapman, E. Stupka, N. Putnam, J. M. Chia, et al. Whole-genome shotgun assembly and analysis of the genome of Fugu rubripes. *Science*, 297(5585):1301–1310, Aug 2002.
- E. Ibarra-Laclette, E. Lyons, G. Hernandez-Guzman, C. A. Perez-Torres, L. Carretero-Paulet, et al. Architecture and evolution of a minute plant genome. *Nature*, 498(7452):94–98, Jun 2013.
- Dave Tang. Genome size versus percent repetitive of 66 vertebrate genomes. 11 2014. URL <http://dx.doi.org/10.6084/m9.figshare.1252036>.
- R. Cordaux and M. A. Batzer. The impact of retrotransposons on human genome evolution. *Nat. Rev. Genet.*, 10(10):691–703, Oct 2009.
- R. E. Mills, E. A. Bennett, R. C. Iskow, and S. E. Devine. Which transposable elements are active in the human genome? *Trends Genet.*, 23(4):183–191, Apr 2007.
- C. Feschotte. Transposable elements and the evolution of regulatory networks. *Nat. Rev. Genet.*, 9(5):397–405, May 2008.

- G. Lev-Maor, O. Ram, E. Kim, N. Sela, A. Goren, E. Y. Levanon, and G. Ast. Intrinsic Alus influence alternative splicing. *PLoS Genet.*, 4(9):e1000204, 2008.
- A. Kapusta, Z. Kronenberg, V. J. Lynch, X. Zhuo, L. Ramsay, G. Bourque, M. Yandell, and C. Feschotte. Transposable elements are major contributors to the origin, diversification, and regulation of vertebrate long noncoding RNAs. *PLoS Genet.*, 9(4):e1003470, Apr 2013.
- C. J. Cohen, W. M. Lock, and D. L. Mager. Endogenous retroviral LTRs as promoters for human genes: a critical assessment. *Gene*, 448(2):105–114, Dec 2009.
- Stephen Jay Gould and Elisabeth S. Vrba. Exaptation; a missing term in the science of form. *Paleobiology*, 8(1):4–15, 1982.
- G. J. Faulkner, Y. Kimura, C. O. Daub, S. Wani, C. Plessy, K. M. Irvine, K. Schroder, N. Cloonan, A. L. Steptoe, T. Lassmann, K. Waki, N. Hornig, T. Arakawa, H. Takahashi, J. Kawai, A. R. Forrest, H. Suzuki, Y. Hayashizaki, D. A. Hume, V. Orlando, S. M. Grimmond, and P. Carninci. The regulated retrotransposon transcriptome of mammalian cells. *Nat. Genet.*, 41(5):563–571, May 2009.
- G. J. Faulkner, A. R. Forrest, A. M. Chalk, K. Schroder, Y. Hayashizaki, P. Carninci, D. A. Hume, and S. M. Grimmond. A rescue strategy for multimapping short sequence tags refines surveys of transcriptional activity by CAGE. *Genomics*, 91(3):281–288, Mar 2008.
- M. Xie, C. Hong, B. Zhang, R. F. Lowdon, X. Xing, et al. DNA hypomethylation within specific transposable element families associates with tissue-specific enhancer landscape. *Nat. Genet.*, 45(7):836–841, Jul 2013.
- D. S. Day, L. J. Luquette, P. J. Park, and P. V. Kharchenko. Estimating enrichment of repetitive elements from high-throughput sequence data. *Genome Biol.*, 11(6):R69, 2010.
- P. Hogeweg. The roots of bioinformatics in theoretical biology. *PLoS Comput. Biol.*, 7(3):e1002021, Mar 2011.
- Lincoln Stein. How Perl Saved the Human Genome Project. http://www.bioperl.org/wiki/How_Perl_saved_human_genome, 1996. Accessed: 2014-06-06.
- Jorge L Contreras. Bermuda’s legacy: Policy, patents, and the design of the genome commons. *Minn. JL Sci. & Tech.*, 12:61–97, 2011.
- P. J. Cock, C. J. Fields, N. Goto, M. L. Heuer, and P. M. Rice. The Sanger FASTQ file format for sequences with quality scores, and the Solexa/Illumina FASTQ variants. *Nucleic Acids Res.*, 38(6):1767–1771, Apr 2010.
- T. Lassmann, Y. Hayashizaki, and C. O. Daub. TagDust—a program to eliminate artifacts from next generation sequencing data. *Bioinformatics*, 25(21):2839–2840, Nov 2009.
- T. Lassmann, Y. Hayashizaki, and C. O. Daub. SAMStat: monitoring biases in next generation sequencing data. *Bioinformatics*, 27(1):130–131, Jan 2011.

- S. F. Altschul, W. Gish, W. Miller, E. W. Myers, and D. J. Lipman. Basic local alignment search tool. *J. Mol. Biol.*, 215(3):403–410, Oct 1990.
- W. J. Kent. BLAT—the BLAST-like alignment tool. *Genome Res.*, 12(4):656–664, Apr 2002.
- H. Li and R. Durbin. Fast and accurate short read alignment with Burrows-Wheeler transform. *Bioinformatics*, 25(14):1754–1760, Jul 2009.
- C. Trapnell and S. L. Salzberg. How to map billions of short reads onto genomes. *Nat. Biotechnol.*, 27(5):455–457, May 2009.
- H. Li, B. Handsaker, A. Wysoker, T. Fennell, J. Ruan, N. Homer, G. Marth, G. Abecasis, and R. Durbin. The Sequence Alignment/Map format and SAM-tools. *Bioinformatics*, 25(16):2078–2079, Aug 2009a.
- Heng Li, Bob Handsaker, Alec Wysoker, Tim Fennell, Jue Ruan, Nils Homer, Gabor Marth, Goncalo Abecasis, Richard Durbin, and 1000 Genome Project Data Processing Subgroup. The sequence alignment/map format and sam-tools. *Bioinformatics*, 25(16):2078–2079, 2009b. doi: 10.1093/bioinformatics/btp352.
- M. Hsi-Yang Fritz, R. Leinonen, G. Cochrane, and E. Birney. Efficient storage of high throughput DNA sequencing data using reference-based compression. *Genome Res.*, 21(5):734–740, May 2011.
- W. James Kent, Charles W. Sugnet, Terrence S. Furey, Krishna M. Roskin, Tom H. Pringle, Alan M. Zahler, and David Haussler. The human genome browser at ucsc. *Genome Research*, 12(6):996–1006, 2002. doi: 10.1101/gr.229102.
- A. R. Quinlan and I. M. Hall. BEDTools: a flexible suite of utilities for comparing genomic features. *Bioinformatics*, 26(6):841–842, Mar 2010.
- B. M. Bolstad, R. A. Irizarry, M. Astrand, and T. P. Speed. A comparison of normalization methods for high density oligonucleotide array data based on variance and bias. *Bioinformatics*, 19(2):185–193, Jan 2003.
- M. D. Robinson and A. Oshlack. A scaling normalization method for differential expression analysis of RNA-seq data. *Genome Biol.*, 11(3):R25, 2010.
- J. C. Marioni, C. E. Mason, S. M. Mane, M. Stephens, and Y. Gilad. RNA-seq: an assessment of technical reproducibility and comparison with gene expression arrays. *Genome Res.*, 18(9):1509–1517, Sep 2008.
- Simon Anders and Wolfgang Huber. Differential expression analysis for sequence count data. *Genome Biology*, 11(10):R106, 2010. ISSN 1465-6906. doi: 10.1186/gb-2010-11-10-r106.
- M. D. Robinson, D. J. McCarthy, and G. K. Smyth. edgeR: a Bioconductor package for differential expression analysis of digital gene expression data. *Bioinformatics*, 26(1):139–140, Jan 2010.

- R. C. Gentleman, V. J. Carey, D. M. Bates, B. Bolstad, M. Dettling, S. Dudoit, B. Ellis, L. Gautier, Y. Ge, J. Gentry, K. Hornik, T. Hothorn, W. Huber, S. Iacus, R. Irizarry, F. Leisch, C. Li, M. Maechler, A. J. Rossini, G. Sawitzki, C. Smith, G. Smyth, L. Tierney, J. Y. Yang, and J. Zhang. Bioconductor: open software development for computational biology and bioinformatics. *Genome Biol.*, 5(10):R80, 2004.
- M. B. Eisen, P. T. Spellman, P. O. Brown, and D. Botstein. Cluster analysis and display of genome-wide expression patterns. *Proc. Natl. Acad. Sci. U.S.A.*, 95(25):14863–14868, Dec 1998.
- Yoav Benjamini and Yosef Hochberg. Controlling the False Discovery Rate: A Practical and Powerful Approach to Multiple Testing. *Journal of the Royal Statistical Society. Series B (Methodological)*, 57(1):289–300, 1995.
- H. C. Lee, S. S. Chang, S. Choudhary, A. P. Aalto, M. Maiti, D. H. Bamford, and Y. Liu. qRNA is a new type of small interfering RNA induced by DNA damage. *Nature*, 459(7244):274–277, May 2009.
- A. R. Muotri, M. C. Marchetto, N. G. Coufal, R. Oefner, G. Yeo, K. Nakashima, and F. H. Gage. L1 retrotransposition in neurons is modulated by MeCP2. *Nature*, 468(7322):443–446, Nov 2010.
- P. J. Skene, R. S. Illingworth, S. Webb, A. R. Kerr, K. D. James, D. J. Turner, R. Andrews, and A. P. Bird. Neuronal MeCP2 is expressed at near histone-octamer levels and globally alters the chromatin state. *Mol. Cell*, 37(4):457–468, Feb 2010.
- H. Wu, J. Tao, P. J. Chen, A. Shahab, W. Ge, R. P. Hart, X. Ruan, Y. Ruan, and Y. E. Sun. Genome-wide analysis reveals methyl-CpG-binding protein 2-dependent regulation of microRNAs in a mouse model of Rett syndrome. *Proc. Natl. Acad. Sci. U.S.A.*, 107(42):18161–18166, Oct 2010.
- S. Djebali, C. A. Davis, A. Merkel, A. Dobin, T. Lassmann, et al. Landscape of transcription in human cells. *Nature*, 489(7414):101–108, Sep 2012.
- K. Struhl. Transcriptional noise and the fidelity of initiation by RNA polymerase II. *Nat. Struct. Mol. Biol.*, 14(2):103–105, Feb 2007.
- F. Spitz and E. E. Furlong. Transcription factors: from enhancer binding to developmental control. *Nat. Rev. Genet.*, 13(9):613–626, Sep 2012.
- T. H. Jensen, A. Jacquier, and D. Libri. Dealing with pervasive transcription. *Mol. Cell*, 52(4):473–484, Nov 2013.
- A. Jacquier. The complex eukaryotic transcriptome: unexpected pervasive transcription and novel small RNAs. *Nat. Rev. Genet.*, 10(12):833–844, Dec 2009.
- L. Yang, J. E. Froberg, and J. T. Lee. Long noncoding RNAs: fresh perspectives into the RNA world. *Trends Biochem. Sci.*, 39(1):35–43, Jan 2014.
- M. J. Hangauer, I. W. Vaughn, and M. T. McManus. Pervasive transcription of the human genome produces thousands of previously unidentified long intergenic noncoding RNAs. *PLoS Genet.*, 9(6):e1003569, Jun 2013.

- S. P. Jackson and J. Bartek. The DNA-damage response in human biology and disease. *Nature*, 461(7267):1071–1078, Oct 2009.
- A. Saxena and P. Carninci. Long non-coding RNA modifies chromatin: epigenetic silencing by long non-coding RNAs. *Bioessays*, 33(11):830–839, Nov 2011.
- A. M. Khalil, M. Guttman, M. Huarte, M. Garber, A. Raj, D. Rivea Morales, K. Thomas, A. Presser, B. E. Bernstein, A. van Oudenaarden, A. Regev, E. S. Lander, and J. L. Rinn. Many human large intergenic noncoding RNAs associate with chromatin-modifying complexes and affect gene expression. *Proc. Natl. Acad. Sci. U.S.A.*, 106(28):11667–11672, Jul 2009.
- A. Wutz and J. Gribnau. X inactivation Xplained. *Curr. Opin. Genet. Dev.*, 17(5):387–393, Oct 2007.
- L. Chakalova, E. Debrand, J. A. Mitchell, C. S. Osborne, and P. Fraser. Replication and transcription: shaping the landscape of the genome. *Nat. Rev. Genet.*, 6(9):669–677, Sep 2005.
- M. Ebisuya, T. Yamamoto, M. Nakajima, and E. Nishida. Ripples from neighbouring transcription. *Nat. Cell Biol.*, 10(9):1106–1113, Sep 2008.
- A. C. Chueh, E. L. Northrop, K. H. Brettingham-Moore, K. H. Choo, and L. H. Wong. LINE retrotransposon RNA is an essential structural and functional epigenetic component of a core neocentromeric chromatin. *PLoS Genet.*, 5(1):e1000354, Jan 2009.
- L. L. Hall, D. M. Carone, A. V. Gomez, H. J. Kolpa, M. Byron, N. Mehta, F. O. Fackelmayer, and J. B. Lawrence. Stable C0T-1 repeat RNA is abundant and is associated with euchromatic interphase chromosomes. *Cell*, 156(5):907–919, Feb 2014.
- D. Kelley and J. Rinn. Transposable elements reveal a stem cell-specific class of long noncoding RNAs. *Genome Biol.*, 13(11):R107, 2012.
- R. Johnson and R. Guigo. The RIDL hypothesis: transposable elements as functional domains of long noncoding RNAs. *RNA*, 20(7):959–976, Jul 2014.
- A. Kapusta and C. Feschotte. Volatile evolution of long noncoding RNA repertoires: mechanisms and biological implications. *Trends Genet.*, 30(10):439–452, Oct 2014.
- A. Fort, K. Hashimoto, D. Yamada, M. Salimullah, C. A. Keya, et al. Deep transcriptome profiling of mammalian stem cells supports a regulatory role for retrotransposons in pluripotency maintenance. *Nat. Genet.*, 46(6):558–566, Jun 2014.